University of Miami
Scholarly Repository

2016-04-27

The Application of Clumped Isotopes to Dolomites

Sean Timothy Murray
University of Miami, smurray@rsmas.miami.edu

Follow this and additional works at: https://scholarlyrepository.miami.edu/oa_dissertations

UNIVERSITY OF MIAMI

THE APPLICATION OF CLUMPED ISOTOPES TO DOLOMITES

By

Sean Timothy Murray

A DISSERTATION

Submitted to the Faculty
of the University of Miami
in partial fulfillment of the requirements for
the degree of Doctor of Philosophy

Coral Gables, Florida

May 2016

UNIVERSITY OF MIAMI

A dissertation submitted in partial fulfillment of
the requirements for the degree of
Doctor of Philosophy

THE APPLICATION OF CLUMPED ISOTOPES TO DOLOMITES

Sean Timothy Murray

Approved:

_____
Peter K. Swart, Ph.D.
Lewis G. Weeks Professor and Chair
of Marine Geosciences

_____
Gregor Eberli, Ph.D.
Professor of Marine Geosciences

_____
James S. Klaus, Ph.D.
Assistant Professor of Geological Sciences

_____
Guillermo Prado, Ph.D.
Dean of the Graduate School

_____
Brad E. Rosenheim, Ph.D.
Assistant Professor of Geological Oceanography
University of South Florida

MURRAY, SEAN TIMOTHY   (Ph.D., Marine Geology and Geophysics)

<u>The Application of Clumped Isotopes to Dolomites</u>   (May 2016)

Abstract of a dissertation at the University of Miami.

Dissertation supervised by Professor Peter K. Swart.
No. of pages in text. (162)

The formation of low-temperature dolomite $(CaMg(CO_3)_2)$ continues to be enigmatic. By using a newly developed carbonate paleothermometer based on the measurement of clumped isotopes, the abundance of which is controlled by a thermodynamic isotope exchange reaction that promotes the combination of multiple heavy isotopes into single molecules with decreasing temperature, it is believed that understanding the environments of formation for dolomites can be elucidated. The advantage of this technique over other carbonate paleothermometers is that the technique is completely independent of the composition of the precipitating fluid, making clumped isotopes ideal for use in ancient carbonates and in dolomites where the formation fluid is difficult to discern.

In this work, the dolomite problem is approached by measuring clumped isotopes in samples from five different cores from the Bahamas, where their relatively young age and comparably simple history make them ideal for calibrating clumped isotopes to dolomites. The first study attempts to measure the temperature of acid digestion fractionation factor in dolomites relative to calcites and aragonites and finds that the fractionation in dolomite (0.153‰) is significantly larger than for calcite (0.089‰) or aragonite (0.091‰). Using the new acid fractionation factor, it is shown that temperatures calculated from clumped isotopes agree with the expected formation temperatures based off previous research and the average fluid temperatures of seawater

in the Bahamas and new insights are made as to the fluid flow regimes that formed the dolomites. Using the clumped isotope temperatures, an attempt to reduce the number of viable $\delta^{18}O_{fluid}$-dolomite calibrations is made.

The clumped isotope technique is then applied to a less ideal sedimentary system, the Clino core, where mixed carbonates and a complex geological history make interpretation difficult. Guidelines are developed for the application of end-member mixing to clumped isotopes in mixed carbonate samples and the implications for having carbonates that formed from different parent fluids and varying temperatures is discussed. Ultimately, the Clino core clumped isotope temperatures do not agree with any known model of formation known from the Bahamas as the temperatures are exceedingly too high. By measuring carbonate associated sulfate $\delta^{34}S$ in the Clino bulk samples and comparing the measurements to sights where clumped isotope temperatures are agreeable, it is found that a unique correlation exists between elevated $\delta^{34}S$ and the formation temperatures recorded by the clumped isotopes in Clino. It is proposed that bacterial sulfate reduction and associated processes is capable of causing disequilibrium in clumped isotopes which has significant implications for the application of clumped isotopes in diagenetic settings.

Preface

The goal of geochemical analysis is to further understanding of the environments of the past to aid in understanding the changing environments of the present. Paleothermometry came to the forefront of geochemistry at the advent of isotopic analysis with the development of the carbonate-water equilibrium exchange paleothermometer described in Urey (1947). Despite the vastness of the field of study that the work of Harold Urey would spawn, the restrictions on the samples that could be studied using his findings would plague research for years. The requirement of needing both the $\delta^{18}O$ of the carbonate and the water it was precipitated from in order to fully understand how a carbonate formed proved to be challenging for any research looking beyond Earth's recent history. In recent years, the development of a new paleothermometer based on the thermodynamics of carbonate equilibrium formation has made the ancient available to study by removing the water from the paleothermometry equation. Based on the natural 'clumping' of rare isotopes in a molecule forming multiply substituted isotopologues as a function of temperature, this new technique can offer the formation temperature through time by the isotopic measurement of carbonates independent of the composition of the fluid. This work will focus on the development of the clumped isotope technique in the Stable Isotope Laboratory at the Rosenstiel School of Marine and Atmospheric Science and its application to diagenetic carbonates from the Bahamas.

The relative novelty of this field has reopened systems that have been looked at in depth previously as well as the many which are still poorly understood. I will discuss my contributions to the application of clumped isotopes to dolomites, a consistently

enigmatic mineral when it comes to isotopic study because of its resistance to being precipitated under controlled conditions in the laboratory at Earth's surface temperatures and pressures. . The importance of understanding the origins of dolomites revolves around its economic importance. According to some estimates, dolostones, rocks predominantly composed of dolomite, compose 80% of North American and 50% or global oil and gas reservoirs (Zenger et al., 1980). This makes understanding dolomites a priority from an economic standpoint and a challenge from an academic perspective.

The kinetics of the precipitation of dolomite has limited its role in geologic research because the dolomites found in abundant expansive blocks in nature appear to have formed at low, earth surface temperatures. However, well-ordered dolomite has only been successfully precipitated synthetically under extreme temperatures and pressures or with the aid of biological processes. The clumped isotope technique side-steps this inhibiting factor and offers a glimpse into the formation history of a mineral that has eluded science since dolomite was originally described over 200 years ago. This work is part of the first attempts at divulging this history and discussing how to approach and interpret the measurement of clumped isotopes in dolomites.

Furthering the development of clumped isotopes as a paleothermometer, we also expand on the relationship between temperature and abundance of multiply substituted isotopologues species by advancing the initial calibrations formulated in Ghosh et al. (2006). By precipitating synthetic calcites at equilibrium under controlled conditions and controlled rates, we develop new and more accurate relations between the clumped isotope signature in low-mg calcite and temperature of formation. By

doing so, we offer guidelines for calibrating and standardizing measurements within the laboratory. This is a necessary step in the progression of the clumped isotope method in furthering its use as more laboratories become integrated into the community.

Table of Contents

List of Figures

List of Tables

Chapter 1 - Introduction to Multiply Substituted Isotopologues

History of Clumped Isotopes

Standard mass spectrometry of CO_2 has revolved around the measurement of masses 44, 45, and 46 which comprise approximately 99.99% of all CO_2 species. Measurement of these species has enabled the determination of the abundance of ^{18}O and ^{13}C. Only by increasing the sensitivity of mass spectrometers and the addition of extra collectors, has it become possible to measure the other 0.01% of CO_2 molecules. At the heavier masses 47, 48, and 49, there resides multiple low-abundance species of CO_2, each of which is considered a multiply substituted isotopologue. These masses are unique in their ability to be interpreted as a universally applicable thermometer.

Multiply Substituted Isotopologues

Multiply substituted isotopologue is the name given to subset of molecules that contain more than one of any rare isotopic species within its molecular structure. A clumped isotope is any multiply substituted isotopologue that has bonds between the rare isotopes.   In the case of CO_2, the rare isotopes would be ^{13}C, ^{17}O, and ^{18}O. In combination, these rare isotopes create eight distinct multiply substituted isotopologues and at least seven clumped isotope species ($^{18}O^{16}C^{18}O$ is a multiply substituted isotopologues, but may not be considered a clumped isotope by definition because there is no direct bond between the rare isotopes) between masses 46 to 49 (Table 1.1), of which the most abundant is $^{13}C^{18}O^{16}O$ at mass 47 which comprises about 44.4 ppm of all CO_2 molecules (the least abundant is $^{13}C^{17}O_2$ which is only

Table 1.1 - Stochastic Abundance* of CO_2 Isotopologues

Molecular Mass	Isotopologue	Stochastic Abudance
44	$^{12}C^{16}O_2$	98.40%
45	$^{13}C^{16}O_2$	1.11%
	$^{12}C^{17}O^{16}O$	748 ppm
46	$^{12}C^{18}O^{16}O$	0.40%
	$^{13}C^{17}O^{16}O$	8.4 ppm
	$^{12}C^{17}O_2$	0.142 ppm
47	$^{13}C^{18}O^{16}O$	44.4 ppm
	$^{12}C^{17}O^{18}O$	1.50 ppm
	$^{13}C^{17}O_2$	1.60 ppb
48	$^{12}C^{18}O_2$	3.96 ppm
	$^{13}C^{17}O^{18}O$	16.8 ppb
49	$^{13}C^{18}O_2$	44.5 ppb

*: Assuming $^{17}O/^{16}O$ and $^{18}O/^{16}O$ ratio are equivalent to VSMOW

and $^{13}C/^{12}C$ equivalent to PDB

- Multiply substituted isotopologues are in highlighted in red

about 1.6 ppb). Because the $^{13}C^{18}O^{16}O$ molecule has the greatest abundance by far of all the clumped isotope species of CO_2, it makes the measurement of mass-47 the focal point of the field.

Zero Point Energy and the Rule of Means

The incentive for measuring clumped isotope species is that the abundance of clumped isotope molecules in a system at equilibrium is directly related to the temperature at which the system is held. With increasing temperature, theory suggests that at equilibrium there should be a decrease in the amount of clumped isotope molecules present as the individual rare isotopes reach a more stochastic distribution amongst all molecules present. The theory behind this was developed during the early days of mass spectrometry (Bigeleisen, 1955; Urey, 1947), and relates to the 'rule of means' and a molecules zero point energy. The zero point energy is the lowest energy state a quantum system can reach. The addition of heavy isotopes to a molecular structure reduces that molecules zero point energy (Figure 1.1). It is commonly assumed, as defined in the rule of means, that each additional heavy isotope that is added to a molecule reduces the bond energy by half (e.g. the H-H bond is twice that of H-D) (Bigeleisen, 1955). Within a system composed of multiple molecules, the rule of means would imply that there is no preferential difference between a system with "clumped" multiply substituted isotopologues and a system with singly substituted isotopologues as the energy in both systems is equivalent (e.g. a system with an H-H and D-D molecule compared to a system with two H-D molecules have equivalent bond energies). However, the rule of means is merely an approximation and the reduction in energy associated with having doubly
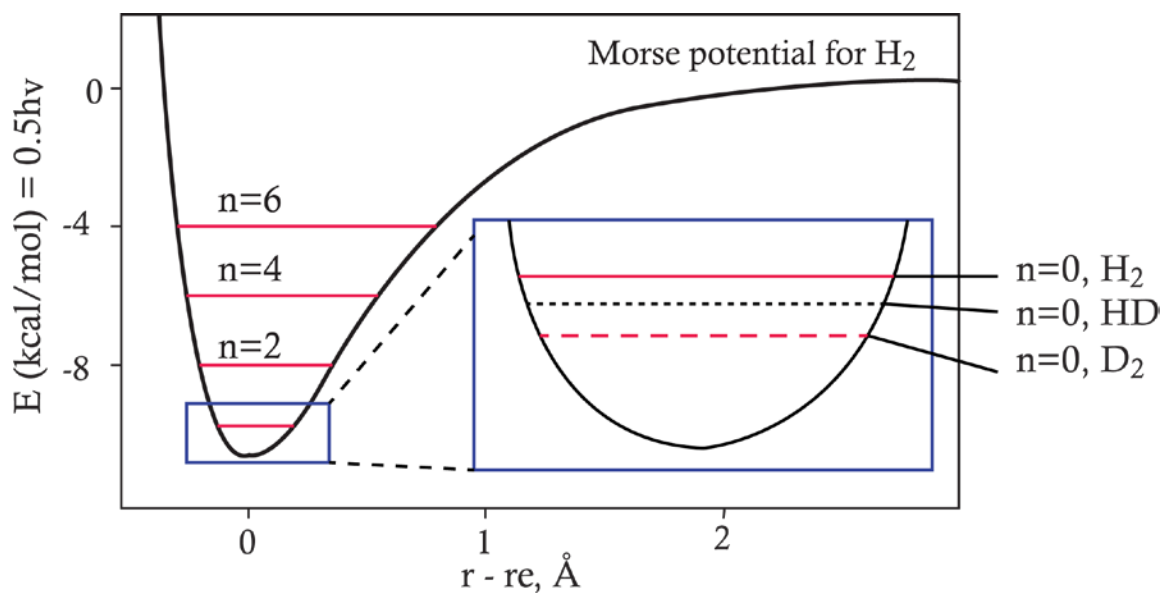
Figure 1.1 - Adapted from Eiler (2007). Solid curve is the Morse potential for molecular hydrogen representing the potential energy (E, kcal/mol) as a function of the bond distance (r-re in angstroms, where r is the molecular radius and re is the optimal bond distance). Horizontal lines are the quantum state of the bonds vibration, with $n = 0$ corresponding to the zero point energy.

substituted isotopologues slightly exceeds what is predicted (Eiler, 2007). This deviation consequently promotes a thermodynamic driving force that promotes the clumping of heavy isotopes into single molecules.

First Practical Applications

This idea was first explored using atmospheric CO_2 in Eiler and Schauble (2004) where they developed the measurement of Δ_{47} which is defined by the abundance of mass-47 CO_2 , in per mil, in a sample relative to the amount of mass-47 that would be expected if the sample were to have a stochastic distribution:

$$\Delta_{47} = \left[\left(\frac{R^{47}}{R^{47*}} - 1 \right) - \left(\frac{R^{46}}{R^{46*}} - 1 \right) - \left(\frac{R^{45}}{R^{45*}} - 1 \right) \right] \times 1000 \qquad (1.1)$$

where R^{47}, R^{46}, and R^{45} are the ratios of the abundance of masses 47, 46, and 45 in the sample relative to mass 44 respectively. The R^{*} values are the values for the corresponding mass ratios if the sample were to have a stochastic distribution amongst all its isotopologues. The stochastic distribution relative to temperature was defined theoretically in Wang et al. (2004). With the foundation laid, the application of clumped isotopes to carbonate-derived CO_2 appeared shortly after in Ghosh et al. (2006), where upon measuring a variety of inorganic calcites precipitated under controlled conditions at known temperatures and organic calcites from shallow and deep water corals precipitated in restricted environments with measured temperatures, it was shown that a measurable difference in Δ_{47} changes linearly with the temperature of precipitation and is independent of the composition of the water. This paper was evidence of a paleothermometer that could be used in carbonates without being hindered by knowing or constraining the composition of the water (Figure 1.2).
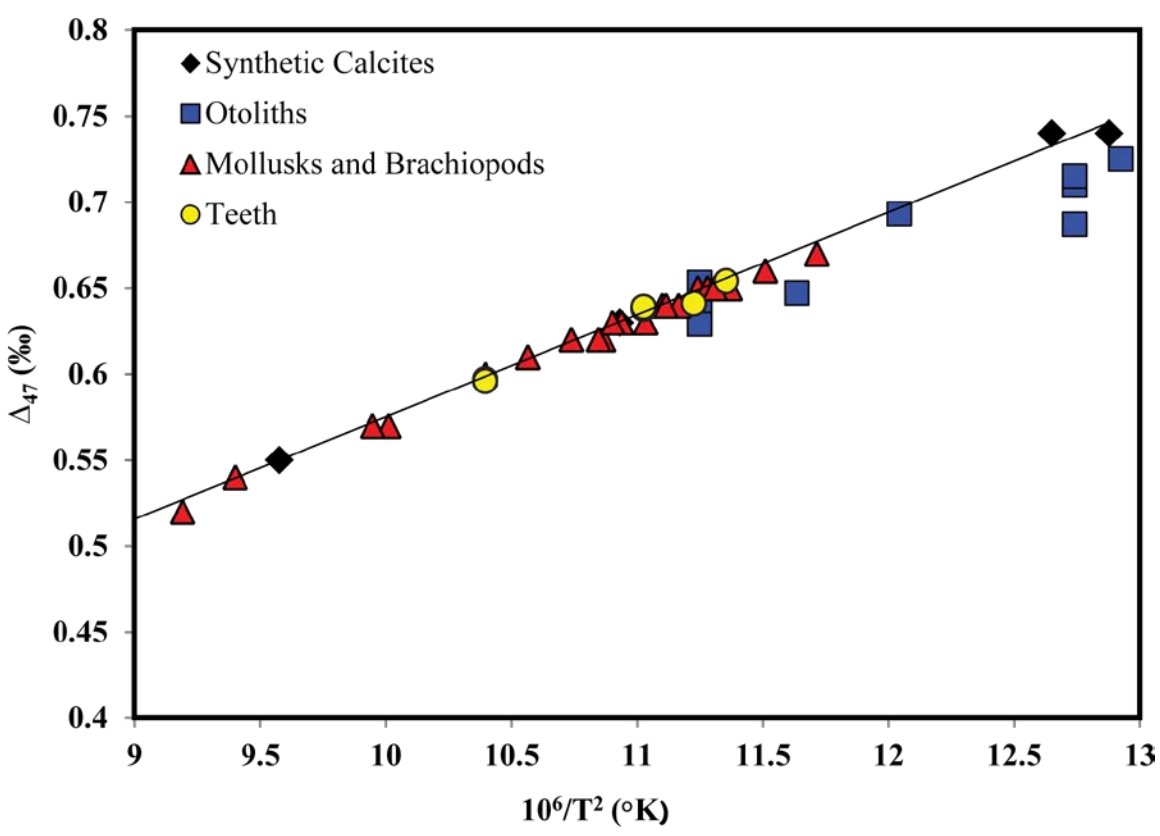
Figure 1.2 - Original clumped isotope calibration line of Ghosh et al. (2006) (synthetic calcites). Additional data derived from Ghosh et al. (2007) (otoliths), Came et al. (2007) (mollusks and brachiopods), Eagle et al. (2010) (teeth).

Δ_{47} Drift over Time

Over the course of time and repeated measurements of clumped isotopes on a Thermo-253 mass spectrometer, it became evident that Δ_{47} measurements on standards began to drift over time. This discovery was not initially understood and only recently have explanations begun to address the problem. The first, identified in Huntington et al. (2009) and corroborated in Passey et al. (2010), involved the fragmentation and recombination that takes place within the source of the mass spectrometer. Initial measurements of samples with known Δ_{47} values suggested that these effects were negligible (Eiler and Schauble, 2004; Ghosh et al., 2006), however improvements in measuring technique have shown that changes within the source can affect the Δ_{47} value by up to 10% (Huntington et al., 2009).

Unfortunately, a simple correction was not possible for this problem as a variety of labs measuring standards on different mass spectrometers showed that the variations in Δ_{47} were neither constant nor predictable between laboratories (Table 1.2). It appeared that each mass spectrometer behaves differently in respect to how its measured Δ_{47} values change over time. This change was later attributed to aging of the filament as well as scattering of the ion beams within the flight tube caused by shielding around the cups being too narrow (Dennis et al., 2011; He et al., 2012; Huntington et al., 2009). These problems are realized as a negative pressure baseline (PBL) measured by the mass spectrometer on each beam. He et al. (2012) describes the problem in detail, but the gist of it is that once gas enters the source, secondary electrons created by the mass-44 beam deflect off the walls of the flight tube and are picked up by other faraday cups. Due to the intensified sensitivity of the mass 47, 48,

Table 1.2: Measurement of clumped isotope standards between multiple laboratories

Standard	Harvard University	Johns Hopkins University	Yale University	California Institute of Technology
NBS-19	-0.512	-0.586	-0.407	not reported
Cararra Marble	-0.643	-0.581	-0.445	-0.402
102-GC-AZ01	-0.326	-0.289	-0.166	-0.235
DSC-45923	-0.228	-0.074	-0.038	-0.098

Data was originally reported in Dennis et al. (2011)

49 cups, the cups respond to the increased signal by creating a negative background

for the baseline which technically cannot go below zero (Figure 1.3). While this is a

common occurrence in typical mass spectrometry, the magnitude of the size of the

beams relative to the magnitude of the size of the negative offset is significantly

larger on the 47, 48, and 49 peaks relative to the much more abundant and therefore

larger signal peaks of 44, 45, and 46 peaks (e.g. 0.005% of the mass 45 ion beam is

equal to 3.0% of the mass 47 ion beam).

Correction for Δ_{47} Drift: The CDES and PBL

To correct for this, two published methods have been presented: the carbon

dioxide equilibrium scale (CDES) developed in Dennis et al. (2011) and an extended

correction to the CDES known as the PBL correction originally described in He et al.

(2012). The CDES improves upon the original reference frame work developed in Ghosh

et al. (2006) (GRF) which used CO_2 gases with a range of δ^{47} heated to 1000°C to

produce "heated gases" which have a stochastic distribution of isotopes amongst all

molecular species ($\Delta_{47} \approx 0$). Because of the negative pressure baseline, the heated gases

produce a sloped line in the relation of δ^{47} and Δ_{47} which is then used to correct for gases

with unknown Δ_{47} values assuming the slope holds true for all Δ_{47} values (Figure 1.4).

The CDES improves upon the GRF by adding additional standard gases with

known Δ_{47} values to the correction based solely on heated gases. These additional gases

can be equilibrated to any temperature, but are typically produced at significantly lower

temperatures to account for the common range of Earth surface temperatures. The lower

temperature gases are produced by equilibrating CO_2 gas with water held at a specific

temperature (typically in a water bath) in order to escape the kinetic barriers of
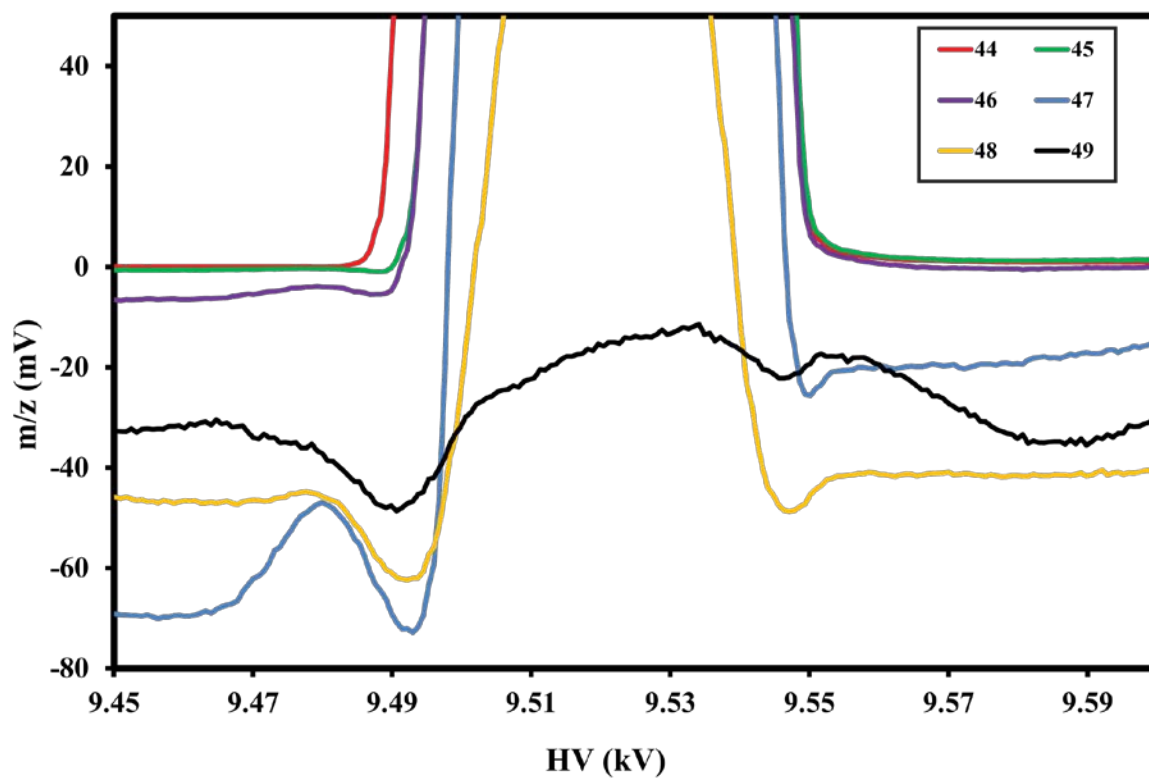
Figure 1.3 - Negative pressure baseline measured on masses 44 to 49 on the Thermo MAT 253 mass spectrometer on April 4, 2016 relative to a set pressure of 12,000 mv on mass 44.
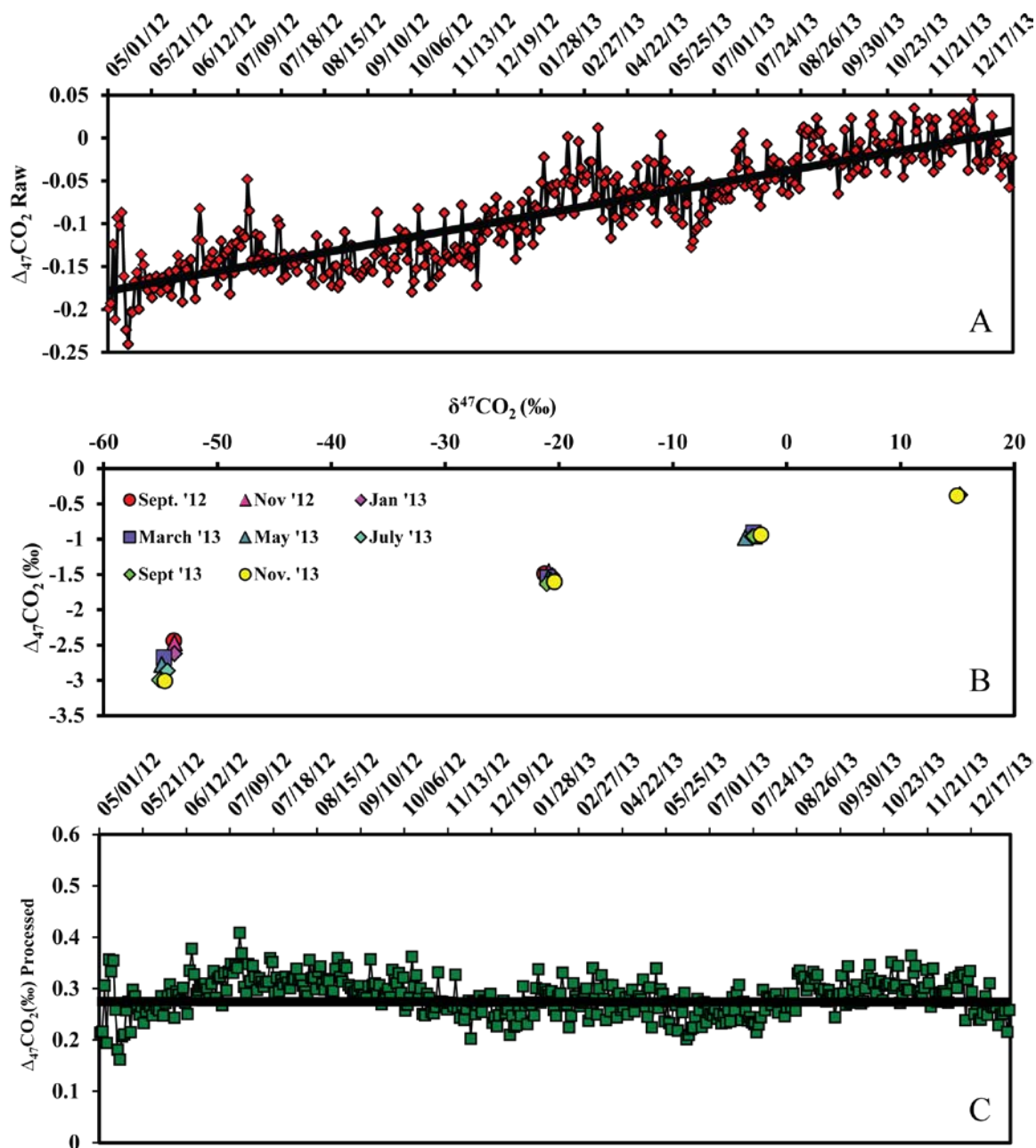
Figure 1.4 - Charts showing the correction of raw Δ_{47} data from the measurement of our Carrara marble standard May, 2012 - December, 2013. A) Raw measured Δ_{47} Carrara showing an increasing trend with time. B) Measured heated gas standard data over the same period of time the Carrara marbles were measured. Some data has been excluded for clarity. There is a decreasing drift in the Δ_{47} of the heated gases. This d rift is used to correct the Carrara Δ_{47}. C) Correct Δ_{47} Carrara values (without acid fractionation) showing the reduction in the increasing Δ_{47} trend seen in panel A after correcting for heated gas drift.

equilibrating gas alone at low temperatures. The CDES framework is developed by measuring the suites of equilibrated waters and heated gases and using their measured Δ_{47} values relative to their expected values as determined in Wang et al. (2004).

The PBL correction takes the CDES one step further by adding an extension to the standard measurement of the peak of the ion beams. To apply the PBL correction, acquisitions are begun and finished with multiple measurements off-peak of the base of the mass 47 peak. In post-processing, these off-peak measurements are used to linearly extrapolate the voltage lost from the on-peak ion beam measurements because of the negative pressure baseline which is then retroactively added back on. This technique has been shown to statistically improve carbonate Δ_{47} measurements over time (Rosenheim et al., 2013).

SIL Clumped Isotope Methods

Sample Preparation and CO_2 Extraction for Common Acid Bath

Whole rock samples were powdered using a Spex SamplePrep Mixer/Mill 8000 or mortar and pestle. Each sample consisted of 8.0 ± 0.2 mg of powder weighed into two K1250A 3.71 mm diameter gas checks plain copper-boats in 4.0 ± 0.1 mg amounts. The sample boats were loaded into a carousel connected to a CAB attached to a stainless-steel line (schematic provided as Figure 1.5). The vacuum line was pumped by two turbo molecular vacuum pumps (Balzer TPU 170 and Edwards 50EX) each protected by molecular sieve foreline traps (Edwards FL20K) and backed by Edwards rotary pumps (E2M2). A dedicated roughing line (Edwards E2M2) with a foreline trap was used for pumping from atmospheric pressures. Typical operating pressure in the main vacuum

line prior to processing was 2 x 10^{-6} mbars. With the exception of the CAB section, which was linked to the main vacuum line using ¼" o.d. stainless steel tubing, the remainder of the vacuum line was constructed of 3/8" stainless steel tubing and Swagelok valves (SS-6BK).

Samples were routinely loaded into the carousel the evening before analysis and evacuated to < 0.0001 mbar overnight using the roughing and turbo molecular pumps. Each sample was then digested in 3.5ml of phosphoric acid (H_3PO_4) which varied in density over the course of this work from 103% to 105%. The time necessary for a complete reaction varied depending on the mineralogy of the sample and temperature of the acid, however, all reactions were allowed to continue until CO_2 bubbles produced during the reaction ceased. While reacting, samples were continuously stirred using a Pyrex™ covered magnetic stir bar in order to encourage digestion and removal of CO_2.

During the reaction, the produced CO_2 was removed and frozen into a U-trap using liquid nitrogen (LN). After the sample had been digested, both the acid bath and the U-trap were isolated and the CO_2 released by replacing the LN with a methanol slush bath (~ -90°C) that stabilizes the temperature to withhold water in a solid phase under vacuum but releases CO_2 gas. The resulting gas pressure was recorded using a capacitance manometer (MKS 220) and then cryogenically transferred to a second U-trap using LN. Once frozen into the trap, any non-condensable gases present were pumped away. During this procedure, a second trap protected the system from any condensable gases possibly back streaming from the vacuum system. The CO_2 was then transferred through a U-trap filled with Porapak™ Type Q 50-80 mesh packing material held at
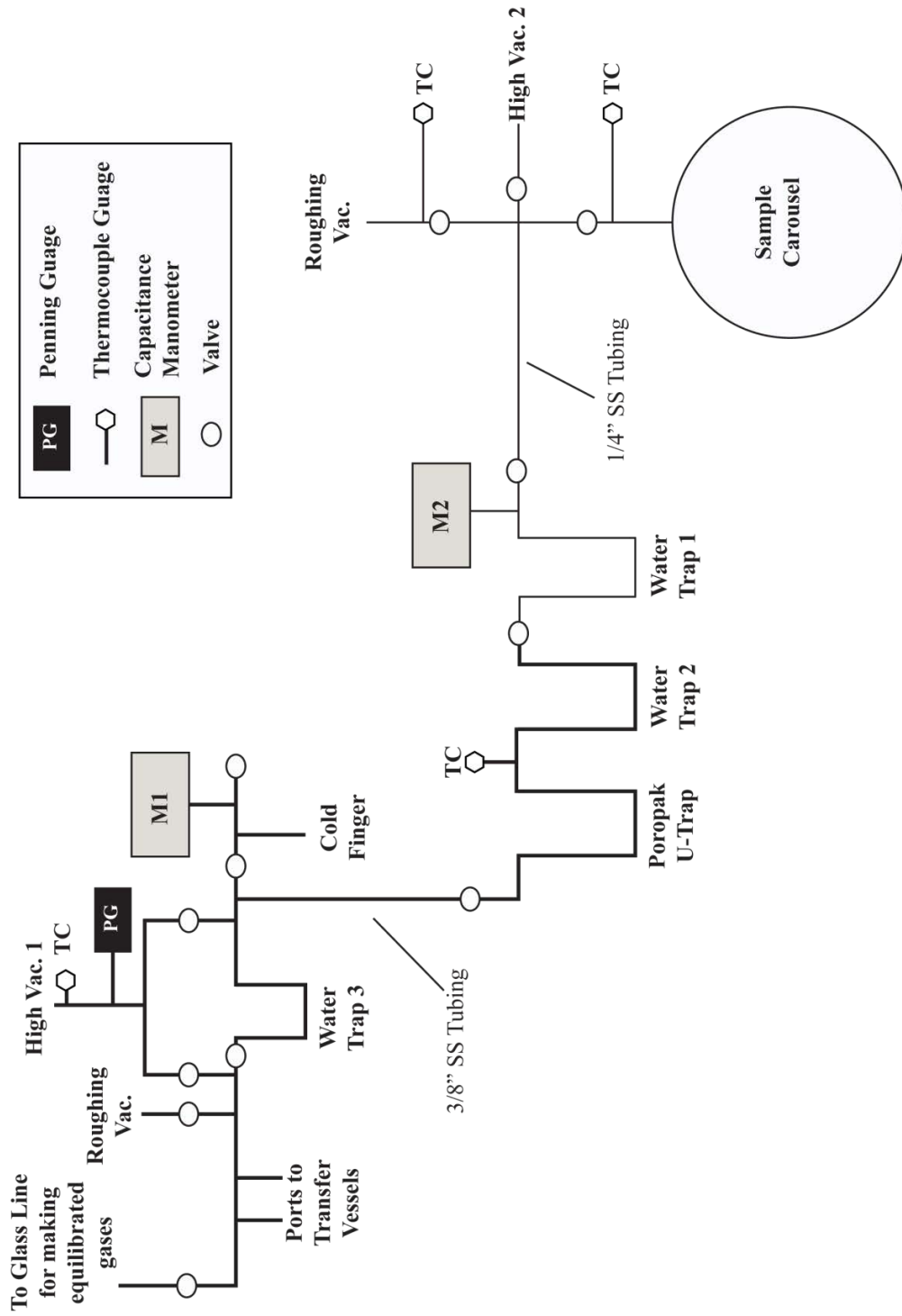
Figure 1.5 - Schematic diagram of the carbonate digestion vacuum-line at the Stable Isotope Laboratory of the Rosenstiel School of Marine and Atmospheric Science

-30.0°C in a methanol bath. This process took between 40 to 45 minutes. Once

completed, the section of the line was isolated and the CO_2 passed through another

methanol trap (-90°C) where the final gas pressure was recorded. The purified CO_2 was

then frozen into a removable glass collection vessel. Before sealing and removal of the

vessel, any non-condensable gas was pumped away, again protected from back streaming

by a methanol trap at -90°C. After vessel removal, the entire line was baked at > 100°C

using nichrome wire (26 gauge) wrapped around the entire stainless steel line and heated

for a minimum of 30 minutes. The Porapak™ trap was heated to +190°C for at least 30

minutes between samples. Before the next sample was digested, the heating wire was

turned off and the entire line allowed to cool to room temperature for ≈10 minutes. Once

cooled, the line was assessed for vacuum pressure and checked to ensure that all systems

had returned to normal before proceeding with the next sample.

Sealed Vessel Reactions

Sealed vessel digestions were performed with 8.0 ± 0.2 mg of sample deposited

into glass tubes sealed at one end. These were placed into a sealed reaction vessel (Ace

Glass valve on a 25 ml pear-shaped vessel) containing 3.0 ml of 103% phosphoric acid

(Figure 1.6). The vessel was then connected to the vacuum line and evacuated overnight.

The following morning, the vessel was sealed, removed from the vacuum line, and then

placed into a water bath held within ±0.5°C of the desired temperature. The acid was

allowed to equilibrate to the temperature of the bath for 24-36 hours and then reacted

with the sample by allowing the acid to run inside the tube resting in the acid. The length

of time samples were allowed to react varied with the temperature of the acid and

Figure 1.6 – Pear-shaped vessel used in both the transferring of sample CO_2 gas from the vacuum line to the mass spectrometer and in all the sealed vessel reactions.

mineralogy. Dolomite samples, because of their slower kinetics during reactions were allowed to react for longer periods of time than calcite and aragonite samples.

After the reaction was complete, the sealed vessel was removed from the water bath and connected to the vacuum line where the CO_2 was removed passing the gas through a methanol trap (-90°C) using LN. The CO_2 was then treated exactly the same as the samples digested using the CAB.

Analytical

The purified CO_2 was measured using a dual-inlet Thermo MAT-253 mass spectrometer. The samples were measured against an in house working-gas that had been cryogenically purified. Each extracted signal was analyzed at a signal intensity of 12V at mass-44. The procedures for a sample run varied over the course of these different studies. Prior to August of 2014, samples processed using the CDES were measured over ten acquisitions of 6 on-peak sample-standard measurements (click-clacks). This procedure was determined to produce the most representative final results while also conserving time. After August of 2014, we developed the use of the PBL method which required a different set of procedures. Samples measured using the PBL were measured over six acquisitions of 15 on-peak click-clacks. Each acquisition was preceded and succeeded by 5 off-peak click-clacks measuring the PBL of the peak. Total run time for non-PBL measurements was typically 2.25 hours and PBL measurements were approximately 3 hours. No statistically significant difference was found between the Δ_{47} values calculated using the CDES or PBL processing techniques. The procedures used on the data presented in this work will be described in each chapter.

Data reduction and normalization for Δ_{47} and temperature calculations followed the methods described in multiple studies (Affek and Eiler, 2006; Huntington et al., 2009). In order to check for contamination, samples were scrutinized based on their offset of δ^{48} and Δ_{48} from that of the standard gases (Huntington et al., 2009).

Heated and Water Equilibrated Gases

In compliance with standard clumped isotope methodology, a suite of heated and water equilibrated gases were routinely processed on a monthly basis. This procedure accounted for the natural drift in Δ_{47} measurements over time and allowed the data to be placed into the CDES. Both heated and water equilibrated gases were composed of our three in house tank CO_2 gases with a range of $\delta^{13}C$ and $\delta^{18}O$ values that are held in sealed bulbs (2000 cm^3) at atmospheric pressure attached to our processing line. Prior to being placed in the bulbs, the gases were cleaned by passing them through traps to remove H_2O and cryogenically cleaned to remove any non-condensable gases.

A heated gas consisted of an aliquot of a tank gas that had been passed through the Poropak™ in the same cleaning procedures as our samples before it was frozen into a quartz tube and sealed with a gas torch. The sealed tube was then placed in a furnace at 1000°C for over two hours then transferred to the MAT-253 mass spectrometer. The transfer time was often immediate, but never more than 24 hours after being removed from the furnace. The tube was then manually cracked allowing the gas to enter the dual inlet. All three tank gases were treated to this procedure with every measurement of heated gases.

The water-equilibrated gases consisted of the same three tank gases as the heated gases frozen into Pyrex™-tubes with 350µl of deionized (DI) water. The tubes were

sealed with a gas torch and placed in either a 25.0°C ± 1.0°C or 50.0°C ± 1.0°C temperature controlled water bath for at least four days. The tubes were then transferred to the processing line where the gas was separated from the water and then passed through a Poropak™-trap following the same cleaning procedures used for carbonate samples before being measured on the MAT-253. The combination of measurements of heated gases and the pair of water equilibrated gases allowed the data to be placed into the CDES (Dennis et al., 2011). All heated gases and equilibrated waters measured during this investigation can be found in the supplementary material (Table S.1)

In order to account for any changes in the mass spectrometer between equilibrated gas measurements, a carbonate standard Carrara marble was measured daily prior to any samples being digested except on days where the temperature of the acid was below 90°C. If any significant variability in the Δ_{47} of the Carrara value was noticed, a new suite of heated and water equilibrated gases were immediately measured.

Some samples in this study had δ^{47} values that exceeded those possessed by the equilibrated gases used in the CDES. This could potentially have produced error associated with the extrapolation of the equilibrated gas lines to higher δ^{47} values. The effect of the extrapolation was shown to produce errors on the final processed Δ_{47} on the order of ±0.04‰. This error is taken into account for any samples measured prior to August, 2013 when an additional heated gas with a δ^{47} more similar to the carbonates being measured was introduced. Once the additional equilibrated gas was added, the associated error from extrapolating the standard gas line was reduced to an insignificant effect on the final Δ_{47} value. It is therefore concluded that this has little influence on the end results of this work.

Isotopes

The $\delta^{13}C$ and $\delta^{18}O$ values were generated simultaneously by measuring masses 45/44 and 46/44 and then correcting for the usual isobaric interferences using a method adapted from Craig (1957) and modified for a multi-collector mass spectrometer. The $\delta^{13}C$ and $\delta^{18}O$ values of the standard gas were calibrated using NBS-19 and data reported relative to Vienna Pee Dee Belemnite (V-PDB). A constant correction of 1.008 was applied to the $\delta^{18}O$ values to account for the differential fractionation of CO_2 produced from dolomite as opposed to calcite during the dissolution in phosphoric acid at 90°C (Land, 1980; Sharma and Clayton, 1965; Vahrenkamp and Swart, 1994). This value could possibly vary between CAB and SV methods as shown for calcite in Swart et al. (1991), but this has not yet been experimentally determined for dolomites.

The Δ_{47} was calculated using the approach outlined in Huntington et al. (2009) and translated into CDES using the methods outlined by Dennis et al. (2011) paired with the 1000°C heated gases and 50°C and 25°C water equilibrated gases. Final Δ_{47} values before application of acid digestion temperature fractionation was determined using linear interpolation between the measurements of standard gases. As no dolomite-based Δ_{47}-temperature calibration has been published in the literature, temperatures for dolomite samples were calculated using CDES converted versions of the calcite and aragonite based Δ_{47}-temperature calibrations utilized in previously published studies (Ghosh et al., 2006; Passey and Henkes, 2012) as well as the dolomite-based theoretical calibration of Guo et al. (2009). Conversion of calibrations into the CDES reference frame were performed using the guidelines described in (Dennis et al., 2011)

X-ray Diffraction and Stoichiometry

The stoichiometry of the dolomites were determined using the method of Lumsden and Chimahusky (1980). In this technique a powdered sample spiked with sylvite (KCl) as an internal standard was analyzed using X-ray diffraction (Panalytical X-pert pro) to determine the precise position of the 104 peak. The corrected d-spacing of this peak was then used to calculate the mol % $CaCO_3$ in the dolomite crystal lattice (N) using equation 1.2:

$$N_{CaCO_3} = Md + B \qquad (1.2)$$

where *d* is the d-spacing of the dolomite, M is 333.33, and B is -911.99 9 (Table 1).

Focus of this work

The chapters to follow will illuminate the application of the clumped isotope technique to dolomites, with a particular focus on dolomites formed in different environments throughout the Bahamas archipelago. The Bahamian archipelago is located about 80 km off the east coast of Florida. The archipelago is composed of a series of shallow-water carbonate platforms which are separated by deep seaways. The nucleus of the various platforms are basement blocks that formed during the opening of the Atlantic and were reactivated during the Cuban orogeny (Masaferro and Eberli, 1999) However for the last 300,000 years, the Bahamas have been tectonically stable (Carew and Mylroie, 1995; Hearty and Kindler, 1995). Seismic data collected from the locations of a multitude of cores drilled in the Bahamas suggests that abundant carbonate precipitation eventually lead to the coalescence of various platforms through extensive progradation which accounts for the present day platform configurations (Eberli and Ginsburg, 1987, 1989). The platforms are

pockmarked by a multitude of Holocene islands which are composed of lithified Pleistocene sands and reefal materials derived during marine high stands (Conrad Neumann and Hearty, 1996; Meyerhoff and Hatten, 1974; Schlager et al., 1985).

Sea level change and the composition of Bahamian platforms are intricately linked as fluctuations throughout the Tertiary have exposed and submerged extensive regions of the platform subjecting the platforms to a variety of diagenetic environments in the seawater realm. The bulk of the sediments that compose the Bahamian platforms are locally derived aragonite precipitation from a variety of organic sources as well as some inorganic precipitation. However through meteoric, mixing zone, and burial diagenesis, a portion of the platforms have been altered to LMC and dolomite (Melim et al., 2004; Swart and Melim, 2000). The LMC varies isotopically from negative to positive suggesting influence from meteoric/mixing zone and sea water respectively. The dolomite tends to only exist below the mixing zone, suggesting the majority of dolomite in the Bahamas formed through suggested seawater dolomitization processes such as Kohout convection (Dawans and Swart, 1988; Melim et al., 2004; Swart and Melim, 2000; Swart et al., 1987). However, most likely associated with sea level change, dolomitization appears to have occurred in multiple stages (Vahrenkamp et al., 1991). There is mention of baroque (saddle) type dolomites in the shallow depths of a core on the southern island of Great Inagua (Pierson, 1982) which are commonly associated with, but not necessarily confirmation of, hydrothermal fluids. No further studies have been conducted on those samples to determine if they actually formed from hydrothermal fluids

Tectonically, the Bahamas has been stable for the past 300,000 years (Carew and Mylroie, 1995; Hearty and Kindler, 1995), with a uniform subsidence rate of 1-2 m per 100,000 years as indicated by the presence of corals which formed above present day sea level during marine isotope stage 5e (MIS 5e) (Carew and Mylroie, 1995; Chen et al., 1991). This would imply that there is little concern for interaction of hydrothermally heated fluids associated with tectonic activity. Because of the tectonic stability of the region with little other known influences on seawater temperature that occur in the Bahamas as well as the young tertiary age of the dolomites being examined in this study, then sea level and its change over time is the largest contributing factor influencing dolomite formation and thusly the clumped isotope values.

Because of the unsettled debate on dolomite formation, aptly called the "dolomite problem" (discussed throughout), the Bahamas offers a unique opportunity for the application of clumped isotopes as the dolomite here have formed in a narrow range of temperatures dictated solely by their depth below the sea surface. On top of that, the many dolomites in the Bahamas show an incredible maturity and high degree of stoichiometry which is comparable to ancient dolomites though most have formed only within the last 5 million years. This makes the dolomites more comparable to ancient dolomites while also limiting the range of influences on the dolomitization process allowing for the constraining of possible formation fluids and temperatures. We hope to take advantage of this unique set of circumstances and use this new technique to help elucidate a dolomite problem.

Chapter 2 – Δ_{47} Phosphoric Acid Fractionation in Carbonates

This chapter is a modified version of a paper published in Geochimica et Cosmochimica Acta titled "Determining the Δ_{47} acid fractionation in dolomites" by Murray et al. (2016). The following contains additional data not published in the original paper with regards to sealed vessel reactions and a measurement of the acid fractionation in aragonite.

Background

The relationship between Δ_{47} and temperature has been determined through a series of calibration studies on materials with known or well constrained temperatures of formation. Calibrations have utilized synthetic calcites (Dennis and Schrag, 2010; Fernandez et al., 2014; Ghosh et al., 2006; Zaarur et al., 2013), naturally produced carbonates (Affek et al., 2008; Came et al., 2007; Ferry et al., 2011; Ghosh et al., 2007; Henkes et al., 2013; Wacker et al., 2014), and theoretical models (Guo et al., 2009; Yuan et al., 2014). To date, there is no Δ_{47}-temperature calibration specifically developed for dolomites using measured samples, the closest being a theoretical calibration proposed by Guo et al. (2009) or a pair of measurements on dolomites formed at approximated temperatures used by Ferry et al. (2011). There is an oft-referenced calibration attributed to Bonifacie et al. (2011), however at the time of writing this dissertation, it has yet to be published in the peer-reviewed literature.

As the initial clumped isotope studies used an acid temperature of 25°C (Affek et al., 2008; Came et al., 2007; Ghosh et al., 2006; Ghosh et al., 2007; Guo and Eiler, 2007), carbonate Δ_{47}-temperature calibrations are by convention normalized to this temperature. This is despite the fact that a majority of clumped-isotope laboratories now react their samples at higher temperatures, typically at 70°C in a Kiel device or at 90°C in a

common acid bath (CAB). The benefit of a higher reaction temperature is that the amount of time required to completely react a sample is significantly reduced. Considering that typical sample sizes for clumped isotopes already approximate 5-10 mg, decreasing the reaction time is almost as much a necessity as it is a matter of convenience, especially when considering the slower reaction kinetics associated with digesting dolomites. Whereas a calcite digested at 25°C would require approximately 18 to 36 hours to fully react (Ghosh et al., 2006; Wacker et al., 2013), an equivalently sized dolomite might require 5 to 7 days (Defliese et al., 2015). The increased reaction times are a result of decreased acid temperature, and the extending timeframe for complete reaction may introduce errors through a number of different mechanisms including: 1) the extended periods of time with which the evolved CO_2 may interact with the phosphoric acid and water produced during the reaction, 2) crystallization of the high density phosphoric acid under vacuum, and 3) possible atmospheric leaks associated with the seals on the vessel containing the reacting sample.

Reacting samples at temperatures greater than 25°C causes a fractionation of the oxygen isotopes which has a measureable effect on the $\delta^{18}O$ and Δ_{47} values. In order to relate samples reacted at different temperatures, these fractionations must be accurately known. Temperature dependent fractionation of $\delta^{18}O$ value during the digestion of carbonates has been discussed in numerous studies (Kim et al., 2007; Kim and O'Neil, 1997; Land, 1980; Rosenbaum and Sheppard, 1986; Sharma and Clayton, 1965; Swart et al., 1991). For calcite, these studies show an approximate 0.012‰ decrease in the $\delta^{18}O$ value for every increase of 1°C in reaction temperature so that CO_2 released at 90°C is approximately 0.8‰ more negative in the $\delta^{18}O$ value than at 25°C. In addition, samples

prepared using the sealed vessel (SV) method appear to be consistently depleted in the heavier isotopes relative to those prepared using a CAB method (Swart et al., 1991). To our knowledge, there have been no studies documenting differences in the reaction temperature dependent fractionation between dolomite and calcite.

Multiple studies have reported differences in Δ_{47} fractionation between calcite or aragonite digested at 90 and 25°C ($\Delta_{47\ 90-25}$). These values range between 0.069‰ (Guo et al., 2009) and 0.081‰ (Passey et al., 2010) in the original Ghosh et al. (2006) reference frame, and 0.092‰ (Henkes et al., 2013), 0.07‰ (Wacker et al., 2013), and 0.082‰ (Defliese et al., 2015) in the Dennis et al. (2011) absolute reference framework (ARF) in the CDES. However, there has been only one published study on the $\Delta_{47\ 90-25}$ of dolomite (Defliese et al., 2015). This is despite the fact that numerous papers have reported clumped isotope data on dolomitized samples (Dale et al., 2014; Defliese et al., 2015; Ferry et al., 2011; Lechler et al., 2012; Loyd et al., 2012; Sena et al., 2014; Swanson et al., 2012; Van De Velde et al., 2013). All of these papers employed $\Delta_{47\ 90-25}$ values similar to that of calcite and aragonite assuming that the value is the same for dolomite. This assumption was examined in Defliese et al. (2015) using a single dolomite sample, National Institute of Standard and Technologies (NIST) dolomite 88b. The conclusion of Defliese et al. (2015) was that dolomite displayed a similar fractionation to calcite and aragonite with a value of 0.082‰.

In this chapter, the temperature dependent fractionation $\Delta_{47\ 90-25}$ value has been reexamined using five different dolomites ranging in chemical composition from $Ca_{0.56}Mg_{0.44}(CO_3)_2$ to $Ca_{0.50}Mg_{0.50}(CO_3)_2$ as well as in two calcite and two aragonite samples.

Samples

All samples were reacted using the CAB method. In addition, a single calcite, aragonite, and dolomite sample were digested over a range of acid temperatures using the SV method. The calcites included a Carrara marble, used by most laboratories as a carbonate standard for clumped isotopes, and a Cretaceous chalk (ETH-3) from Northern Germany which had been made available to the clumped isotope community to facilitate interlaboratory comparison by the clumped isotope laboratory of Eidgenössische Technische Hochschule (ETH), Zürich. The aragonites were from two modern aged coral specimens formed in the Caribbean.

The dolomite samples used in this study were chosen to exhibit a range of Mg and Ca concentrations. The NIST 88b sample, the same as analyzed by Defliese et al. (2015), is a stoichiometric dolomite ($Ca_{0.50}Mg_{0.50}(CO_3)$) sourced from the Galena-Platteville Groups in Skokie, Illinois. The second dolomite (ME-1) is of Jurassic age and also has a near stoichiometric composition ($Ca_{0.51}Mg_{0.49}(CO_3)$). It is believed to have formed from higher temperature fluids than any of the other dolomites in this study. The last three dolomites were all derived from various depths in a 168 m deep core from the island of San Salvador, Bahamas that penetrated Pleistocene to Miocene aged sediments. These possess varying Mg/Ca ratios with two being calcian ($Ca_{0.56}Mg_{0.44}(CO_3)$) and the third being of near stoichiometric composition ($Ca_{0.50}Mg_{0.50}(CO_3)$).

In order to validate the fractionation factors determined in this study, the series of Δ_{47} measurements from the San Salvador samples were converted to temperature using various Δ_{47}-temperature calibrations because these samples are known to have formed in a restricted environment. Based on $^{87}Sr/^{86}Sr$ ratios and U-Th dating, the age of

dolomitization of the San Salvador samples has been constrained to between 150 ka and 500 ka (Swart et al., 1987; Vahrenkamp et al., 1991). Their formation was attributed to either Kohout convection (Kohout, 1967; Simms, 1984) or as a result of movement of seawater associated with the discharge of freshwater through the mixing zone (Vahrenkamp and Swart, 1994). Hence it was concluded that these dolomites formed from normal seawater at near-surface temperatures (Dawans and Swart, 1988; McNeill et al., 1988; Supko, 1970, 1977; Swart et al., 1987; Vahrenkamp et al., 1991) .

Methods

Sample Reactions

       Samples were digested using both the SV and CAB methods as described in chapter one. The time necessary for the reaction varied depending on the mineralogy and temperature, however, all reactions were allowed to continue until CO_2 bubbles produced during the reaction ceased. All samples used in the CAB fractionation study were digested at 90°C, 75°C, and 50°C, while some were also digested at 60°C and 35°C. The digestion time was extended with decreasing temperatures. For the calcites and aragonites, reactions continued for 30 minutes, 60 minutes, 2 hours, 3 hours, and 4 hours for 90°C, 75°C, 60°C, 50°C, and 35°C digestions respectively. For dolomites, these times were extended to 45 minutes, 2 hours, 3.5 hours, 7 hours, and 15 hours for the same respective temperatures. For lower temperature CAB reactions, the water bath used to maintain acid temperature was allowed to heat the acid overnight prior to the first sample being digested in order to ensure the oxygen atoms within the molecular structure of the acid had reached equilibrium with the set temperature.

Temperature Dependent Acid Fractionation

Previously published methods for measuring Δ_{47} temperature dependent acid fractionation used a combination of the CAB and SV methods (Defliese et al., 2015; Henkes et al., 2013; Wacker et al., 2013). Samples reacted at higher temperatures used a CAB, while those reacted at 25°C employed the SV. The SV method was necessary for dolomite reactions at 25°C as a result of the lengthy time required for complete reactions. However, because the work of Swart et al. (1991) identified significant differences in the fractionation of the $\delta^{18}O$ value between the SV and CAB methods, the possibility arises that the type of method may also influence the Δ_{47} value. In order to address this possibility, we measured a full suite of digestion temperatures using both techniques for the NIST 88b dolomite, the Carrara marble, and the aragonite grind samples.

The $\Delta_{47\,90\text{-}25}$ fractionation was determined using a weighted least-squares regression through the measured Δ_{47} values of each individual digestion and extrapolation of the best-fit line to 25°C with error determined on a 2-tailed t-distribution with n-2 degrees of freedom corresponding to a 68% confidence interval correlating to ±1 standard deviation. The reported $\Delta_{47\,90\text{-}25}$ value is based on subtracting the 90°C value on the regression line from the 25°C value and does not take into account the 0.268‰ theoretically determined fractionation of Δ_{47} at 25°C because this value was determined for calcite and is not necessarily the same for dolomite (Guo et al., 2009; Passey and Henkes, 2012). In the cases where samples were measured using both the SV and CAB extractions, results have been considered both separately and together.

Dolomite stoichiometry was measured and calculated using the XRD methodology described in Chapter 1 (Table 2.1).

Table 2.1 - X-ray diffraction d-space and calculated % $MgCO_3$

Sample I.D.	SS212.0	SS381.5	SS424.9	ME-1	NIST 88b
Sylvite d-space measured	3.149	3.146	3.145	3.146	3.143
Dolomite d-space measured	2.888	2.904	2.904	2.889	2.884
Calculated Mole % $MgCO_3$	50	44	44	49	50

Results

Acid Fractionation

The acid fractionation results are summarized in Table 2.2 and Figure 2.1. The dolomite Δ_{47} fractionation values ($\Delta_{47\ 90\text{-}25}$) ranged from +0.163‰ to +0.137‰ using the CDES reference frame with an average value for all the dolomite samples of +0.153 ± 0.011‰ (±1σ S.D.). The calcite and aragonite fractionations were statistically different in the CDES reference frame than the dolomite fractionation with average $\Delta_{47\ 90\text{-}25}$ values of +0.089 ± 0.013‰ and +0.091 ± 0.026‰ respectively. The fractionation at any digestion temperature between 90°C and 25°C based on our results can be calculated by equation 4-6:

$$\text{Dolomite: } 1000 \ln \alpha_{\text{Reaction T-25}} = \frac{0.041757(\pm 0.011195) \times 10^6}{T^2} - 0.469746\ (\pm 0.034347) \qquad (2.1)$$

$$\text{Calcite: } \quad 1000 \ln \alpha_{\text{Reaction T-25}} = \frac{0.0243974(\pm 0.013178) \times 10^6}{T^2} - 0.274458\ (\pm 0.040431) \qquad (2.2)$$

$$\text{Aragonite: } 1000 \ln \alpha_{\text{Reaction T-25}} = \frac{0.024784(\pm 0.003490) \times 10^6}{T^2} - 0.278811\ (\pm 0.078517) \qquad (2.3)$$

where α is the Δ_{47} fractionation factor and T is the temperature of reaction in degrees Kelvin and errors are ± 1 standard deviation.

In all three cases of S.V. extractions, the calculated $\Delta_{47\ 90\text{-}25}$ differed from the C.A.B. value although the samples are considered identical. However, the difference was neither consistent nor statistically significant which leads us to conclude that any difference between the two methods is either non-existent or currently unresolvable and the application of the results should be treated as such.
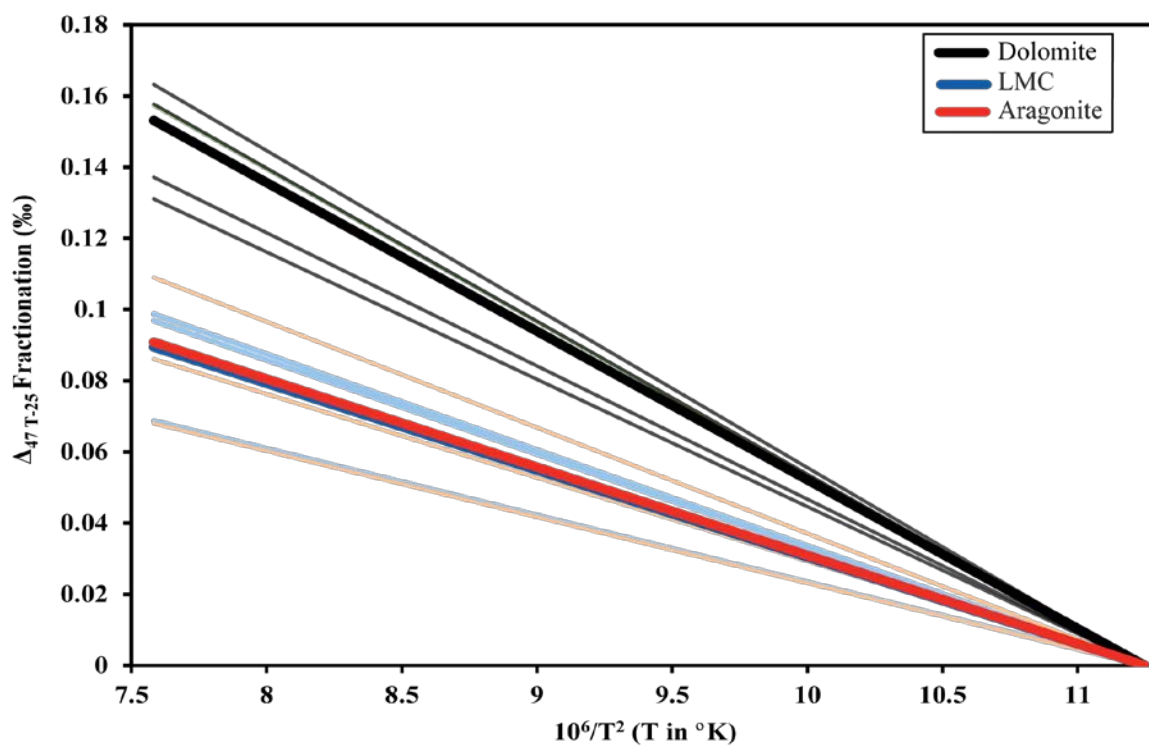
Fig 2.1 - Graphical representation of the Δ_{47} acid digestion fractionation between 90 °C and 25 °C. Bold lines are the average value for the mineralogy type. The faded lines are the individual samples. Image shows that dolomites behave significantly different than both low-mg calcite (LMC) and aragonite with respect to the fractionation in Δ_{47}.

Table 2.2 - Average acid fractionation results for varying mineralogies

Sample I.D.	Method of Digestion	Mineralogy	Δ47 (ETF)[b] 90°C React. (‰)	Δ47 (ETF)[b] 75°C React. (‰)	Δ47 (ETF)[b] 60°C React. (‰)	Δ47 (ETF)[b] 50°C React. (‰)	Δ47 (ETF)[b] 35°C React. (‰)	Δ47 (ETF)[b] 25°C React. (‰)	Weighted Slope m	Weighted Intercept b	90°C Extrapolation (‰)	25°C Extrapolation[c] (‰)	± 1 S.D. (‰)	Acid Correction (‰)
SS212.0	C. A. B.	Dolomite	0.521	0.516	-	0.588	0.660	-	0.043	0.180	0.506	0.663	0.031	0.157
SS381.5	C. A. B.	Dolomite	0.518	0.566	-	0.600	-	-	0.045	0.180	0.518	0.681	0.028	0.163
SS424.9	C. A. B.	Dolomite	0.504	0.544	-	0.590	-	-	0.043	0.182	0.508	0.665	0.029	0.158
ME-1	C. A. B.	Dolomite	0.454	0.447	-	0.540	-	-	0.042	0.129	0.445	0.598	0.038	0.153
NIST88b	C. A. B.	Dolomite	0.529	0.537	0.585	0.591	0.637	-	0.036	0.253	0.524	0.655	0.011	0.131
NIST88b	S. V.	Dolomite	0.529	-	-	0.583	-	0.668	0.037	0.240	0.524	0.661	0.032	0.137
NIST88b[a]	C. A. B. & S.V.	Dolomite	0.529	0.537	0.585	0.589	0.637	0.668	0.037	0.246	0.523	0.657	0.007	0.134
												Dolomite Average:	1σ S.D.	0.153 0.011
Cararra	C. A. B.	Calcite	0.294	0.305	-	0.313	0.365	-	0.019	0.154	0.296	0.365	0.032	0.069
Cararra	S. V.	Calcite	0.310	-	-	0.379	-	0.399	0.026	0.111	0.311	0.408	0.025	0.097
Cararra[a]	C. A. B. & S.V.	Calcite	0.300	0.305	-	0.332	0.365	0.399	0.022	0.130	0.295	0.376	0.015	0.080
ETH-3	C. A. B.	Calcite	0.594	0.626	-	0.649	-	-	0.027	0.394	0.598	0.697	0.013	0.099
												Calcite Average:	1σ S.D.	0.089 0.013
Aragonite Coral	C. A. B.	Aragonite	0.587	0.627	-	0.648	-	-	0.030	0.370	0.595	0.704	0.037	0.109
Aragonite Grind	C. A. B.	Aragonite	0.638	0.669	-	0.688	0.711	-	0.023	0.464	0.643	0.729	0.013	0.086
Aragonite Grind	S. V.	Aragonite	0.666	-	-	0.684	-	0.747	0.019	0.523	0.664	0.732	0.012	0.068
Aragonite Grind[a]	C. A. B. & S.V.	Aragonite	0.656	0.669	-	0.686	0.711	0.747	0.020	0.504	0.654	0.727	0.009	0.073
												Aragonite Average:	1σ S.D.	0.091 0.026

a : Associated data is a combination of both common acid bath and sealed vessel measurements

b : Δ47 values are in the Dennis et al. (2011) reference frame. Dashes indicate no measured data.

c : Extrapolated values based on the fitting of a weighted least squared regression through all data points measured for the particular sample. Associated standard deviation is based on a 2-tailed t-distribution with n-2 degrees of freedom using a 68% confidence interval.

San Salvador Dolomites

Temperatures calculated for the dolomite samples from San Salvador using acid fractionation corrections of +0.082‰ and +0.153‰, with commonly used Δ_{47}-temperature calibrations for dolomites converted into the CDES (Ghosh et al., 2006; Guo et al., 2009; Passey and Henkes, 2012), are presented in Table 2.3. Temperatures calculated using an acid correction of +0.082‰ range from 50°C to 68°C and temperatures using an acid correction of +0.153‰ range from 30 to 38°C.

Dolomite Stoichiometry

An inverse correlation was found to exist between the Δ_{47} and concentration of Mg within the dolomites. A Spearman's rank correlation coefficient returned a ρ value of -0.60, which is not statistically significant at the 95% confidence limits ($p = 0.28$). The absence of any correlation may be real or may be a result of the relatively small sample size ($n = 5$).

Discussion

Acid Fractionation and Application to San Salvador

Previous work has suggested that the San Salvador dolomites formed at normal sea water temperatures ($\approx 25°C$) and from fluids similar to seawater (Dawans and Swart, 1988; McNeill et al., 1988; Supko, 1970, 1977; Swart et al., 1987; Vahrenkamp et al., 1991). However, calculating temperatures from Δ_{47} values with an applied $\Delta_{47\,90\text{-}25}$ of +0.082‰ as proposed by Defliese et al. (2015) produced temperatures that were too warm and unrealistic for the Bahamas regardless of which Δ_{47}-temperature calibration is used (Table 2.3). An explanation of these high temperatures would require unreasonable

geologic processes or undocumented influences on clumped isotope measurements. Using the measured average $\Delta_{47\ 90-25}$ of +0.153‰ as measured in this work, the calculated temperatures fell to within acceptable ranges that agree with previously discussed models of San Salvador formation (Dawans and Swart, 1988; Supko, 1970, 1977; Swart et al., 1987; Vahrenkamp et al., 1991).

Combining these lower temperatures with the $\delta^{18}O_{fluid-dolomite}$ value equation of Fritz and Smith (1970) provided estimates of the $\delta^{18}O_{fluid}$ value between 0.1‰ and 3.5‰. Such values are suggestive of formation by normal seawater to slightly evaporated marine waters which are consistent with previous models of formation. In contrast, using the +0.082‰ acid correction results in $\delta^{18}O_{fluid}$ values that are between 3.3‰ and 6.6‰. In order to produce such dolomites, an extensive and highly evaporated water source would have to have been present in the Bahamas. Based on our current knowledge of the climate and hydrology of the Bahamas, such values seem unrealistic.

Application of New Δ_{47} Fractionation Value to Previous Works

Several previously published studies which have measured the Δ_{47} values of dolomites have reported that calculated temperatures using various calcite based Δ_{47}-temperature calibrations were warmer than expected compared to temperatures produced from other paleoproxies. For example, Loyd et al. (2012) measured dolomites in concretions collected from the Miocene aged Monterey Formation and found that dolomites yielded temperatures up to 9.6°C warmer than values estimated using the $\delta^{18}O$ carbonate-water paleothermometer. In another study, Van De Velde et al. (2013) investigated dolomitic paleosol nodules from the Paleocene-Eocene boundary in central Utah. When compared to paleofloral studies from the same region and time period (Wilf,

2000), clumped isotope temperatures were 10 to 20°C warmer and did not faithfully reproduce mean summer air temperature and pore water fluid composition. In a third example, Lechler et al. (2012) measured a single dolomite sample associated with calcitic micrites from the Basin and Range Province of western North America. The dolomite produced a Δ_{47} temperature which was 10°C higher than associated calcites.

Both Loyd et al. (2012) and Van De Velde et al. (2013) invoked a range of explanations in order to account for the discrepancies in the temperatures calculated from Δ_{47} values (a combination of exposure to higher than known temperatures and diagenetic processes). Lechler et al. (2012) on the other hand resolved their discrepancy by invoking a 7.2°C difference in their averaged Δ_{47}-temperature value for the sample citing the difference in Δ_{47}-temperature response between calcite and dolomite predicted in Guo et al. (2009). The anomalies in all of these studies would be significantly reduced using the fractionation factor proposed here.

Applying the 0.153‰ acid fractionation with the same Δ_{47}–temperature equations utilized in the original studies, the temperature of the dolomite determined by Lechler et al. (2012) would be 23°C using eq. 9 of Dennis et al. (2011), similar to that obtained from calcitic micrites at the same location. The dolomite samples of Van De Velde et al. (2013) would yield temperatures of 11 to 25°C using the dolomite calibration of Guo et al. (2009). This range of temperatures is in good agreement with estimates of the temperature from the same sample location using paleofloral data (Wilf, 2000). Only the data of Loyd et al. (2012) shows continued disagreement with their proposed model as their temperatures would be between 10 and 20°C using the formula eq. 9 from

Table 2.3 - Calculated temperatures of San Salvador dolomites

Sample I.D.	Acid Correction	Δ_{47} (ARF)	Ghosh et al. (2006)[a]	Guo et al. (2009)[b]	Passey and Henkes (2012)
	(‰)	(‰), ± 1. s.e.	(°C)	(°C)	(°C)
SS212.0	0.082	0.603 ± 0.006	50	60	59
SS381.5	0.082	0.600 ± 0.013	51	62	60
SS424.9	0.082	0.586 ± 0.003	55	68	67
	Average	0.596 ± 0.009	52	63	62
SS212.0	0.153	0.674 ± 0.006	33	33	30
SS381.5	0.153	0.671 ± 0.013	34	34	31
SS424.9	0.153	0.657 ± 0.003	37	38	36
	Average	0.667 ± 0.009	34	35	33

[a] Indicates the equation of Ghosh et al. (2006) in the absolute reference frame as described in equations 9 of Dennis et al. (2011)

[b] Indicates equation 20 of Guo et al. (2009). Newly calculated temperatures are calculated using the same equation placed into the absolute reference frame using a tertiary reference frame with a measured Δ_{47} value of 0.334‰ (Guo et al., 2009) relative to an accepted value of 0.392‰ (Dennis et al., 2011).

Table 2.4. - $\Delta_{47\ T-25}$ measurement on previous dolomite studies

Original Work	Sample ID	Original Δ_{47} (‰)	Formula used	Reported Temperature (°C)	New Δ_{47} (‰)	New Temperature (°C)
Lechler et al. (2012)	10SP02	0.666	Ghosh et al. (2006)[a]/Dennis et al. (2011)[a]	35 / 38	0.724	22 / 16
Loyd et al. (2012)	MSCP-1	0.673	Ghosh et al. (2006)[a]	33	0.734	20
	MSC-3	0.706		26	0.767	14
	MMC8-RB	0.723		23	0.784	11
	MMC9-M	0.689		30	0.750	17
Van De Velde et al. (2013)	NH060110	0.66	Guo et al. (2009)[b]	27	0.732	15
	NH060113	0.624		39	0.696	25
	NH060114	0.674		22	0.746	11
Sena et al. (2014)	E36	0.623	Ghosh et al. (2006)[a]	45	0.695	28
	G5	0.621		46	0.693	29
	I4	0.628		44	0.700	27
Dale et al. (2014)	PC10B6	0.631	Passey and Henkes (2012)	43	0.715	14
	PC10D5	0.62		48	0.704	17
	PC10G5	0.608		53	0.692	21
	PC13 B2	0.595		58	0.679	25
	PC13 B3	0.612		51	0.696	20
	PC13 B4	0.664		31	0.748	4
	PC13 B6	0.626		45	0.710	15
	PC12 E1	0.573		68	0.657	33
	PC12 E4	0.666		30	0.750	3

New temperatures were calculated using the same formulas as in the original work. Original Δ_{47} values had the acid fractionation applied in the original work removed prior to adding a fractionation of 0.153‰ to produce the New Δ_{47}.
[a] Referenced formulas of Ghosh et al. (2006) and Dennis et al. (2011) indicate the equations of Ghosh et al. (2006) and Dennis and Schrag (2010) in the absolute reference frame as described in equations 9 and 10 of Dennis et al. (2011)
[b] Indicates equation 20 of Guo et al. (2009). Newly calculated temperatures are calculated using the same equation placed into the absolute reference frame using a tertiary reference frame with a measured Δ_{47} value of 0.334 (Guo et al., 2009) relative to an accepted value of 0.392 (Dennis et al., 2011).

Dennis et al. (2011). This range of clumped isotope temperatures is lower than temperatures obtained from the $\delta^{18}O_{fluid}$-carbonate paleothermometer using the same data. This could be a consequence of an incorrect estimate of the pore water composition used to calculate temperature from the $\delta^{18}O$ value of the dolomite, error in the $\delta^{18}O_{fluid}$-carbonate paleothermometer itself, or an influence of stoichiometry on the applied acid fractionation. These results can be seen in Table 2.4 along with results from other previously published dolomite clumped isotope studies.

Dolomite Stoichiometry and Acid Fractionation

The dolomites measured in this study produce an acid fractionation that decreases with increasing Mg in the crystal structure (Figure 2.2). While not statistically significant, this trend is counterintuitive considering that all reported calcite Δ_{47} acid fractionations are less than for dolomite (Defliese et al., 2015; Guo et al., 2009; Henkes et al., 2013; Passey et al., 2010; Wacker et al., 2013). It is expected that if the fractionation varies, it would become more positive with increasing mol % $MgCO_3$, similar to the 0.0375‰ increase seen in the $\delta^{18}O$ value for every mol % increase in $MgCO_3$ shown by Vahrenkamp and Swart (1994).

Conflicting Dolomite Δ_{47} Fractionation Values

A discrepancy that needs to be addressed is the difference in the reported $\Delta_{47\,90\text{-}25}$ for sample NIST 88b in this study and that measured by Defliese et al. (2015). Both studies report nearly identical average values for Δ_{47} measured at 90°C (0.524 ± 0.013‰ in Defliese et al. (2015), 0.529 ± 0.011‰ in this work) suggesting good agreement between results. However, there is an almost 0.06‰ difference in the reported Δ_{47} of the
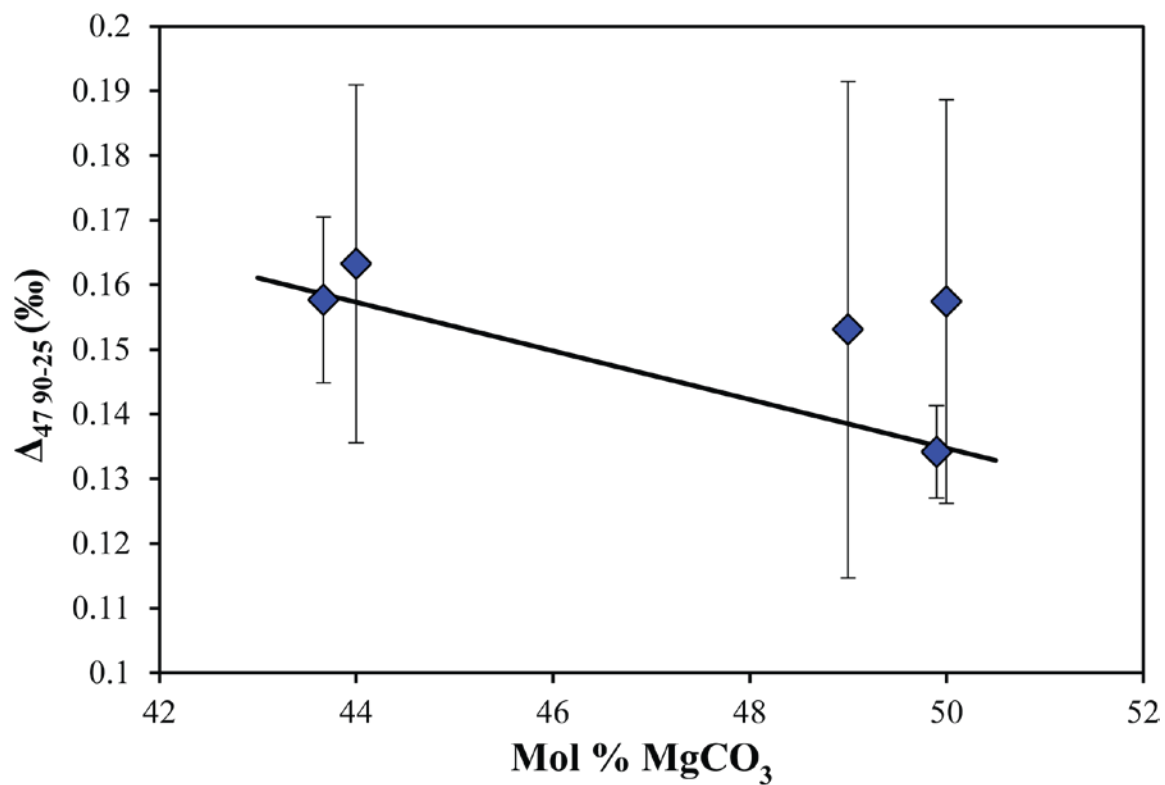
Figure 2.2: Weighted least square regression line plotted through the $\Delta_{47\ 90\text{-}25}$ fractionation relative to the stoichiometry of the dolomite samples as determined through X-ray diffraction. Error bars are $\pm 1\sigma$ S.D.
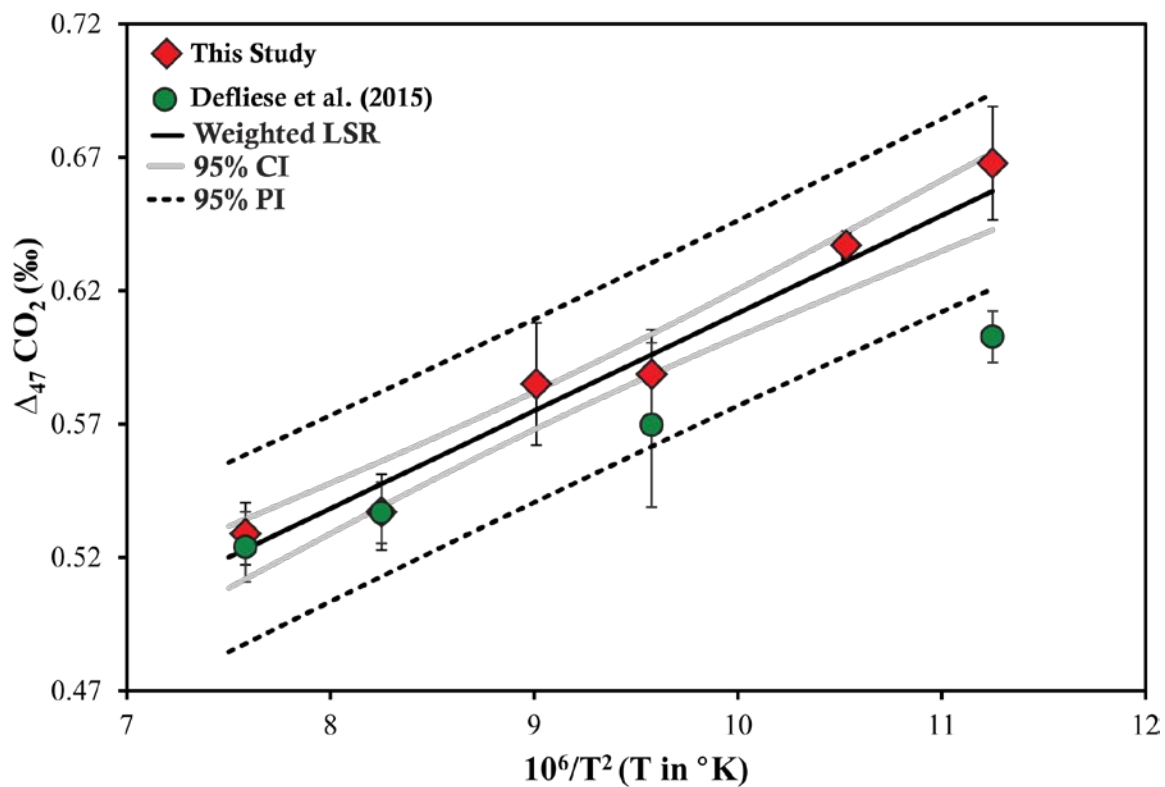
Figure 2.3 - Comparison of acid fractionation results of this work and Defliese et al. (2015) for dolomite NIST 88b. X-axis represents temperature of reaction. Error bars are ±1σ S.D. Solid black line is the weighted least squares regression (LSR) through the data measured in this study. The red solid line is the 95% confidence interval (CI) and the dashed line is the 95% prediction interval (PI) of the NIST 88b data in this study.

25°C measurements in Defliese et al. (2015) (0.603 ± 0.010‰) when compared to our

Δ_{47} at 25°C (0.661 ± 0.032‰). Both 25°C values were derived using the SV technique.

Furthermore, a comparison of individual regression lines through the NIST 88b Δ_{47} data

measured in this study and Defliese et al. (2015) shows the regression lines deviating

significantly between 90 and 25°C (Figure 2.3).

It is unlikely that analytical error can account for the deviation in regression lines.

Using 95% confidence limits and a 95% predictive band derived from a one-factor

ANOVA (r^2 of 0.89), it was found that the 25°C Δ_{47} results between the two studies were

statistically different. This was supported by the measurement of covariance between the

slope of the two regression lines using ANCOVA which resulted in a statistically

significant covariate (the temperature of reaction) ($p < 0.0001$).

There also is little reason to believe that the disparity was a result of any

differences in methodology of reaction as the methods used for digestion of the dolomites

and the cleaning of CO_2 were nearly identical between both studies. One notable

difference in the methods presented in this paper and that of Defliese et al. (2015) was

sample size; 8 mg was used in this study compared to 4-6 mg in the study of Defliese et

al. (2015). Wacker et al. (2013) reported that during acid digestions at lower

temperatures, sample sizes below 7 mg generally gave more dispersed Δ_{47} values than

their larger counterparts. However, the smaller sample sizes in Wacker et al. (2013)

trended towards higher Δ_{47} values than larger samples, opposite to that seen in the NIST

88b data. Also, as stated in Defliese et al. (2015), their data produced at 25°C show little

scatter and possess better external precision than the data obtained at other temperatures.

The differences were also not likely to be a result of sample heterogeneity considering the

certified homogenization by NIST as well as the consistently steeper temperature of digestion fractionation slopes in all the dolomites presented in this work.

Two factors which cannot be ruled out in explaining the discrepancies between our data and that of Defliese et al. (2015) were differences arising from variations in the composition of the acid and fractionation associated with incomplete reaction of the samples or incomplete recovery of CO_2 from the acid. The acid used in Defliese et al. (2015) was created by hydrating heated polyphosphoric acid ($H_6P_4O_{13}$) until a density of 1.92 g/ml was reached. The acid used in this study, initially 85-88% phosphoric acid (H_3PO_4), was boiled until it reached the desired density. It is possible that either of these methods or the methods used to produce the source of the acid introduced a fractionation to the oxygen atoms within the acid. These kinds of issues are not unfounded considering the various problems identified with determining fractionation of the $\delta^{18}O$ value in carbonates (Guo et al., 2009; Kim et al., 2007; Kim and O'Neil, 1997; Rosenbaum and Sheppard, 1986; Sharma and Clayton, 1965; Swart et al., 1991). The problem with this theory is that both acids produce nearly identical Δ_{47} values for NIST 88b with 90°C reactions suggesting that if there were a contributing factor from the acid, it is most pronounced when the kinetics of reactions are slowed. This would suggest that better agreement between laboratories would be achieved if all carbonate clumped isotope digestions were performed at 90°C.

Some fractionation might be associated with recovery of the CO_2 from the reaction vessel. This might be a greater issue with smaller sample amounts as a greater proportion of CO_2 would be retained within the acid. At low temperatures, this effect could be compounded as the viscosity of the acid is increased thus trapping more CO_2. A

method employed both in Defliese et al. (2015) and in this work for gauging the completion of a reaction was noting the absence of bubbles in the acid. This method guaranteed neither a complete reaction nor complete recovery of the CO_2. Defliese et al. (2015) mentioned discarding samples with low yields which may have eliminated samples that were not completely reacted, however a baseline for what constitutes a low yield can be difficult to establish when considering all the factors that go into preparing and digesting samples. In investigating the recovery of CO_2 from the carbonate-acid reaction, shorter low temperature digestions were attempted where the collection of CO_2 was stopped once bubbling had all but ceased. It was found that not only were the yields of these reactions less than predicted, but the reactions would resume if the temperature of the acid was increased. It should also be noted that due to the anhydrous nature of phosphoric acid, the risk of acid crystallization increases with extended periods of time under vacuum at low temperatures. This could inhibit complete reaction or complete collection of CO_2 while also being difficult to identify.

This disagreement of fractionation results parallels another major clumped isotope discrepancy, i.e. the inconsistent slopes for Δ_{47}-temperature calibrations measured in different laboratories. It was suggested by Fernandez et al. (2014) that the inconsistencies in slopes between calibrations could be a result of the method of reaction, whether online in a CAB or offline in a SV. This idea is not consistent with results of the NIST 88b fractionation measurements using both SV and CAB methods presented in this work which showed no statistically significant difference between the Δ_{47} values produced using the two methods.

Conclusions

Based on the analyses of five different dolomites, this study has shown that there is a $+0.153 \pm 0.011$‰ difference in Δ_{47} between the reaction of dolomite at 25 and 90°C in phosphoric acid. This value is significantly larger than previously reported fractionation values for calcites, aragonites, and dolomites. It has been shown that using the fractionation factor measured in this study produced realistic temperatures and $\delta^{18}O_{fluid}$ values for dolomite samples derived from a core on the island of San Salvador, Bahamas. Applying this greater fractionation value to previously published studies reduced the estimated temperatures and $\delta^{18}O_{fluid}$ values and in several instances makes the interpretation of the data more consistent with geological models. Based on the analysis of one of the dolomite samples using both SV and CAB methods, no statistically significant differences were found between the different methods of CO_2 extraction.

Chapter 3 – Applications of the Clumped Isotopic Method to the Study of Dolomitization in the Bahamas: Implications for the Interpretation of Clumped Isotopes in Dolomites

Background

Dolomite forming in association with Cenozoic island dolomites are commonly believed to have formed by ocean water and its derivatives (Land, 1985). When reconciling the dolomites formation, there is little question as to the necessary supply of Mg bearing fluid being present, which allows the focus to be shifted to fluid flow models, fluid composition, and timing of dolomitization. Budd (1997) described six different commonly proposed fluid flow models for dolomitization with drivers based on differences in elevation or differences in fluid density. These models include 1) tidal pumping, 2) seepage infiltration/influx, 3) differential sea surface elevation 4) brine reflux, 5) coastal mixing, and 6) thermal convection. There is no concrete method for differentiating between these models and it is possible for the different regimes to work in concert. However, given an intricate and detailed understanding of the geological history and the composition of the contributing fluids, it might be possible to narrow down the possible modes of dolomitization.

Fluid Equilibrium Composition

Fluids can be differentiated by their isotopic and elemental composition, however the relationship between a fluid and the dolomite that is formed is a highly debated and controversial subject (Budd, 1997; Goldsmith and Graf, 1958; Land, 1980, 1983, 1985; Warren, 2000). The reason for this is that the equilibrium state, the point where chemical

exchanges between and within the fluid and the dolomite is at a steady state over observable time, for any isotope or element is uncertain.

One of the early methods that attempted to determine the precipitating fluids $\delta^{18}O$ composition was to examine coevolved calcites and dolomites (Degens and Epstein, 1964; Friedman and Hall, 1963; Sheppard and Schwarcz, 1970). Considering that the equilibrium relationship between calcite and the precipitating fluid has been fairly well constrained (Friedman and O'Neil, 1977; Kim and O'Neil, 1997), any differences between the calcite and dolomite would have been attributable to the equilibrium value of the dolomite (Budd, 1997; Land, 1980, 1983; Warren, 2000). This had limited success considering the difficulty in proving calcite and dolomite formed simultaneously from the same fluids, however these workers and others have shown that dolomite consistently has much higher $\delta^{18}O$ values than co-occurring calcite on the order of 3-6‰ (Degens and Epstein, 1964; Land, 1980)

Another method for determining a fluids $\delta^{18}O$ value relies on experimentally (Fritz and Smith, 1970; Horita, 2014; Land, 1980; Matthews and Katz, 1977; Northrop and Clayton, 1966; O'Neil and Epstein, 1966; Sheppard and Schwarcz, 1970; Vasconcelos et al., 2005) and theoretically derived equations (Zheng, 1999) which relate the $\delta^{18}O$ value of the fluid, the $\delta^{18}O$ value of the dolomite, and the temperature of formation. Most of these experimental equations were derived at high temperatures and therefore require extrapolation to the low temperature range where many dolomites are believed to have formed. This extrapolation results in large errors in the calculation of the fractionation factor (α) at reasonable sedimentary temperatures. The various equations for

calculating α result in a range of ~1.032 – 1.035 at 25°C, a range large enough (3‰) to render the $\delta^{18}O$ value of little use in distinguishing between different accepted models.

Comparing the results of the $\delta^{18}O$ values of dolomites formed during the Cenozoic on islands from across the globe has shown that they tend to fall in a narrow range of values between +0.5‰ and 4.5‰ (Budd, 1997). Compared to Holocene calcian protodolomites which formed from near normal sea water and have a $\delta^{18}O$ value of +2‰ (Mazzullo et al., 1995) and accounting for variability in the $\delta^{18}O$ value of waters in the Cenozoic, it can be presumed that most Cenozoic island dolomites were formed by normal seawater. It would be expected that dolomites formed from a more evaporated source would trend towards the heavier endmember and those from fresher waters towards the lower endmember; however drawing any distinction between them would require a geologic context to be successful.

The equilibrium fractionation between a dolomite and its parent fluid is also controlled by the temperature during formation. This is often overlooked when considering Cenozoic island dolomites as they form in the narrow range of fluid temperatures of surface waters (20-30°C in the Bahamas). However, when taking into account sea level change over the Cenozoic and the geothermal gradient associated with dolomites formed both in islands and also on the shelf, then the range of possible fluid temperatures is considerably larger. With the recent advances in measuring multiply substituted isotopologues and their associated paleothermometer which is independent of fluid composition, it has become possible to further narrow down the possible contributing fluids and flow regimes which have formed island dolomites. In this study, we will be using clumped isotopes on a suite of Cenozoic island dolomites from the

Bahamas paired with well-developed geologic contexts to constrain their models of formation.

Samples

San Salvador

The samples from San Salvador (SS) were selected from a ≈168 m core drilled on the northern tip of the island which is located on the far eastern edge of the Bahamas island chain (Figure 3.1). The core penetrated Pleistocene to Miocene aged carbonate sediments as determined through biostratigraphy (Supko, 1970, 1977), Sr-isotopes (Swart et al., 1987) and magnetostratigraphy (McNeill et al., 1988). A 110 m interval between 35 and 145 m depth was pervasively dolomitized with well ordered, near stoichiometric (43 to 50% $MgCO_3$) dolomite (Dawans and Swart, 1988; Supko, 1970, 1977).

The sediments in the core were originally composed of aragonite and high-Mg calcite (HMC) derived from calcareous organisms and the prevalent non-skeletal carbonate grains produced in the Bahamas. A series of dolomitization events identified using Sr-isotope and the uranium disequilibrium series (Swart et al., 1987; Vahrenkamp et al., 1991) occurred that suggested the LMC was diagenetically altered to dolomite over anywhere from two to five different dolomitization periods between the early Miocene and the modern (<150 k.a.). In total, 37 dolomite samples between 37 m and 134 m depth were collected for this study along with a single LMC sample from 158.5 m depth.
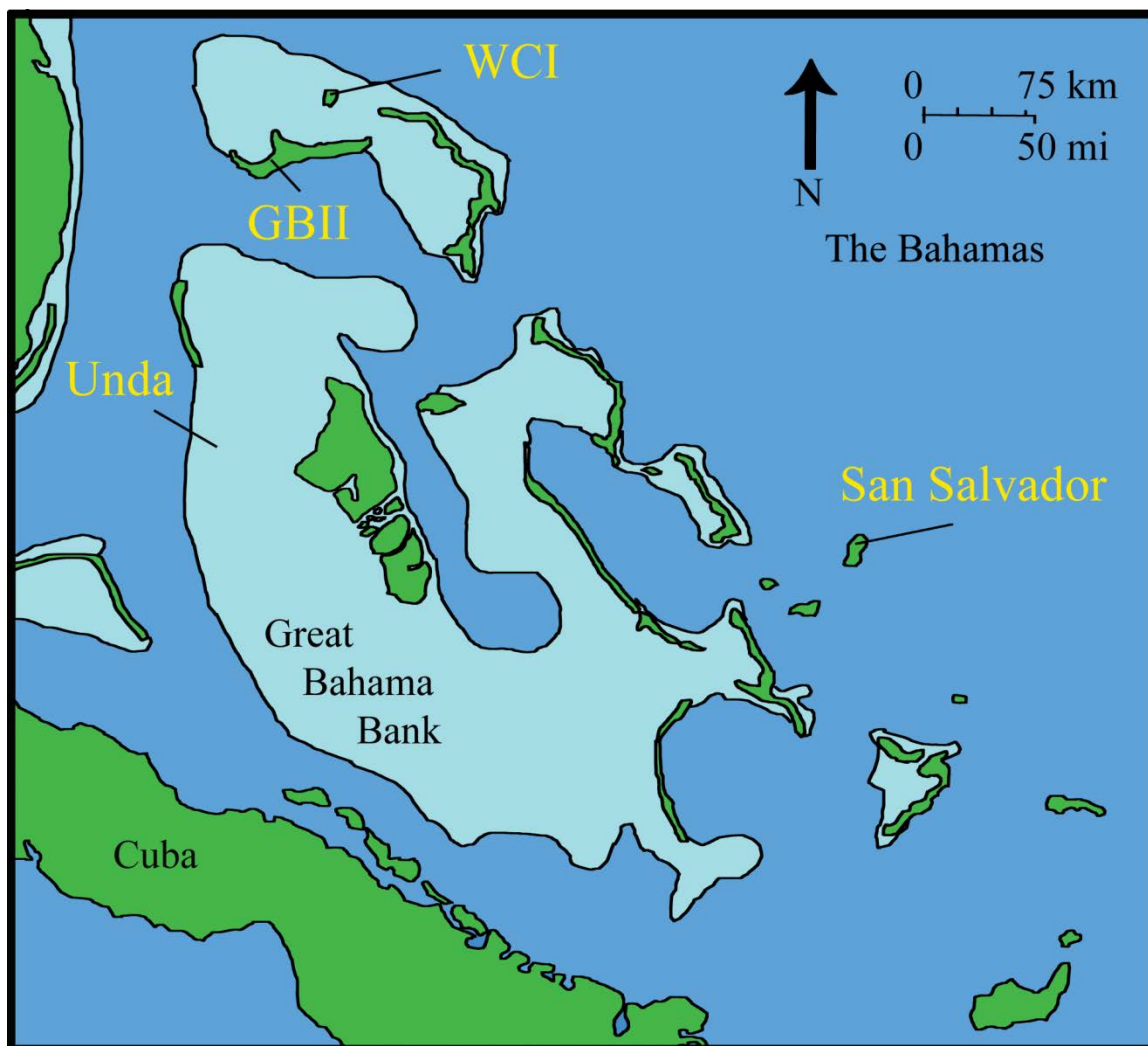
Figure 3.1- Map of the Bahamas including the locations of the four core sites used in this study.

Little Bahama Bank

Two different cores just less than 100 m in length, WCI and GBII, were collected on Walkers Cay and Grand Bahama Island respectively. Twelve distinct samples were collected from WCI between 52.1 and 92 meters depth, all of which were 100% dolomite except for the sample at 52.1 m which was pure LMC and samples at 59.1 m, 61.0 m, and 64.6 m which were all between 76% and 90% dolomite with the remnant portion being LMC. Eleven samples were collected from GBII between 48.2 m and 89.9 m depth, all of which were 100% dolomite. These locations are both situated on Little Bahama Bank, the northern most platform in the Bahamas archipelago, however are separated by 70 km of NE-SW distance. Both cores were studied previously with the original descriptions made in Williams (1985), followed by measurements of magnetostratigraphy (McNeill, 1989), Sr-isotope (Vahrenkamp and Swart, 1990; Vahrenkamp et al., 1991) and δ^{13}C and δ^{18}O values (Vahrenkamp and Swart, 1994). The cores can be separated mineralogically into three distinct sections, with the top most section in both cores containing no dolomite. This is followed by a transition section which is partially dolomitized, and the bottom section which is completely dolomitized. The dolomitized section exceeds the length of both cores which limits the understanding of the extent of dolomitization across the bank.

Interest in drilling these cores originated with the discovery and defining of the Lucayan formation (Beach, 1982; Beach and Ginsburg, 1980), a non-skeletal carbonate grain stone, as well as the sudden transition to a skeletal rich pre-Lucayan wackestone further which had been suggested to be the transition from the Pliocene to the Pleistocene (Vahrenkamp, 1988). The extent of the Lucayan and pre-Lucayan sections were found to expand across Great Bahama Bank (Beach, 1982; Beach and Ginsburg, 1980) to the

south-eastern Bahamas (Pierson, 1983). By examining these cores on Little Bahama Bank, it would be possible to trace these sections across the entirety of the Bahamas. In lieu of discussing the extent of the Lucayan formation, the main focus on studies of these cores was the traceability of the large dolomite formation across Little Bahama Bank (Vahrenkamp, 1988; Vahrenkamp and Swart, 1994; Vahrenkamp et al., 1991). Some sections linked up to other studies on carbonate cores drilled across Bahamas and show the same dolomite crystal structures as described elsewhere are present in these cores (Dawans and Swart, 1988; Supko, 1970, 1977; Vahrenkamp, 1988).

Based on previous works, the cores have been dated to between the Middle Miocene and Pleistocene, with three distinct dolomitized sections broken into three events which took place in the Late Miocene, Late Pliocene, and Early Pleistocene (Vahrenkamp, 1988; Vahrenkamp et al., 1991). The dolomitization events produced different textures of dolomite (discussed below) with the earliest event in the Late Miocene associated with dense sucrosic dolomites which are texturally mature and fabric destructive and the latter two events producing less mature, fabric preserving sucrosic dolomites with the presence of calcite still lingering. Multiple subaerial exposure surfaces and erosional boundaries indicated a complicated relationship with sea level change and exposure to meteoric fluids. Based on the timing of the events and extent of dolomitization, it has been suggested that the dolomites formed near the seawater sediment interface which implied formation by normal marine seawaters or waters slightly altered by either evaporation or dilution.
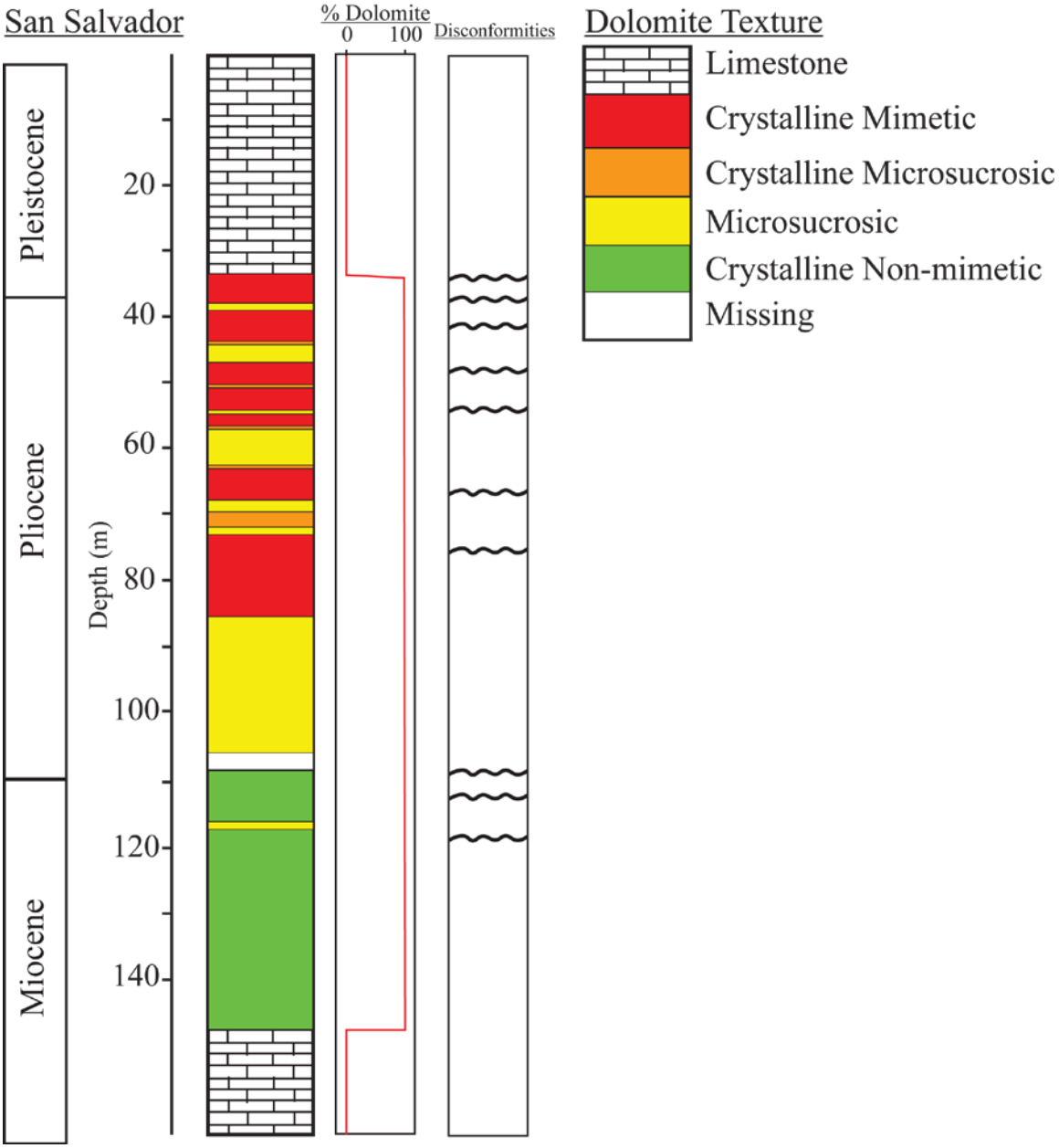
Figure 3.2 - Adapted from Dawans and Swart (1988). San Salvador core description based on dolomite textural types, percent dolomite abundance as determined by X-ray diffraction, and identified disconformities (∿∿).
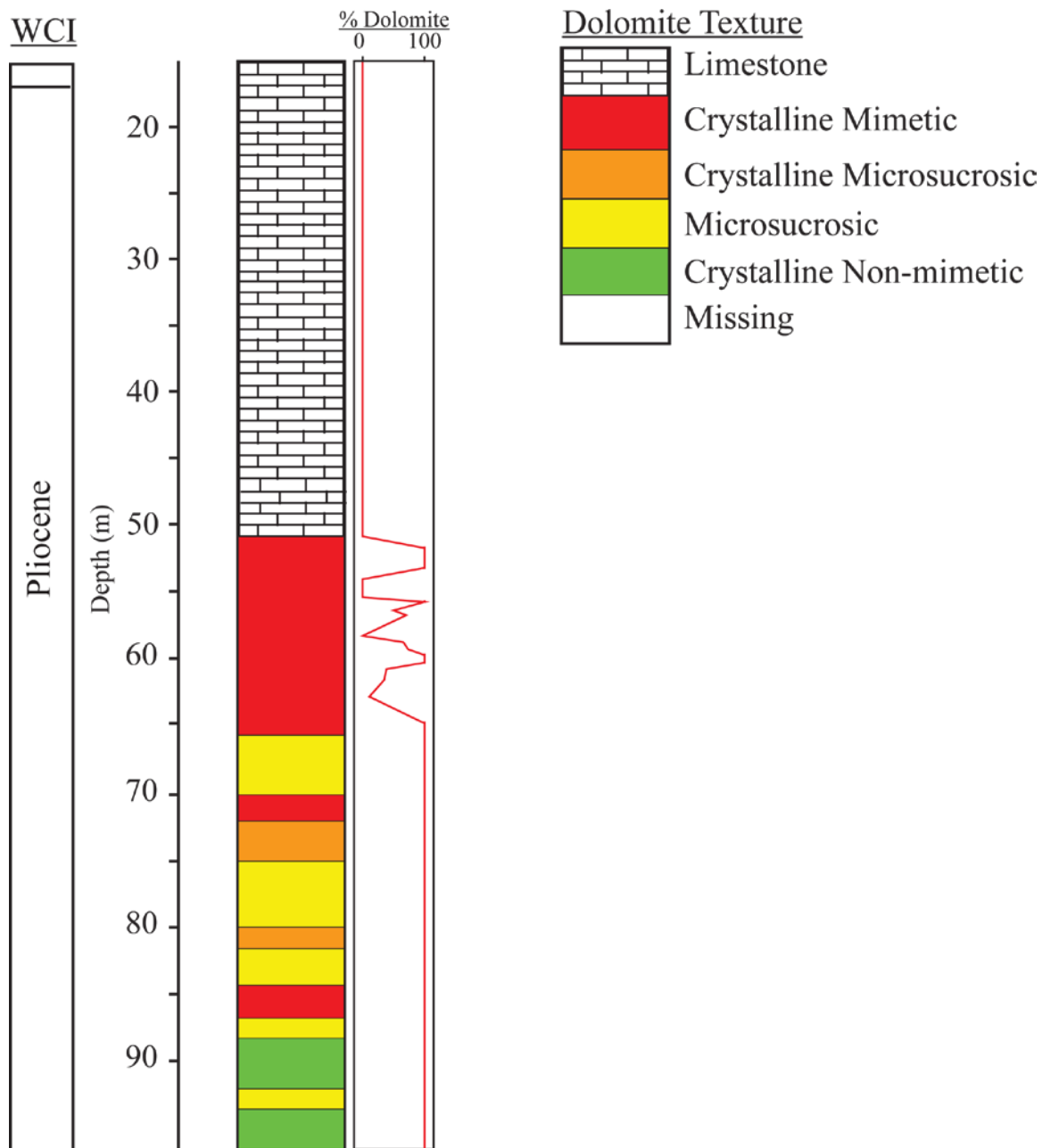
Figure 3.3 - Adapted from Vahrenkamp and Swart (1994). Dolomite textural types and percent dolomite abundance, as determined by X-ray diffraction, distributed throughout the Walkers Cay core.
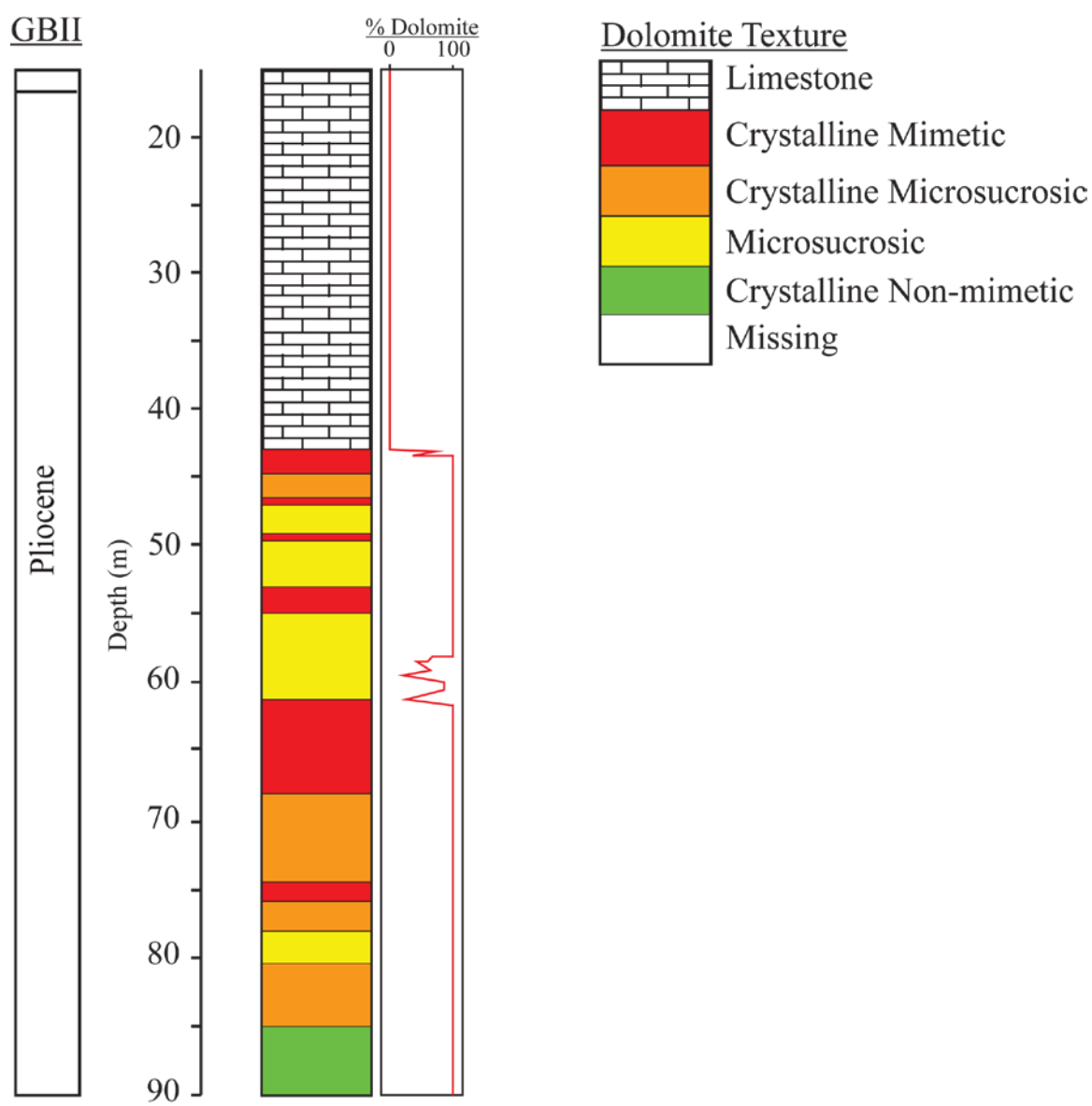
Figure 3.4 - Adapted from Vahrenkamp and Swart (1994). Dolomite textural types and percent dolomite abundance, as determined by X-ray diffraction, distributed throughout the Grand Bahama Island II core.
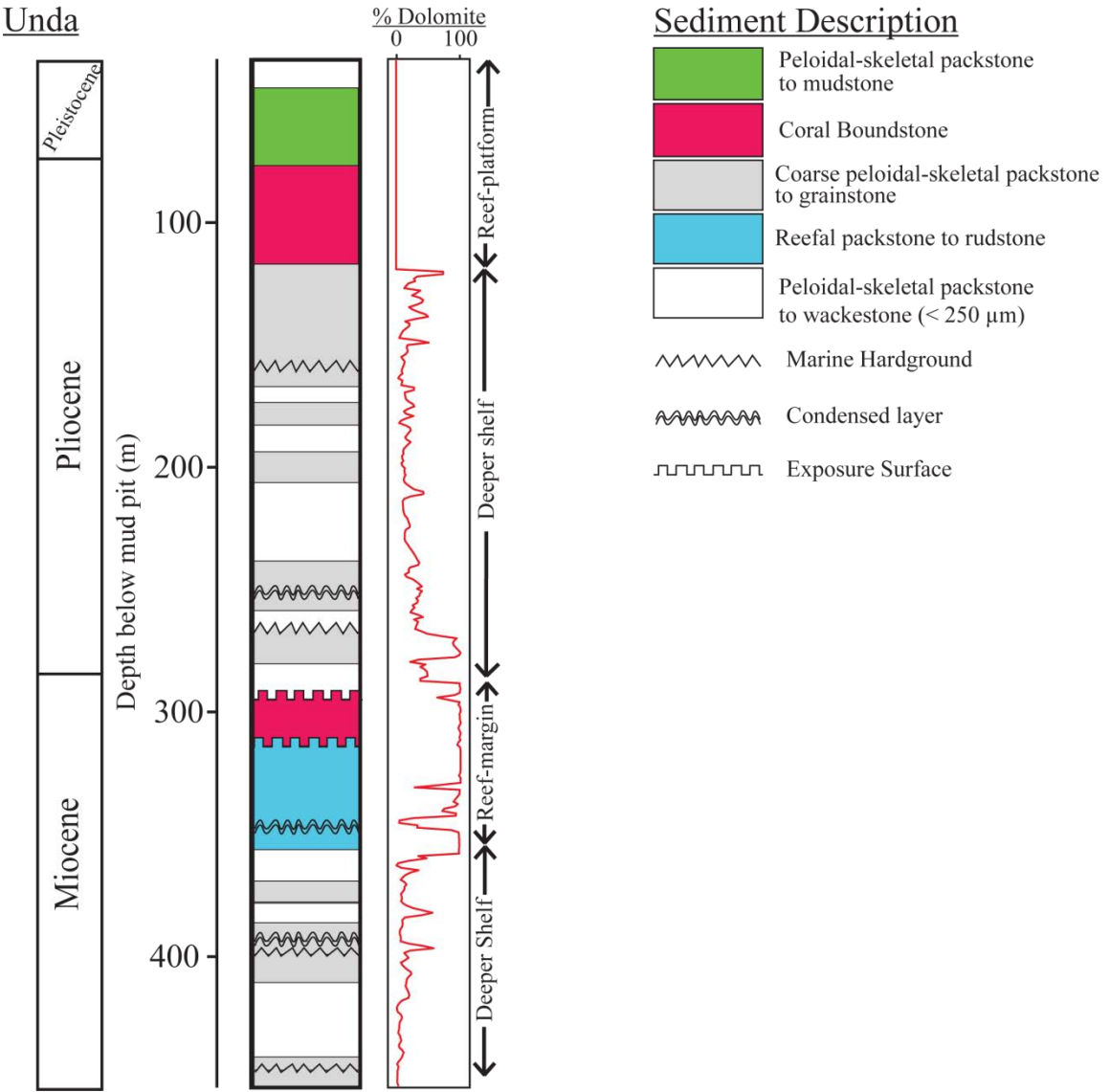
Figure 3.5 - Adapted from Eberli et al. (1997). Image displays the lithology and description of the Unda core with percent dolomite abundance as determined by X-ray diffraction.

Unda

Core Unda was drilled on the North-Western Bahamian shelf as part of the Bahamas Drilling Project (Eberli et al., 1997) along the same geophysical line as core Clino (discussed in Chapter 4). Unda is composed mostly of reefal deposits and platform derived sediments with some deeper marginal deposits towards the bottom of the core (Swart and Melim, 2000). Trace amounts of dolomite were first identified below 108.1 m with increasing abundances (up to 80%, but typically 20-40%) from 108-235 m and 354-452 m depth. From 292-360 m depth just below the Miocene-Pliocene boundary, a section of platform to middle-reef sediments is 100% dolomitized. These dolomites show nearly identical fabrics, both microsucrosic and crystalline mimetic, to those found elsewhere in the Bahamas including San Salvador (Dawans and Swart, 1988) and Little Bahama Bank (Vahrenkamp, 1988).

Analysis of δ^{13}C and δ^{18}O in bulk sediments of Unda revealed a sudden and distinct transition from negative δ^{13}C and δ^{18}O (δ^{13}C = -1.6‰ ± 1.7‰, δ^{18}O = -3.0‰ ± 0.7‰) values in the upper 108m of core to positive values (δ^{13}C = 3.0‰ ± 0.9‰ ; δ^{18}O = 0.9‰ ± 0.3‰ and 3.4‰ ± 0.3‰ for calcite and dolomite respectively) (Melim et al., 1995). This transition has been suggested to be a shift from the influence of meteoric diagenesis to marine pore fluid diagenesis and cannot strictly be because of the geothermal gradient as the shift in the δ^{18}O value would suggest a 14°C temperature change which is unreasonable considering the location and depth (Eberli et al., 1997; Melim et al., 1995; Swart and Melim, 2000).

In total, 12 samples were taken from the completely dolomitized reefal section of Unda between 292 and 332 m depth. Each sample was analyzed for composition on the

XRD and the majority were 100% dolomite with less than 1% LMC present in two of the samples and 3% aragonite found in a third sample. This section was identified as falling within *diagenetic zone II* in Melim et al. (2001). Within this zone, multiple diagenetic events are believed to have occurred in relation to sea level falling below the upper extent and subsequently rising. While most of the section is completely dolomitized, there are a few isolated pockets of preserved LMC and aragonite grains associated with restricted fluid flow from cementation and fracturing.

Dolomite Textures

The dolomites present in all of these cores were classified according to the scheme originally described in Vahrenkamp (1988) and Dawans and Swart (1988). Four different textural types of dolomites were identified: two distinct fabrics, crystalline mimetic and (micro)sucrosic, and two intermediate fabrics, crystalline non-mimetic (CNM) and crystalline microsucrosic (CMS) (Figures 3.2-3.5). The crystalline mimetic (CM) dolomites were characterized by the preservation of the original structure of the precursor fabric. They were mostly composed of clear crystals which act as void filling cements. The sucrosic dolomites were differentiated by their fabric destructive nature.

The original grains in the cores were composed of carbonate grainstones and framestones that had either been dissolved away or mimetically replaced. The CM dolomites were typically calcian (mol % $MgCO_3$ = 44-46%) with slightly positive $\delta^{18}O$ values (+2‰ (V-PDB)). The sucrosic dolomites were separated into both micro (10-50 μm) dolomites (MS) and macro (>100 μm) dolomites (S). They show extensive recrystallization with crystals that are tightly interwoven with cloudy centers and clear rims similar to those described in Sibley (1982). The crystals were fabric destructive,

typically forming in mudstones and wackestones, however were nearly stoichiometric (mol % $MgCO_3$ = 48-50 %) with higher $\delta^{18}O$ values (~ +4‰ (V-PDB)). The $\delta^{13}C$ values were similar in the two dolomite types ranging between +1.7‰ to +2.4‰. The intermediate phase, described as crystalline non-mimetic (CNM), was composed of both CM and MS style fabrics. CNM dolomites were fairly fabric destructive suggesting extremes in the amount of recrystallization, and were composed of varying sized anhedral and euhedral crystals. Based on the stoichiometry of the dolomites in the cores, samples from the San Salvador core were believed to be more stable and mature than those from Unda, WCI, and GBII, as most, but not all, samples from those cores were found to be calcian and disordered (Dawans and Swart, 1988; Melim et al., 2001; Vahrenkamp and Swart, 1994).

Information from Coral Skeletons

Fabric preservation granted by the presence of the CM dolomite fabric within the cores made it possible to identify individual species of corals despite complete dolomitization. Fossil corals, including *Acropora cervicornis* and *A. palmata,* were identified as prominent components of these cores (Supko, 1970; Williams, 1985). The presence of these species, which are extant in modern Bahamian sea waters but are also known to have limited tolerance for sea water temperatures (Hoegh-Goldberg, 1999), would have suggested a similar range of sea surface temperatures in the Plio-Pleistocene as the modern Bahamas.

Age of Dolomitization from Sr-isotopes

The age of dolomitization has been constrained in the cores using the $^{87}Sr/^{86}Sr$ ratio of the dolomite (Swart et al., 2001; Swart et al., 1987; Vahrenkamp, 1988; Vahrenkamp and Swart, 1990; Vahrenkamp et al., 1991). This method works because during the Pliocene and Pleistocene, the $^{87}Sr/^{86}Sr$ ratio of seawater had been steadily increasing (Burke et al., 1982; DePaolo, 1986). During this period, it is assumed that the only sources of strontium composing the Sr in the carbonate lattice was derived from the seawater at the time of dolomitization and the precursor carbonate. This enables a comparison of the $^{87}Sr/^{86}Sr$ ratio of the dolomite with the ratio in seawater which produced the oldest possible age of dolomite formation as well as the youngest age of the original sediments (Saller, 1984; Swart et al., 1987; Vahrenkamp et al., 1991). This technique depended upon the precursor mineralogy of the dolomite; if the precursor was LMC then the Sr-isotopes predicted actual dolomitization age, however if the precursor was aragonite or HMC, then some possible Sr-contribution from the precursor needs to be accounted for and could affect results.

In the case of San Salvador, the $^{87}Sr/^{86}Sr$ ratio throughout the core showed an increasing trend from 0.70851 at the bottom of the core to 0.70912 at the Plio-Pleistocene boundary and the $^{87}Sr/^{86}Sr$ values generally agree with the corresponding value of sea-water at the time of deposition (Swart et al., 1987). There is however some deviation in the $^{87}Sr/^{86}Sr$ ratio based on the chronostratigraphy of the core. In particular the $^{87}Sr/^{86}Sr$ of the dolomites between 53 m and 79 m which were dated to have formed at some point during the Pliocene are as radiogenic as modern seawater (0.70923). These values suggest dolomitization in this interval occurred less than 500,000 ybp. This age

was further constrained using $^{234}U/^{230}Th$ ratios to approximately 150,000 ybp. As dolomitization could not have taken place when the sediments were exposed to meteoric fluids, this age places the timing of formation to periods when sea level was as high as the modern sea level such as during MIS 5e, or during other sea level changes associated with the current high stand.

The Little Bahama Bank cores showed evidence for three distinct phases of dolomitization (Vahrenkamp et al., 1991). The first phase was shown to have occurred between 11.5 and 8.3 Ma (0.70893 to 0.70894) to limestones that were deposited in the Middle to Late Miocene. This was followed by a second major phase of dolomitization at the end of the Pliocene between 2.8 and 2.2 Ma (0.70899 to 0.70809). A third minor phase was shown to have occurred shortly after the second phase, separated by a non-diagenetically altered limestone layer on top of the phase II dolomites. This unit is dated to have formed between the Latest Pliocene and Early Pleistocene (0.70912).

The $^{87}Sr/^{86}Sr$ ratio on bulk samples of Unda suggests ages that are mostly coincident to those calculated based on chronostratigraphic ages determined by magnetostratigraphy and biostratigraphy (McNeill et al., 2001). The agreement between the two proxies would suggest that diagenesis occurred shortly after deposition. On isolated dolomites from the core, the $^{87}Sr/^{86}Sr$ ratios are slightly more radiogenic than the surrounding carbonate material suggesting dolomitization occurred post-deposition (Swart et al., 2001). Samples near the top of the core show a gradual decline in Sr isotope values until a hiatus at 292.91 m depth where a subaerial exposure surface is associated with a sudden shift to more negative values suggesting a major unconformity. Based on

foraminifera in the core, the unconformity has been identified as the Miocene-Pliocene boundary (McNeill et al., 2001).

Mechanisms of Dolomite Formation

Studies on cores throughout the Bahamas have almost ubiquitously found the presence of shallow subsurface dolomites that show the textural maturity of ancient dolomites despite having formed in the Neogene (Beach, 1982; Dawans and Swart, 1988; Goodell and Garman, 1969; Pierson, 1983; Supko, 1970; Williams, 1985). The formation of these dolomites is often questioned as the viable contributing fluids and pathways of fluid flow are extensive when considering the complex relationship between sea level change and the evolution of the platform. The fluid most readily available for dolomitization of these cores is the surrounding seawater as it is the only source with enough magnesium to produce an equivalently sized dolomite. Seawater in the Bahamas has a typical $\delta^{18}O$ value of 0.0-1.0‰ (Baldini et al., 2007). The island of San Salvador is also covered by a multitude of evaporative pools that are fed by seeps connected to the surrounding ocean or by fresh water lenses (Baldini et al., 2007; Davis and Johnson Jr., 1990; Dupraz et al., 2013; Hagey and Mylroie, 1995; Teeter, 1995). These pools have measured salinities either slightly more concentrated than, or up to twice as concentrated than, the surrounding ocean (Davis and Johnson Jr., 1990). The fluids have published $\delta^{18}O$ values of 0 to 1.5‰ (Baldini et al., 2007), though these values were all measured in a single study during one visit to the island in December of 2000. Unpublished data from salt ponds on Little Darby Island have measured fluid $\delta^{18}O$ values from 1.3 to 4.9‰ (Piggot, 2014). Similar restricted lakes exist elsewhere in the Bahamas including Lee Stocking Island (Dix, 2001) and Eleuthera (Dupraz et al., 2004; Glunk et al., 2011) which

has a measured fluid composition of 2.8 to 2.9‰, possibly making them major role players in carbonate diagenesis throughout the Bahamas.

San Salvador

The original model of dolomitization in San Salvador, proposed by Supko (1970), suggested that the magnesium was supplied by the reflux of evaporated seawater at the surface. This conclusion was based on the observation that the dolomites were enriched in ^{18}O relative to calcite in the core. However, since dolomites contain more positive δ^{18}O values relative to calcite (Fritz and Smith, 1970; O'Neil and Epstein, 1966) formed at the same temperature, Supko (1970) revised his interpretation to favor a model in which dolomitization occurred as a result of the mixing of marine and meteoric waters according to the mixing-zone or Dorag hypothesis (Badiozamani, 1973). This model has been invoked by numerous workers to explain early dolomites (Humphrey, 2000; Ward and Halley, 1985), but its applicability has been questioned as a result of the fact that dolomite has only been rarely found associated with modern mixing-zones (Hardie, 1987; Melim et al., 2004; Plummer et al., 1976; Smart et al., 1988; Stoessell et al., 1989).

Dawans and Swart (1988) identified ten different shallowing upwards sequences throughout the length of the core, each of which was capped by a subaerial-exposure surface, an erosional boundary, or a sudden change in facies type. These boundaries were interpreted as evidence for changes in the relative position of sea level. Within each sequence, there is a general trend in changes of dolomite facies type. At the bottom of each sequence, there are typically MS dolomites replacing wackestones and mudstones composed of skeletal and non-skeletal sediments. This is followed CM dolomites in a

grading upwards sequence of coral laden boundstones into sediments indicative of a shallow subtidal and peritidal carbonate environment.

The present consensus is that the San Salvador dolomites formed as a result of the flushing of normal seawater through the sediments, at temperatures slightly lower than surface seawater. This flushing has been proposed to have been driven by processes such as Kohout convection (Kohout, 1967; Simms, 1984) or as a result of movement of seawater associated with a discharge of freshwater through the mixing-zone (Vahrenkamp and Swart, 1994). This conclusion is further supported by the more positive $\delta^{18}O$ and $\delta^{13}C$ values of the dolomite which are consistent for precipitation by cooler seawater and compare similarly to other dolomites formed by geothermally induced seawater circulations (Aharon et al., 1987). None of these models proposed that temperatures could have been in excess of the modern sea surface temperatures.

Little Bahama Bank

The WCI and GBII cores have a muddled gradient of transition from the overlying Pleistocene LMC body to the completely dolomitized section of the core which occurs over ≈10m in both cores (Williams, 1985). The dolomites also show extensive variation in their texture, porosity, and permeability. This is most likely associated with the dolomites interaction with shallow subsurface diagenetic processes. The extensive nature of the dolomite bodies across the length of LBB (≈70 km) gives credence to the all-encompassing nature of the dolomitizing fluids that contributed to their formation. This eliminates many of the smaller scale fluid flow models that could not have possibly provided the resources required for such events. However, no large scale bank-wide controls were found to have preferentially influenced the dolomitization process

including both facies type and relative position to the bank edge. Williams (1985) initially concluded that these dolomites had to have been associated with dolomitization from fluids in the mixing zone which were associated with the rapid changes in sea level that occurred throughout the Neogene. Based on the geometry of the dolomite body across LBB, Vahrenkamp and Swart (1994) agreed with a mixing zone conclusion with seawater being driven by an overlying mixing zone during periods of exposure. This is further supported with a trend in the $\delta^{18}O$ values of the dolomites that departs negatively away from expected marine values which suggests the dolomites formed from fluids with a depleted $\delta^{18}O$ value or were hot.

Unda

The Sr-concentration profile of the pure dolomites of the Unda core suggests formation from normal marine seawater (Swart and Melim, 2000). The dolomites had an average Sr concentration of 230 ppm which is comparable to a calculated expected Sr value for seawater of 190 ppm. The dolomites used in this study are derived from a reefal section that extends from a non-depositional surface at 292.8m down to 354.7m core depth which has been extensively dolomitized. The dolomitization is believed to have occurred after burial to a depth of 50 to 100m to account for the entire length of the dolomite body these samples were taken from which extends from 260 to 354.7m in core depth. Outside of this heavily dolomitized section, dolomite typically comprised less than 10% of the bulk composition in was described as a background dolomite (Swart and Melim, 2000). Some deviation from the background dolomites have been associated with marine hardgrounds found at 108.1 and 393.8m core depth where dolomite abundance increases significantly before tapering off to background levels with increasing depth.

Both the background and hardground type dolomites can be associated with dolomitization by pore fluids and exposure at the seawater sediment interface. This model of dolomitization does could not have formed the large body of reefal dolomites where the samples in this study are taken from, however no fluid flow models have been proposed for their formation (Swart and Melim, 2000).

Methods

Clumped Isotopes

The SS samples were measured for clumped isotopes from June 2012 to July of 2013 and the Unda, WCI, and GBII samples were measured from March to November of 2015. Sample preparation and CO_2 cleaning procedures followed the same methods described in Chapter 1. Dolomite and LMC samples were determined using XRD and are corrected using the appropriate acid temperature digestion fractionation factors ($\Delta_{47\ 90-25}$) of 0.153‰ and 0.091‰ as measured in Chapter 2 of this work. The SS samples were processed using the standard CDES method while Unda, WCI, and GBII were processed using the PBL. Any mixed carbonate sample was corrected using a linear mixing model between the two $\Delta_{47\ 90-25}$ endmembers for calcite and dolomite. Temperatures were calculated using the CDES construction of the Ghosh et al. (2006) calibration presented in Dennis et al. (2011). The $\delta^{18}O_{fluid}$ values were calculated using the dolomite formula of Fritz and Smith (1970) and the calcite formula of Kim and O'Neil (1997).

Results

All measured data for Chapter 3 can be found in supplementary table S.2.

San Salvador

The SS dolomites had Δ_{47} values between 0.657‰ and 0.738‰ after being translated into the CDES. These values translate to a temperature range of 19°C to 37°C with an average value of 28 ± 5°C. The one calcite at a depth of 158.5 m had an average Δ_{47} value of 0.690‰ which when converted to temperature is 29°C. The calculated $\delta^{18}O_{fluid}$ values for the dolomite temperatures averages 1.8 ± 1.0‰ and 2.0 ± 0.4‰ for the calcite sample. The large standard deviation on the $\delta^{18}O_{fluid}$ values of the dolomites is because of the presence of two different temperature signals present in the clumped isotopes (discussed below). A graphical representation of the temperature and $\delta^{18}O_{fluid}$ values can be seen in Figure 3.6 A-D.

Little Bahama Bank

Corrected using the PBL, GBII dolomite sample Δ_{47} values ranged from 0.720‰ to 0.762‰. This range produced an average calculated temperature of 20 ± 3°C and $\delta^{18}O_{fluid}$ value of 1.3 ± 0.6‰ (Figure 3.7A-D).

The WCI core measurements had Δ_{47} values between 0.712‰ and 0.752‰. This equated to an average temperature of 20 ± 3°C for the pure dolomites. The LMC sample produced an average temperature of 32 ± 3°C and the three mixed dolomite/LMC samples had temperatures ranging from 16 to 26°C. Based on these temperatures, the dolomites were formed from a fluid with a $\delta^{18}O$ value of 1.5 ± 0.5‰, the transitional impure dolomites from fluids of 0.0 ± 1.0‰, and the LMC from a fluid of 1.0 ± 0.6‰ (Figure 3.7A-C).
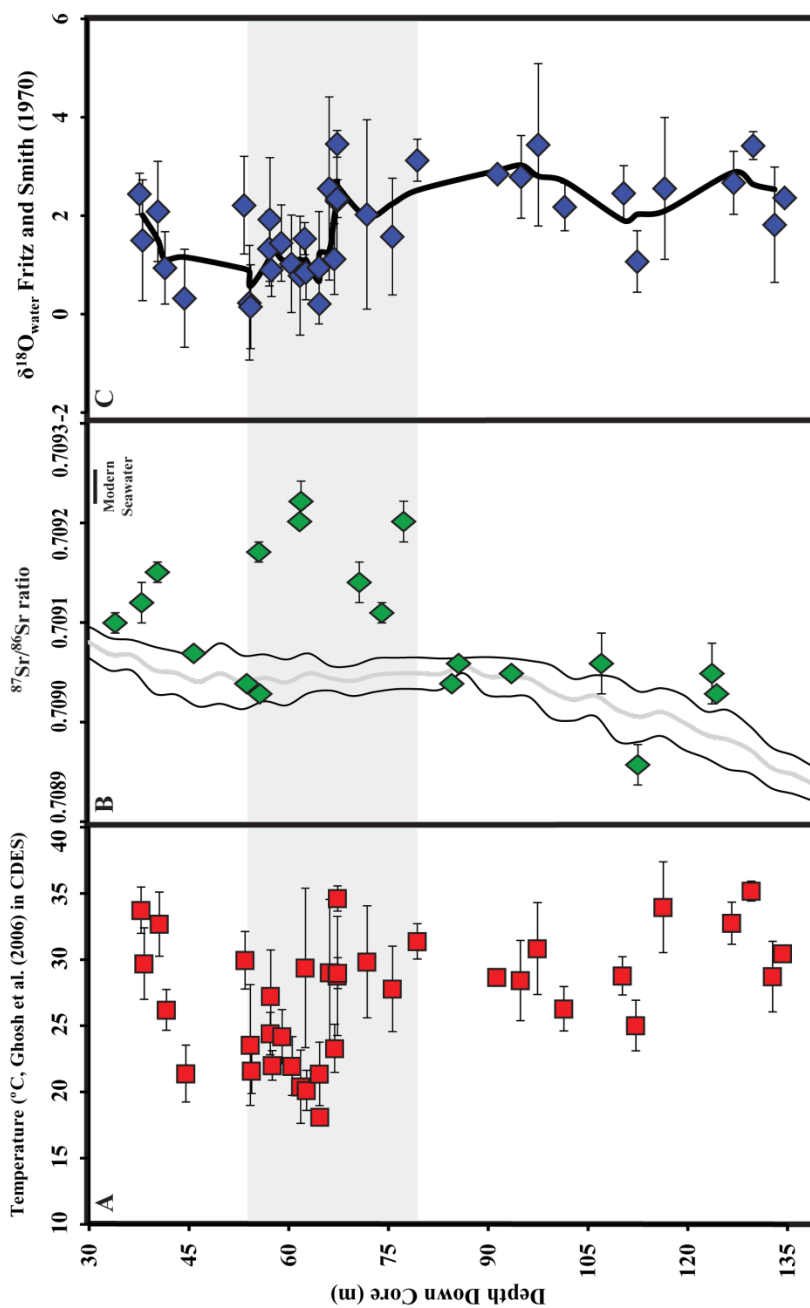
Figure 3.6 - Summary plots of the San Salvador dolomite data. Faded blue horizontal bar across all three plots indicates the zone of near modern $^{87}Sr/^{86}Sr$ values that correlate with decreased clumped isotope temperatures and $\approx$ 0 ‰ $\delta^{18}O_{fluid}$ values. Error bars on all three plots represent $\pm$ 1σ. A) Clumped isotope temperatures converted using the calibration of Ghosh et al. (2006) placed into the CDES in Dennis et al. (2011). B) $^{87}Sr/^{86}Sr$ values measured in Swart et al. (1987). Vertical gray line indicates an average measured $^{87}Sr/^{86}Sr$ for seawater through the time frame of deposition of the San Salvador sediments as measured in Depaulo (1986) with corresponding $\pm$ 1σ indicated by the black lines. Modern day Sr isotope seawater value is indicated by the black horizontal line at the top of the graph. C) Calculated $\delta^{18}O_{fluid}$ values using the corresponding clumped isotope temperatures and the formula of Fritz and Smith (1970). Black line represents a three-point moving average of the data. Error bars are $\pm$ 1σ.
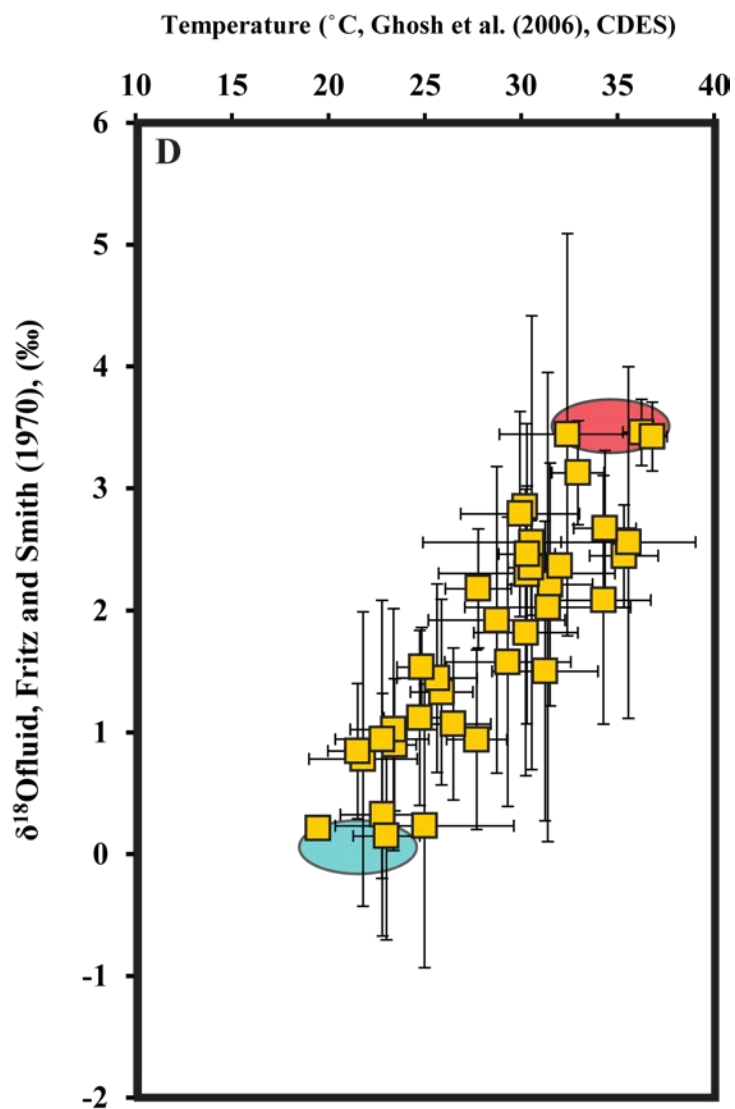
Figure 3.6D - Plot of the compositional fluid as determined by the calibration of Fritz and Smith (1970) against the temperature of formation calculated using Ghosh et al. (2006) in the CDES. Data suggests a mixture of two endmember fluids, a normal seawater type fluid (blue oval) and a more evaporative fluid (red oval).
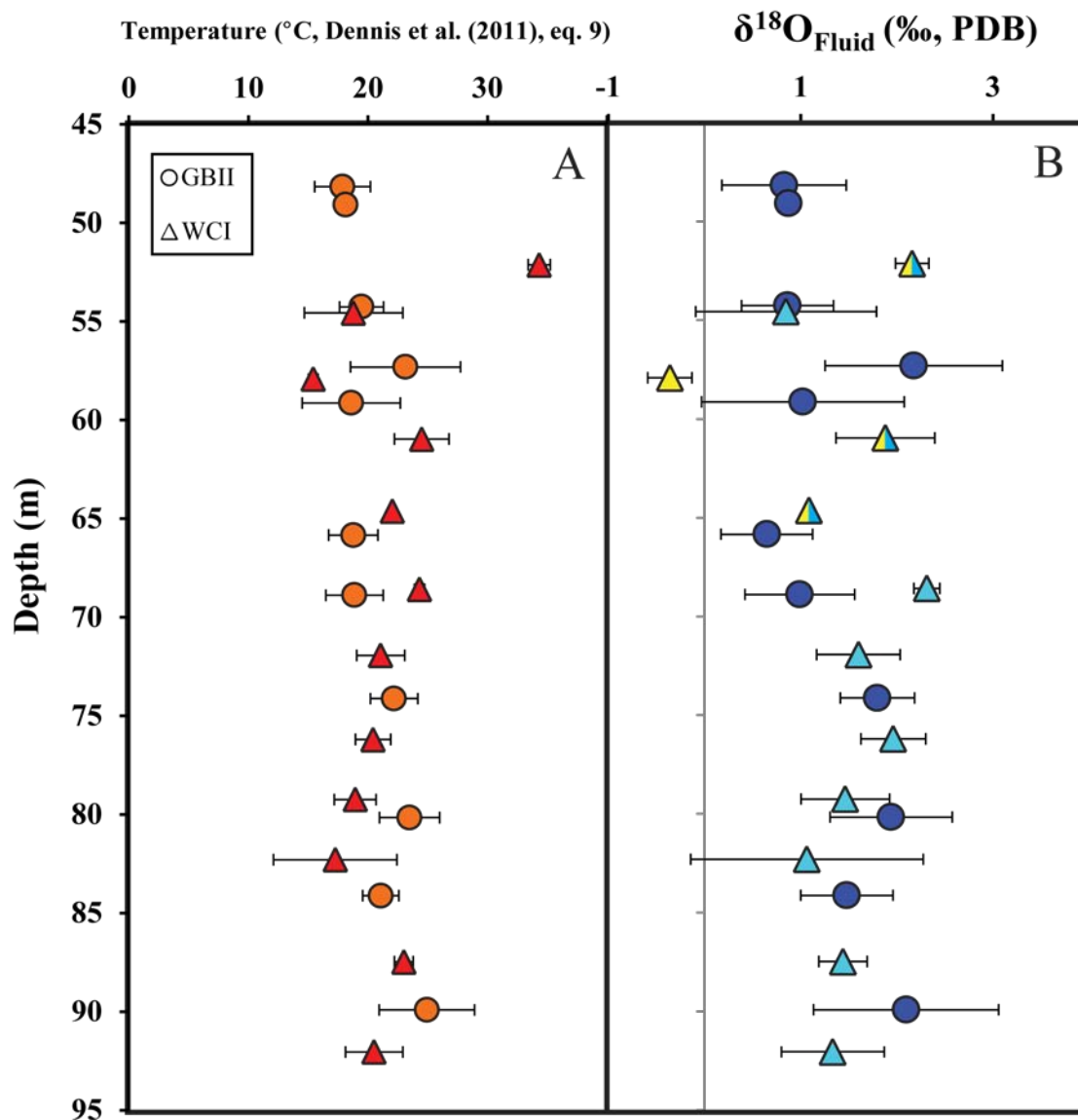
Figure 3.7 - Calculated clumped isotope temperatures and corresponding $\delta^{18}O_{fluid}$ values for cores GBII and WCI on Little Bahama Bank. Temperatures were calculated using the calibration of Ghosh et al. (2006) placed into the CDES from Dennis et al. (2011). $\delta^{18}Ofluid$ values were calculated using the calibration of Fritz and Smith (1970) for the pure dolomite samples and in combination with Kim and O'Neil (1997) for the mixed carbonate samples (split blue and yellow) and the pure LMC sample (completely yellow). The effects of acid digestion temperature were taken into account when calculating the Δ_{47} used for mixed
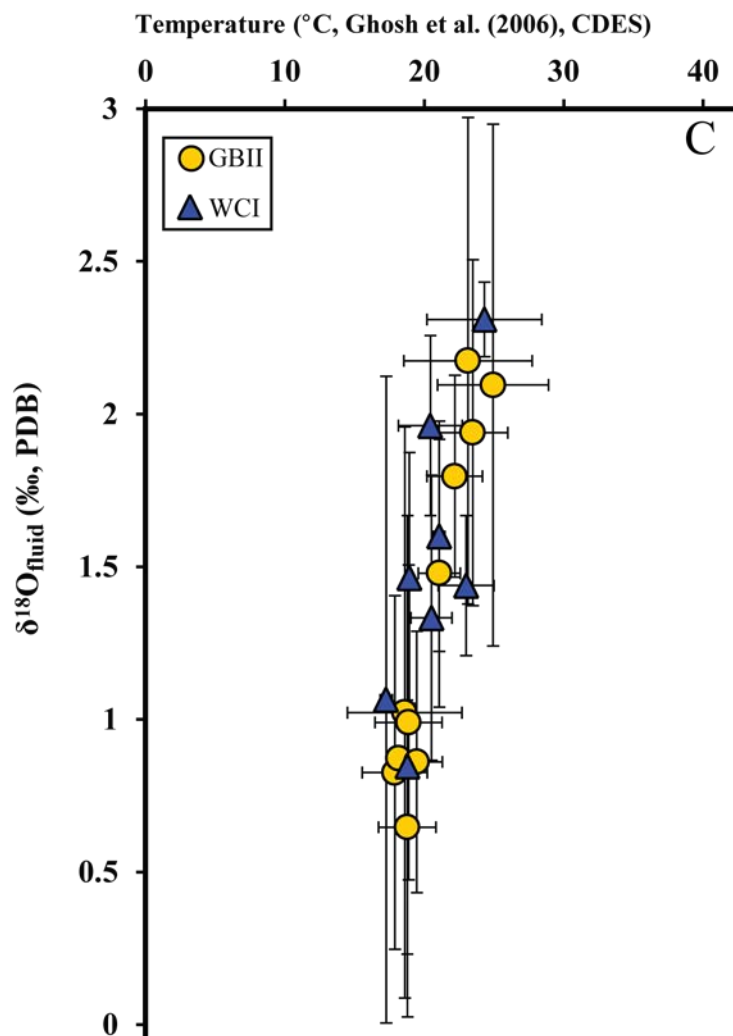
Figure 3.7C - Plot of the composition of the dolomitizing fluid of the Little Bahama Bank cores as calculated using the calibration of Fritz and Smith (1970). Temperatures were calculated from clumped isotopes using the calibration of Ghosh et al. (2006) in the CDES. Error bars represent ± 1σ.

Unda

The 12 Unda samples were measured 2-3 times between March and July of 2015. All data reported are with the PBL correction. Clumped isotope results throughout the length of the core vary little, with Δ_{47} results ranging between 0.740‰ and 0.758‰. This range results in calculated temperatures using Dennis et al. (2011) of 16-19°C and an average fluid value of 1.1 ± 0.3‰ using the calibration of Fritz and Smith (1970). (Figure 3.8A-C)

CM and MS Dolomites

Applying a two-tailed Student's t-test with a 95% confidence interval with unequal variances to the Δ_{47} results samples of the SS core between 53m and 79m depth have shown that there is a significant difference ($p < 0.001$) between CM and MS dolomites. The CM dolomites within this section had Δ_{47} values that averaged 0.682 ± 0.014‰ and MS dolomites averaged 0.715 ± 0.015‰ (Figure 3.9). All data measured for Chapter 4 can be found in supplementary table S.3.

Discussion

Unda

The clumped isotope calculated temperatures and fluid values suggest that the completely dolomitized reefal section of Unda was formed by a normal marine seawater at depths below sea level. This is in agreement with the conclusions of Swart and Melim (2000) where they stated that dolomitization of this section had to have occurred in 50-100 m burial depth and there assessment that the Sr-concentration within the dolomites (≈230 ppm) is a good indicator of the formation fluid and not extensively contaminated
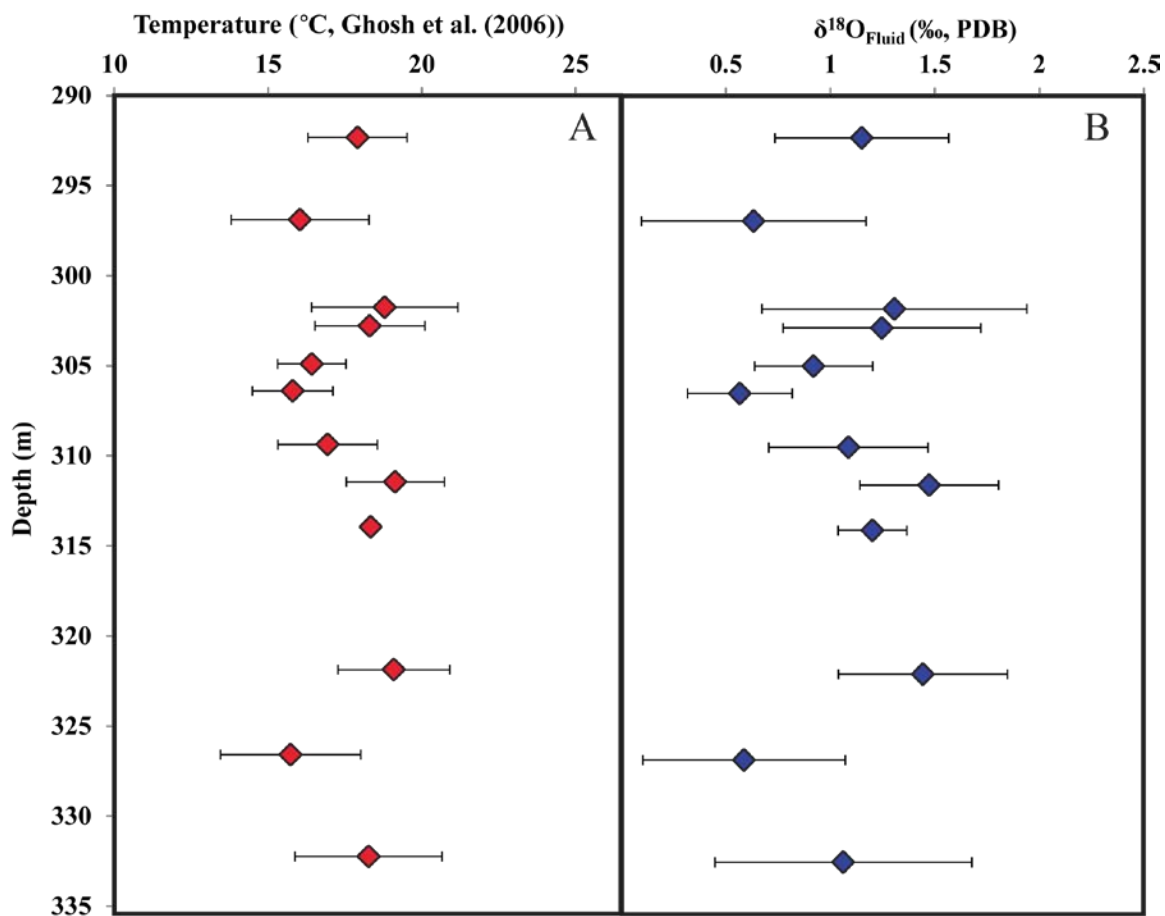
Figure 3.8 - Calculated clumped isotope temperatures and corresponding $\delta^{18}O_{fluid}$ values for the Unda core. Temperatures were calculated using the calibration of Ghosh et al. (2006) placed into the CDES from Dennis et al. (2011). $\delta^{18}O_{fluid}$ values were calculated using Fritz and Smith (1970) for the pure dolomite samples and in combination with Kim and O'Neil (1997) for the mixed carbonate samples. The effects of acid digestion temperature were taken into account when calculating the Δ_{47} used for mixed carbonate samples. Error bars represent ± 1σ.
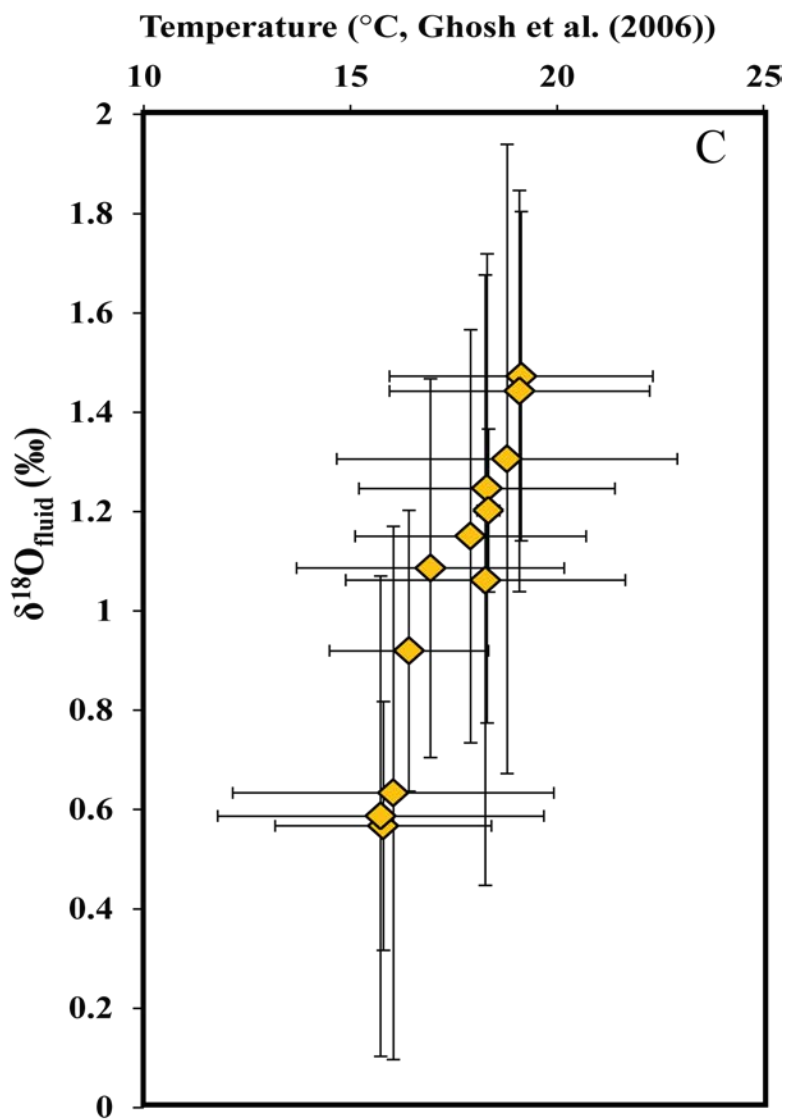
Figure 3.8C - Plot of the composition of the dolomitizing fluid of the Unda core as calculated using the calibration of Fritz and Smith (1970). Temperatures were calculated from clumped isotopes using the calibration of Ghosh et al. (2006) in the CDES. Error bars represent ± 1σ.
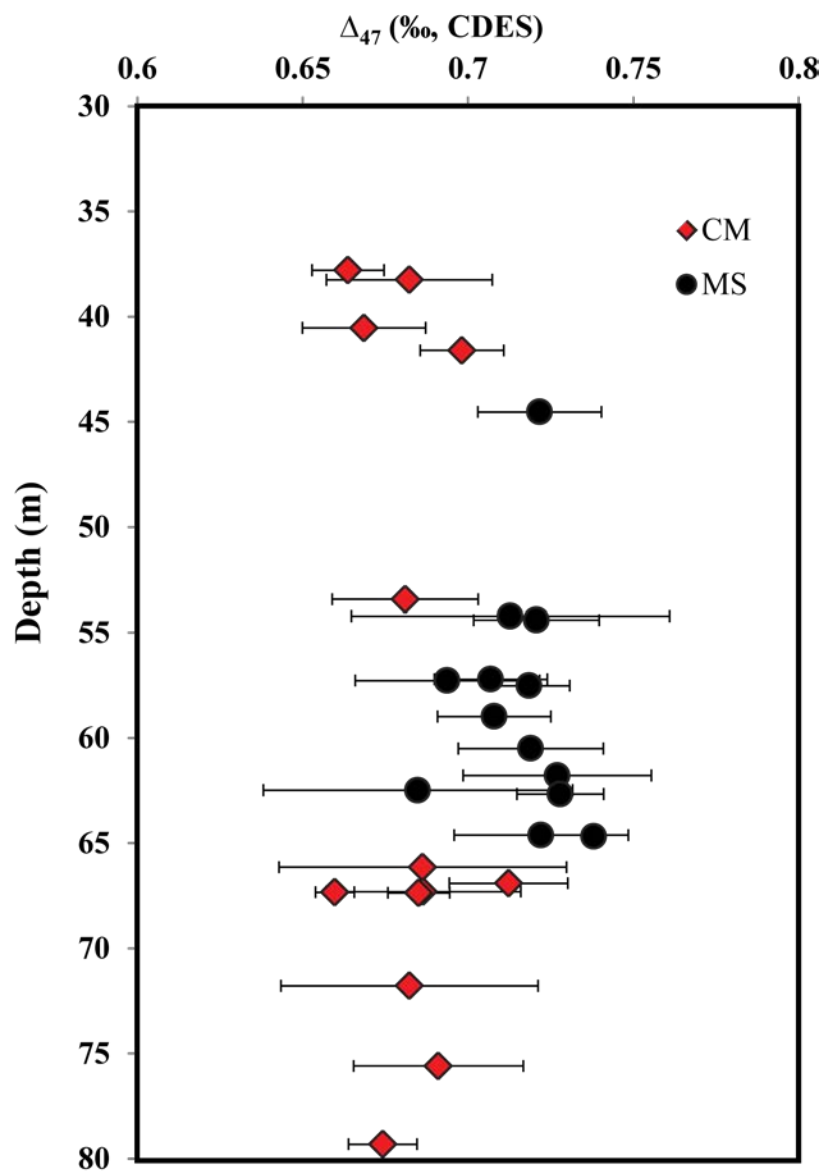
Figure 3.9 - Plot showing the different dominant dolomite fabrics: crystalline mimetic (CM) and microsucrosic (MS), within the upper portion of the San Salvador core relative to their measured Δ_{47} value. Error bars represent $\pm 1\sigma$.

by the dissolution of precursor aragonite or HMC. This conclusion would suggest that the dolomites formed after the reefal section was completely altered to LMC and any remnant Sr was swept away by fluids before dolomitization began. Although only samples from the completely dolomitized reefal section were measured in this study, the results do lend credence to the formation of the background and hard-ground associated dolomites having formed through different processes, and possibly different fluids, than the dolomites in this section.

San Salvador

This study corroborates the results of previous research that these dolomites formed at low, earth surface temperatures and from normal to slightly evaporative seawaters (Dawans and Swart, 1988; Supko, 1970, 1977; Swart et al., 1987). This is also true for the LMC sample which produced nearly identical results for the temperature and $\delta^{18}O_{fluid}$ values to the dolomites despite using the significantly different acid fractionation corrections as discussed in Chapter 2.

The temperature and fluid data suggests that the SS dolomites were formed by at least two distinct fluid sources, 1) a ≈20 to 25°C fluid with composition similar to seawater which is apparent in the section of the core from 53m to 79m depth, 2) a warmer, ≈30 to 35 C evaporative fluid (+2 to +3.5‰) fluid that has contributed to the rest of the dolomitized section (Figure 3.6). This would suggest that at least two separate dolomitization episodes have occurred.

The most likely source of the evaporative fluids was the restricted, hypersaline pools that are present on the island of San Salvador (Baldini et al., 2007; Dupraz et al., 2013; Hagey and Mylroie, 1995). Based on modern measured values, these pools have

greater $\delta^{18}O$ than the surrounding ocean and can be expected to reach greater temperatures considering the heat capacity of a restricted pool is less than the oceans. These fluids would have to have been moved through the island by a brine reflux mechanism. The reflux mechanism has been shown to exist on Great Bahama Bank (Whitaker and Smart, 1990; Whitaker and Smart, 1993) and has been suggested to be a viable fluid driver with increases in salinity to as little as 37 to 42‰ (Simms, 1984). Measurements of salinity in Salt Pond, one of the many evaporative pools on San Salvador, suggested salinity varied in the pool from 60 to 170 psu (Paerl et al., 2003). Based on the dating of dolomitization from Sr isotopes (Swart et al., 1987) and the correlation with the timeframe of deposition as determined by magnetostratigraphy and biostratigraphy (McNeill et al., 1988; Supko, 1970, 1977), it can be suggested that these brines have been a consistent source of dolomitizing fluid throughout` the history of San Salvador.

The other fluid characterized by the clumped isotope results is similar to seawater. It is most identifiable in the section of the core between 53m to 79m depth with possible other samples suggesting similar influence. This fluid has a lower $\delta^{18}O$ value, typically between 0‰ and 1‰ and temperatures as low as 20°C. Considering that seawater is external to the island, it could have been driven in through tidal pumping, seepage influx, or Kohout convection. Otherwise, the fluid could have been sourced from the island pools during marine high stands. In order to produce a less evaporative fluid, the pools would have to have an increased connectivity with the surrounding seawater causing more exchange which is easiest explained by increased sea level

Sr-isotopes measured from the dolomitizes suggest that this dolomitization event occurred significantly later than the dolomitization that occurred throughout the rest of the core from the evaporative fluid, even approaching modern times and fluids. The only time when seawater was high enough to overtake the island of San Salvador in recent history is during marine isotope stage 5e which does correlate well with the age suggested by U/Th dating of 150,000 ybp (Swart et al., 1987). With the formation of a deep freshwater lens, the seawater could have been driven to the depths where dolomitization occurred by fluid density differences, similar to the conclusions for the dolomitization of Little Bahama Bank in Vahrenkamp and Swart (1994). The other possibility is that with elevated sea level shut down the brine reflux fluid flow leading to dominance of Kohout convection throughout the interior of the island. This would have driven normal seawater upwards providing a magnesium source for dolomitization.

The representation of this modern day fluid dolomitization event is clearly associated with the MS dolomites within the 53 to 79 m section of the core. The MS dolomites and CM dolomites have been shown to have statistically different Δ_{47} values within this section with the MS dolomites being enriched relative to the CM dolomites. The CM dolomites in this section have comparable Δ_{47} values to other sections of the core, and elsewhere, MS dolomites are indistinguishable from the other dolomite textures. This implies that the fluid was restricted to within this layer of the core, most likely by the density of the dolomite below or by fluid density associated with a mixing zone. The reasons for why the low temperatures are constrained to MS type dolomites is difficult to determine as it is impossible to tell if the precursor to these MS dolomites were less mature dolomites or LMC. Most likely, the reason involves a combination of

density of the rock allowing preferential exchange of fluids to certain layers and the maturity of the different dolomite layers.

A single shallowing upwards sequence between 52 and 68 m core depth was measured in detail to see if there are any associated changes with clumped isotopes and the compositional fluids (Figure 3.10). It can be seen that temperatures are elevated at both the top and bottom of the section where the sea level cycle was interpreted previously to be at a minimum. As the sea level deepened, it is seen that clumped isotope temperatures decrease suggesting less influence from the interpreted warmer evaporative pools and a greater influx of seawater contributing to dolomitization. This is corroborated by the calculated $\delta^{18}O$ fluid values which show a similar trend.

Little Bahama Bank

The dolomite samples from GBII and WCI are relatively similar to each other with respect to the $\delta^{13}C$, $\delta^{18}O$, and Δ_{47} values, and calculated temperature (Figure 3.11). This would imply a common origin for the dolomites found in these cores and that there is a direct link of fluids across the bank which agrees with the results of previous work on these cores (Vahrenkamp, 1988; Vahrenkamp and Swart, 1994; Vahrenkamp et al., 1991; Williams, 1985).

The clumped isotopes suggest that dolomitizing fluids were approximately 20°C in both cores. This is a few degrees lower than modern day summer-high sea surface temperatures on Little Bahama Bank, but well within an acceptable range of temperatures for the latitude of the Bahamas. Using the dolomite fluid calibration of Fritz and Smith (1970), the calculated fluids throughout both cores show a slight increase in $\delta^{18}O_{fluid}$ with depth, possibly suggesting a greater influence from an evaporative fluid, but the bulk of
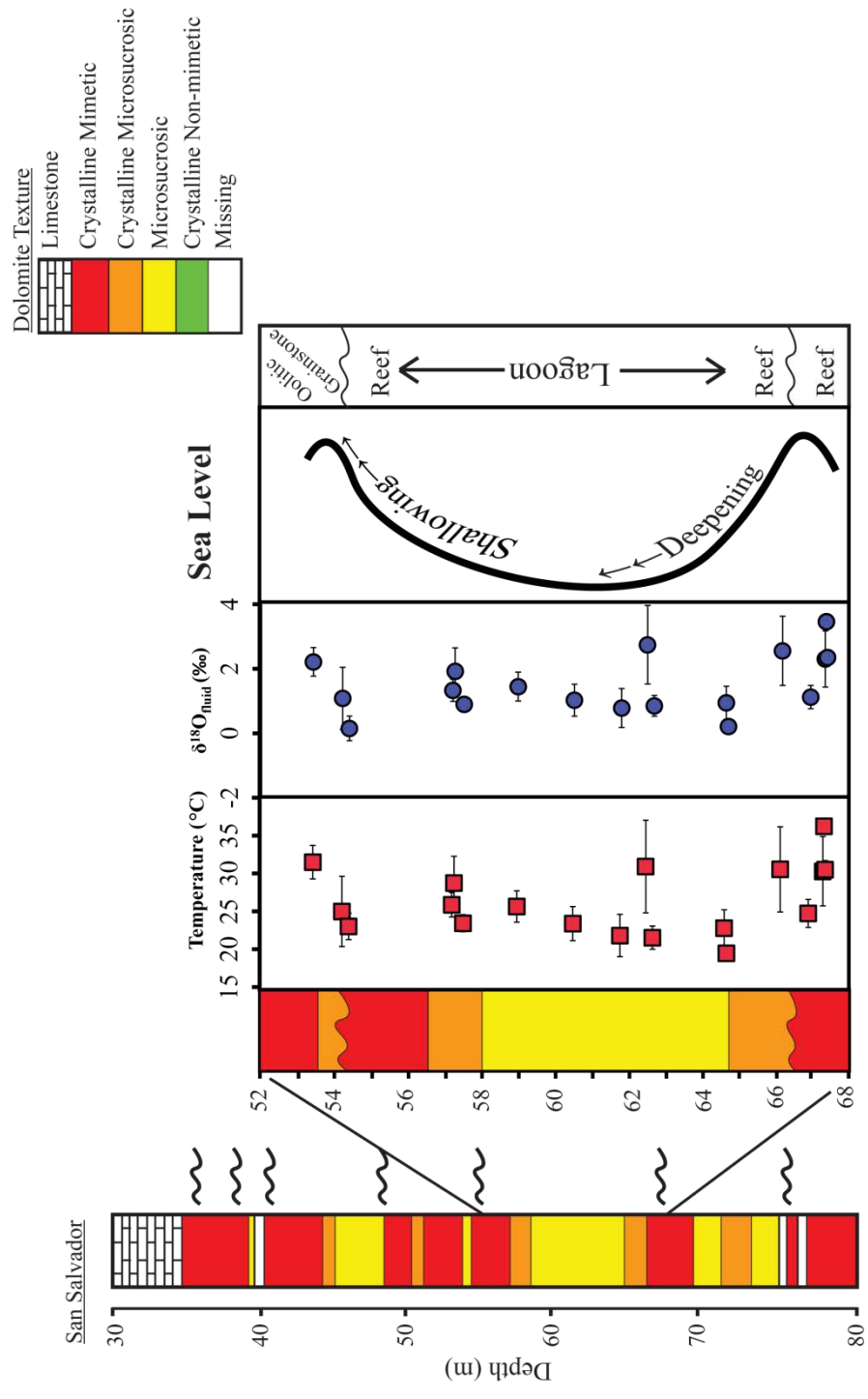
Figure 3.10 - San Salvador section showing a number of subaerial exposure surface unconformities (〰) throughout the length of the core indicating multiple sea level cycles. A zoomed in core description of one sea level cycle between 52 m and 68 m depth paired with clumped isotope temperatures (Ghosh et al., 2014, CDES) and $\delta^{18}O_{fluid}$ values (Fritz and Smith, 1970). Adapted from Dawans and Swart (1988).
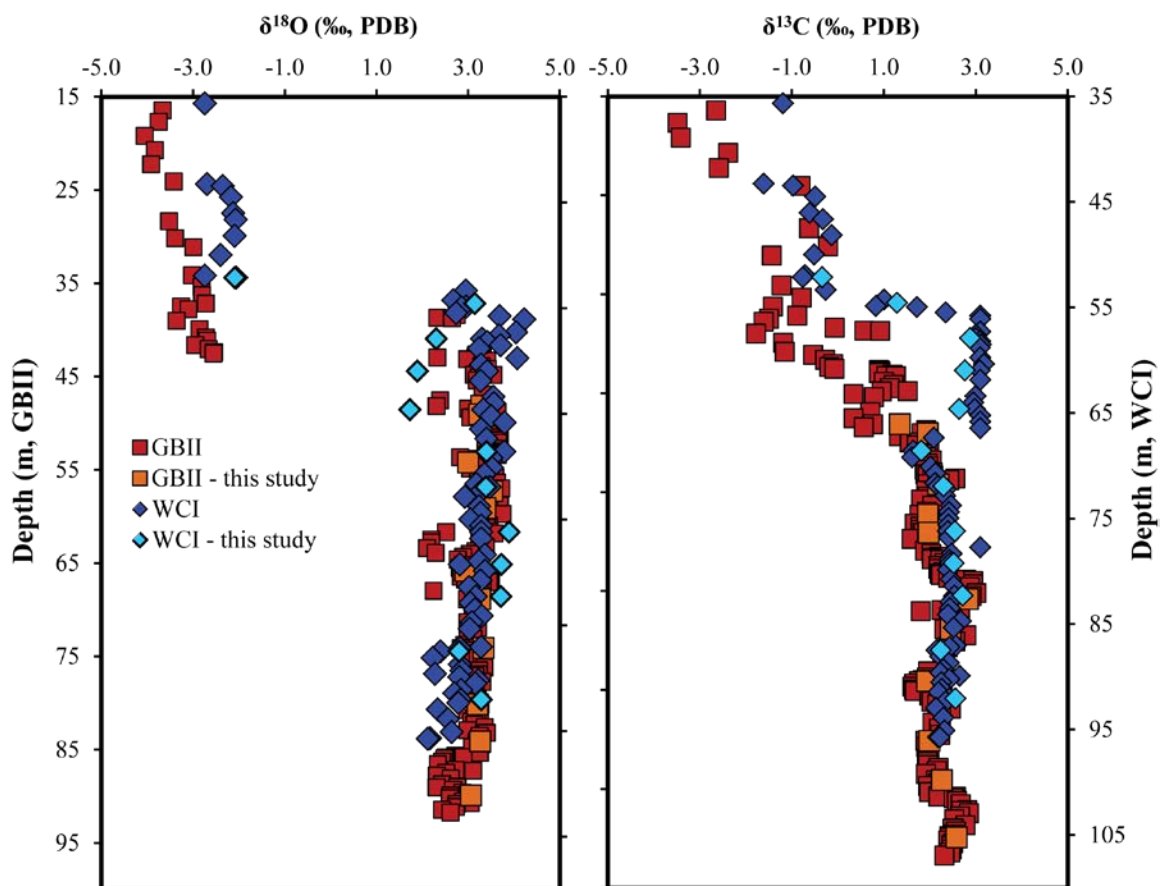
Figure 3.11 - Carbon and oxygen isotopes for the cores from Little Bahama Bank. Error bars represent ± 1σ, though they are typically smaller than the symbol size. Data not indicated as being from this study are taken from the work of Vahrenkamp and Swart (1994). Oxygen isotopes have been corrected for the difference in acid digestion fractionation between LMC and dolomite of 0.8‰ based on the bulk % dolomite present in the sample as determined by X-ray diffraction.

signal appears to be similar to normal marine sea-water. If the increasing trend with depth were seen in deeper cores, it may be indicative of a brine reflux occurring across Little Bahama Bank.

Interpretation of Dolomite Textures

In the section of the SS core between 53m and 79m depth, there had been shown to be a statistically significant difference between the CM and MS dolomite textures; however the difference breaks down outside of this section. This agrees with Dawans and Swart (1988), which showed using the student's t-test that there was a statistically significant difference at the 99% confidence level for the oxygen isotopes of CM and MS dolomites in this core but not in the carbon isotopes. Based on the collective evidence of different clumped isotope temperatures, calculated fluid composition, and age of precipitation (as determined with Sr and U/Th isotopes (Swart et al., 1987; Vahrenkamp et al., 1991)), the logical conclusion is that these MS dolomites are predecessors to the original dolomite fabric which would have formed around the same time frame as the dolomites above and below. This would suggest that the MS dolomite texture is not associated with the original composition of the carbonate, but is a more evolved form of the CM dolomite texture. This agrees with the original definition of CM and MS dolomites in Dawans and Swart (1988) as the MS dolomites trend towards being more stoichiometric than CM dolomites, as CM dolomites never reach a stoichiometric composition, suggesting a more prolonged period of time being exposed to dolomitizing fluids. This interpretation also agrees with the textures seen in the GBII and WCI cores as the presence of the MS dolomite fabric is more abundant towards the bottom of the cores where exposure time has been the longest.
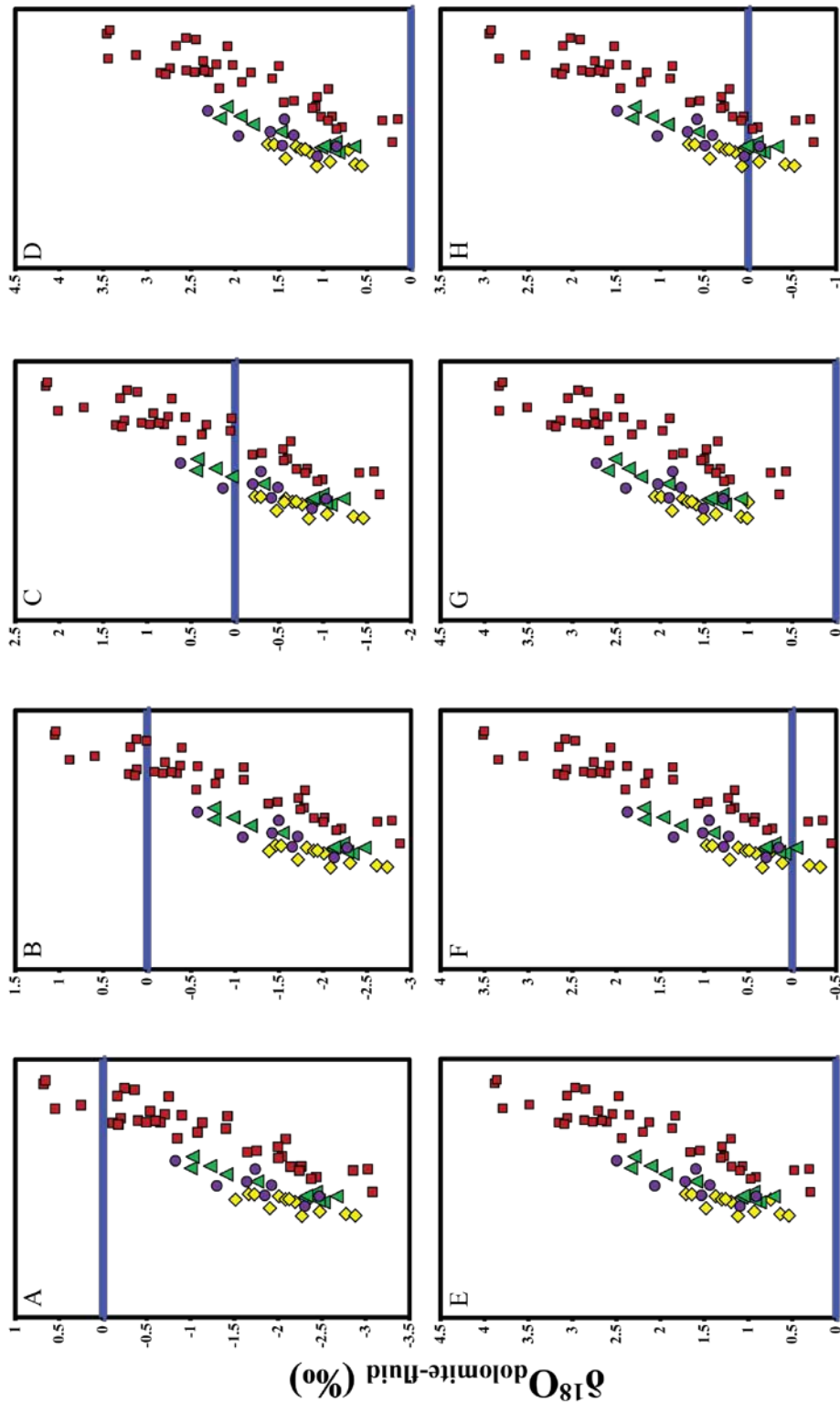
Temperature (°C, Ghosh et al. (2006), CDES)

Figure 3.12 - Clumped isotope temperatures for the four dolomite core sites: San Salvador (■), Unda (◇), GBII (▲), and WCI (●), plotted against the δ¹⁸O$_{dolomite-fluid}$ calculated using eight different known calibrations. The x-axis is always from 0 to 40 °C with increasing temperature to the right. The blue horizontal line represents 0‰ δ¹⁸O$_{dolomite-fluid}$ on the y-axis. The δ¹⁸O$_{dolomite-fluid}$ calibrations include **A)** Northrop and Clayton (1966), **B)** O'Neil and Epstein (1966), **C)** Shepard and Schwarz (1970), **D)** Fritz and Smith (1970), **E)** Matthews and Katz (1977), **F)** Zheng (1999), **G)** Vasconcelos et al. (2005), and **H)** Horita (2014).

Appropriate Dolomite-Fluid Formula

Multiple calibrations have been proposed for the relationship between the isotopic composition of the dolomite and the equilibrium temperature and composition of the parent fluid (Fritz and Smith, 1970; Horita, 2014; Matthews and Katz, 1977; Northrop and Clayton, 1966; O'Neil and Epstein, 1966; Sheppard and Schwarcz, 1970; Vasconcelos et al., 2005; Zheng, 1999). To date, there has been no consensus on which of these formulas is most appropriate for use with dolomites. Using clumped isotope temperatures as a fluid-independent approach for addressing this problem, some conclusions can be drawn about which formulas produces fluid values that are the least realistic for these Bahamian dolomite samples (Figure 3.12).

Working under the assumption that none of these dolomites have been precipitated from fresh water (δ^{18}O < 0‰), nor are they associated with extremely evaporative brines beyond what was found on San Salvador (δ^{18}O > 3‰), multiple calibrations can be ruled out as inappropriate for these samples. All three of Northrop and Clayton (1966), O'Neil and Epstein (1966), and Sheppard and Schwarcz (1970) produce fluid compositions that are too negative, with the bulk of the measurements falling below the zero line to values as negative as -3‰. Utilizing both Zheng (1999) and Horita (2014) result in comparably more positive and reasonable values, but produce a low-end which still suggests dolomitization by fresh water up to -1‰. The other three formulas, Vasconcelos et al. (2005), Fritz and Smith (1970), and Matthews and Katz (1977) all produce fluid compositions that are in line with the criteria of dolomite formation with the calibration in Vasconcelos et al. (2005) producing the most extreme fluid values up to 4‰, though in all cases the San Salvador dolomites exceed 3‰ fluid

value. This constraint could be relaxed if it can be assumed that during sea level low-stands the evaporative pools on San Salvador would become more saline as fluid supply is restricted. This line of evidence leads to the conclusion that the dolomite-fluid calibration best suited for the Bahamian dolomites is one of these three formulas, or a formula similar to these.

Summary

It has been shown that there is good agreement between previously published models of dolomitization and the interpretable results from clumped isotope paleothermometry on a suite of dolomite samples from cores taken on San Salvador, Great Bahama Bank, and Little Bahama Bank in the Bahamas. Both locations produced realistic temperatures from converted Δ_{47} values for precipitation by normal or slightly altered seawater in the Caribbean, however San Salvador dolomites produced temperatures that were $\approx 10°C$ warmer than those from Little Bahamas Bank. This can be related directly to the source of the fluids. Based on this work, the San Salvador fluids are derived from external seawater or from the warm evaporative pools located on the island. The Grand Bahama Island and Walkers Cay cores suggest dolomite formation from normal seawater most likely sourced from Little Bahama Bank with slightly more influence from an evaporative fluid with depth. These varying fluid sources have contributed to different dolomite textures that show evolution through time being controlled more by exposure to saturated fluids than by original fabric composition.

Chapter 4 – Clumped Isotope Variations in a Mixed Calcite-Dolomite Interval from a Constrained Geologic Setting

Background

The majority of clumped isotope studies have focused on a single mineralogical phase. This has been prudent during the developing stages of clumped isotopes as it has reduced the abundance of variables that could influence variations in results between studies. However, initial mineralogy, vital effects, and the composition of the parent fluid were thought to have little influence on the Δ_{47} value of a carbonate material (Came et al., 2007; Eiler, 2007; Ghosh et al., 2006).

As shown in chapter 2 of this work, calcite, dolomite, and aragonite do not behave identically in all aspects in regards to measuring clumped isotopes. This makes samples of a mixed mineralogy more difficult to properly measure than originally presumed. A conclusion similarly reached by previously published theoretical works including Guo et al. (2009) and Yuan et al. (2014) that have shown the Δ_{47}-temperature relationship between calcite, aragonite, and dolomite can vary by as much as 0.037‰ at 25°C. A situation in which all mineralogies do not behave similarly isotopically would restrict the application of clumped isotopes to more realistic mixed-mineralogy settings until a complete understanding on Δ_{47}-temperature relationships is determined.

Multiple contributing factors could play a role in causing incorrect clumped isotope results from mixed carbonate samples. A factor previously discussed in this work is the application of acid digestion fractionation corrections. This issue is most

applicable to samples containing dolomites as the difference in fractionation between LMC, aragonite, and siderite (Fernandez et al., 2014) show little difference in measured acid digestion fractionation values. However, as more research is done and these numbers are refined, they may become significant.

The other major factor is the non-linear mixing relationship between CO_2 gases with different $\delta^{13}C$, $\delta^{18}O$, and δ^{47} values. This concept has been reviewed with respect to CO_2 and N_2O (Affek and Eiler, 2006; Eiler, 2007; Eiler and Schauble, 2004; Schauble et al., 2006) with a few studies mentioning its impact on carbonate samples (Bristow et al., 2011; Defliese and Lohmann, 2015; Henkes et al., 2013). These studies have shown that Δ_{47} values deviate from a linear mixing model when the endmembers have large difference in $\delta^{13}C$, $\delta^{18}O$, and δ^{47} values, with Affek and Eiler (2006) measuring a deviation up to 0.042‰ in a mixture of car exhaust and atmosphere. There are documented cases of disagreement between measured growth temperatures of carbonates, such as in corals (Saenger et al., 2012) and speleothems (Affek et al., 2008; Daeron et al., 2011), relative to their calculated temperature of formation from clumped isotopes. It is possible that the homogenizing of a variety of carbonates with differing composition in order to meet the 8-10 mg sample requirement for clumped isotopes is causing significant effects on the measured Δ_{47} value.

In order to approach the problem of measuring clumped isotopes in mixed carbonates, samples from the Clino core, a mixed carbonate core from the Bahamas containing LMC, aragonite, and dolomite in varying abundances were collected. These samples have been extensively studied with a well-developed depositional

history as well as constraints on the timing of dolomitization events. Samples were treated multiple times with a weak acid to remove the less stable carbonate minerals until the sample had a homogenous dolomite composition. This dolomite endmember along with the bulk material and all treatments were then measured for clumped isotopes and mixing models were developed to determine the influence of varying mixed compositions on the resulting Δ_{47} value.

Samples

The Clino core was drilled off the western margin of Great Bahama Bank as part of the Bahamas Drilling Project and penetrated more than 670 meters into Mio/Pliocene inclined slope carbonates. Multiple studies have reported on the composition and interpretation of this core which will be summarized here (Eberli et al., 1997; Melim et al., 2004; Melim et al., 1995; Melim et al., 2001; Swart and Melim, 2000). The original composition was a combination of marine-derived aragonite and LMC in the form of skeletal packstone to grainstone as well as a shallowing upwards sequence of peloidal and skeletal wackestone or coral framestone (Melim et al., 2002) and its mineralogy has evolved over time by a combination of meteoric, mixing zone, and marine burial diagenesis (Fig 4.1).

The modern core can be broken into three distinct lithologic layers: 1) An upper layer of reefal deposits and shallow water platform derived sediments (21.6 to 197.4 m), 2) a middle layer which is mostly non-skeletal fine-grained sediments with periodic layers of skeletal material (197.4 to 367.03 m), and 3) a deep layer that is a mixture of skeletal and fine-grained non-skeletal sediments (367.03 to 677.27 m)
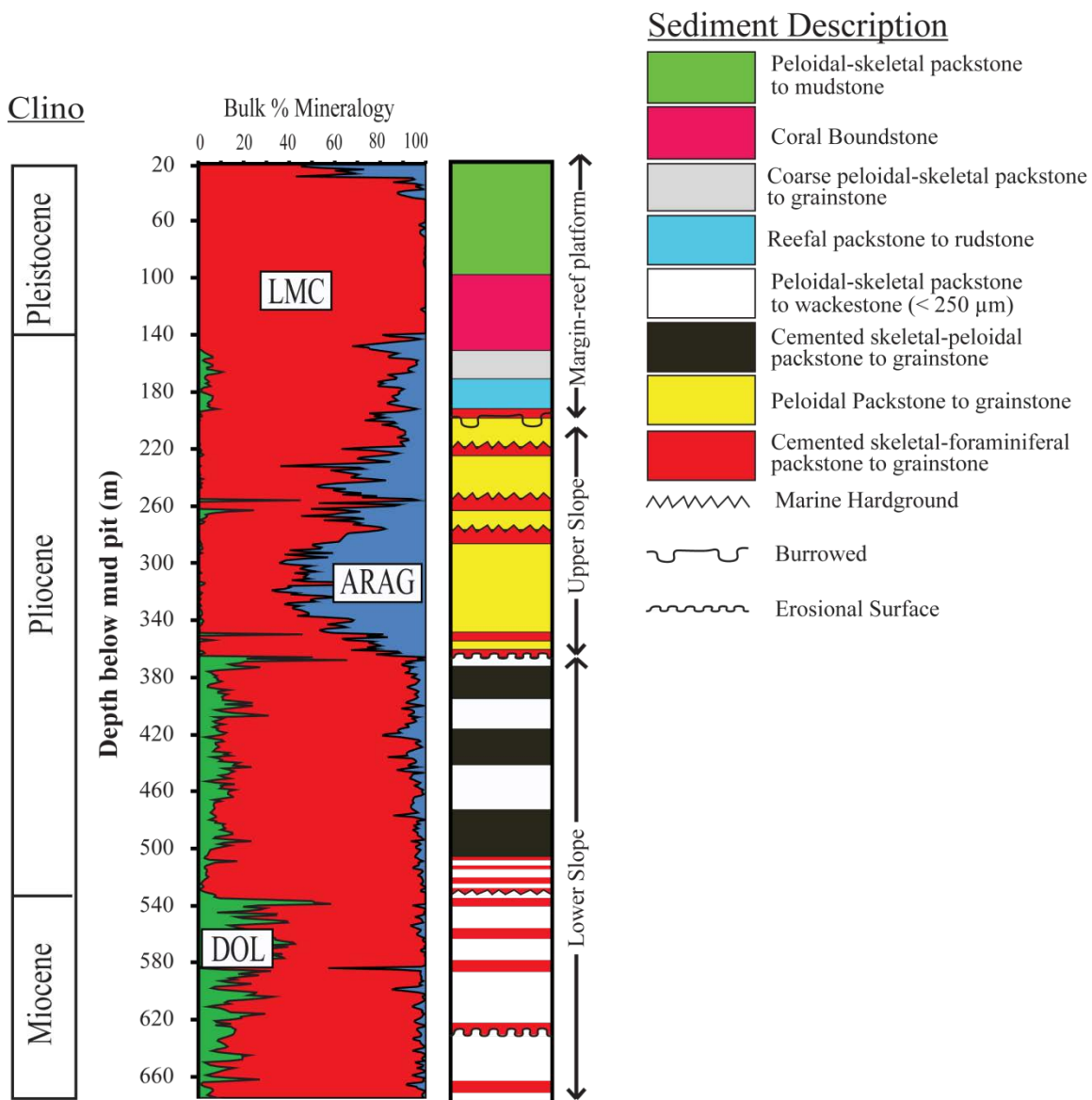
Figure 4.1 - Adapted from Eberli et al. (1997). Lithology and sediment description of the Clino with bulk mineralogy as determined through X-ray diffraction.

diagenesis to positive values more expected of marine burial diagenesis. The greatest abundance of dolomite in the core is found to be associated with marine hard grounds, lithified sediments that have been extensively cemented from extended periods of exposure and non-deposition on the seafloor (Wilson and Palmer, 1992), but dolomite rarely exceeded more than 50% of the bulk composition, and typically much less. The dolomites were calcium-rich, ranging from 41.8 to 45.8 mol % magnesium, with increased stoichiometry related to increased abundance (Swart and Melim, 2000). Whereas some dolomitic cements were present, most dolomite was found replacing previous carbonate grains (Swart and Melim, 2000). Some of the skeletal debris was still easily identifiable including red algae, echinoderm spines, and *Halimeda*.

The $\delta^{18}O$ values measured in the dolomites in Clino were approximately 3‰ heavier relative to the associated carbonate (Swart and Melim, 2000). This agrees with the equilibrium difference between co-precipitated calcite and dolomite as suggested in Land (1980). Swart and Melim (2000) suggested that a depletion in the $\delta^{18}O$ value with depth below hard ground surfaces found in both the dolomite and LMC in a co-trending fashion suggests that the original aragonite sediments were diagenetically altered to LMC prior to dolomite formation indicating that the LMC and dolomite would have reached equilibrium with the same fluid.

The strontium concentrations range from 70 to 2378 ppm showing an increase with decreasing bulk percent dolomite. This change in Sr correlates with depth below hard ground surfaces (Swart and Melim, 2000). This trend in strontium is similar to profiles seen in the pore fluids from deep sea and periplatform

sediments which arise from the diagenesis of less stable forms of carbonate including aragonite and HMC that contain more strontium relative to LMC (Swart and Guzikowski, 1988). The strontium profile is taken as evidence that the dolomites formed in a deep sea environment relative to their shallow water precursor carbonates, which in the Bahamas is taken to suggest colder waters than seen at the surface, probably in the range of 10 to 15°C.

Based on this previous work, it has been concluded that the sediments of the Clino core were exposed primarily to two temperature regimes: 1) the warm sea surface where the original grains formed between 20 to 30°C, and 2) the deep bottom waters of the slope and rise which is estimated to be between 10 to 15°C.

Methods

Sample Treatment with Buffered Acetic Acid

Twenty-two mixed calcite/aragonite/dolomite samples were collected throughout the dolomitized sections of the Clino core from 365 to 650 m depth. Each bulk rock sample was mechanically ground then sifted to acquire portions smaller than 63 μm. This 63 μm portion was weighed and then a 75% of the total amount was treated using a buffered acetic acid solution for 2 to 3 hours with the other 25% stored for later measurement. The treated sample was then rinsed with DI water and allowed to dry in a 40°C oven over night. This cycle was repeated 2-3 times per bulk rock sample until the sample obtained a ≈100% dolomite composition as determined by X-ray diffraction and scanning electron microscopy.

Measurement of Isotopes

The Clino treatments were measured for clumped isotopes primarily between March of 2013 and June of 2014 with a few repetitions in 2015. Samples were digested and measured following the methods described in chapter 1 of this work.

Linear Mixing Models and the Application of Isotopic Corrections

In post processing, the Δ_{47} values are adjusted for the fractionation that occurs during dissolution of carbonates at 90°C relative to 25°C. To this author's knowledge, no previous study has ever addressed the proper application of differing fractionation factors in mixed carbonate samples. This is particularly true, as prior to this work there was no reason to believe that carbonate clumped isotopes measurements had significantly different acid digestion fractionations. The approach taken in this work was to simply apply a linear mixing model between the two acid fractionation values (0.092‰ for calcite and aragonite (Henkes et al., 2013) and 0.153‰ for dolomite (Murray et al., 2016)) and the percent dolomite remaining in the sample as determined by XRD.

This method of equal application of fractionation factors may be inaccurate as one mineralogical state may overshadow the influence of the other in terms of Δ_{47}, especially considering the difference in rate of reaction within phosphoric acid between LMC and dolomite which could promote a greater LMC signal if the reaction does not go to 100% completion. To justify a linear mixing model, an experiment was conducted where two pure endmember carbonates, LMC and dolomite, derived from similar localities to Clino in the Bahamas were mixed in various known proportions and their clumped isotopes
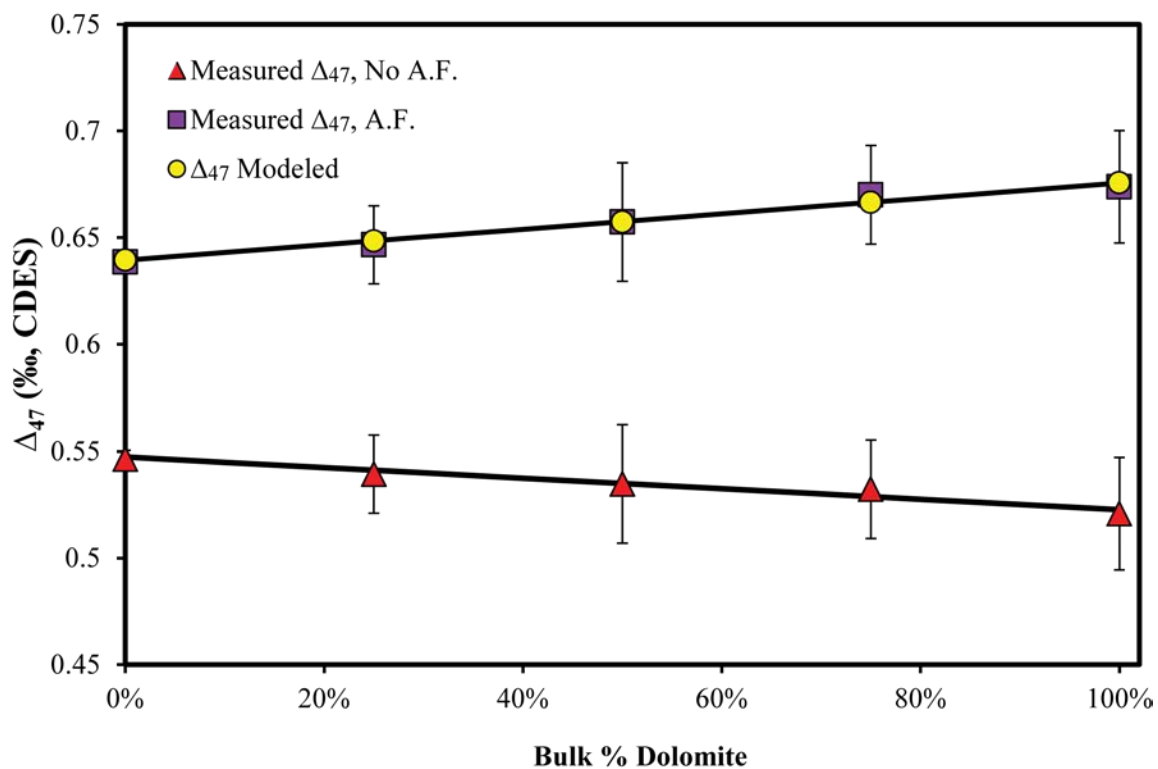
Figure 4.2 - Manually mixed dolomite and LMC endmembers shown with and without the addition of the acid fractionation (A.F.) of 0.153‰ (Murray et al., 2016). This is compared with the non-linear mixing model of Defliese and Lohmann (2015).

measured (Figure 4.2). The results of the experiment were then compared to the endmember mixing model of Defliese and Lohmann (2015). The results suggest that with respect to Δ_{47}, $\delta^{18}O$, and $\delta^{13}C$ values, that a linear mixing model is appropriate within error.

The same problem persists when calculating the temperature of mixed carbonates from clumped isotopes. This problem is more difficult to resolve as there is no designated dolomite clumped isotope calibration, while calcite and aragonite samples have more than could reasonably be discussed in a single work. Again, the simplest approach is taken: all Δ_{47} values are converted to temperature using a single formula, Dennis et al. (2011) equation 9.

With respect to other isotopes, a linear mixing model is also employed in order to calculate the endmember compositions for LMC and dolomite. While most dolomite endmembers are directly measured from the final acetic acid treatment which was typically 100% dolomite, the LMC endmember had to be determined as no sample in the study was originally 100% LMC. All reported endmember isotopic values were determined by a weighted least squares regression through the measured data relative to the percent dolomite remaining in the sample. Errors on the isotopic endmember values are determined by a 95% confidence interval. Because no calcite endmember was directly measured, the 95% confidence interval produces significantly larger errors for the calcite endmember than the dolomite endmember, especially in bulk samples that were originally a greater percentage dolomite.

Defliese Mixing Model

To take into account any possible influence from the mixture of CO_2 gases derived from varying sources (LMC and Dolomite endmembers), a modeling program used by Defliese and Lohmann (2015) was employed. The program uses endmember composition, in this case the calcite and dolomite endmembers as determined by weighted least-square regression, and calculates the Δ_{47} offset that would occur through their mixture. Defliese and Lohmann (2015) concluded that significant offsets were only seen between samples that had differences in $\delta^{18}O$ and $\delta^{13}C$ values on the order of 2‰ between both isotopes or 15‰ in a single isotope. Because of the shared origin of the Clino LMC and dolomite samples, they do not tend to meet either of these requirements as the offset in the $\delta^{18}O$ value is up to 3‰, but the difference in the $\delta^{13}C$ value is typically only 1‰. Despite this, any significant offset from a linear mixing model created by the combination of CO_2 endmembers will be taken into account and quantified as this method may become more applicable in systems where the dolomite and LMC are not both formed from similar sources.

Results

$\delta^{13}C$ and $\delta^{18}O$ Values

According to XRD, the dolomite percentage in all the bulk samples before any acetic acid treatments ranged from 5 to 83 %. Over this range of composition, bulk samples had $\delta^{13}C$ values from 2.1 to 3.8‰ (Figure 4.3) and $\delta^{18}O$ values from 0.4 to 3.2‰ (Figure 4.4). Acetic acid washes enabling the measurement of the dolomite endmember showed a strong trend ($r^2 = 0.89$) between dolomite percentage and an increasing $\delta^{18}O$ value that suggests the dolomite endmembers are 3‰
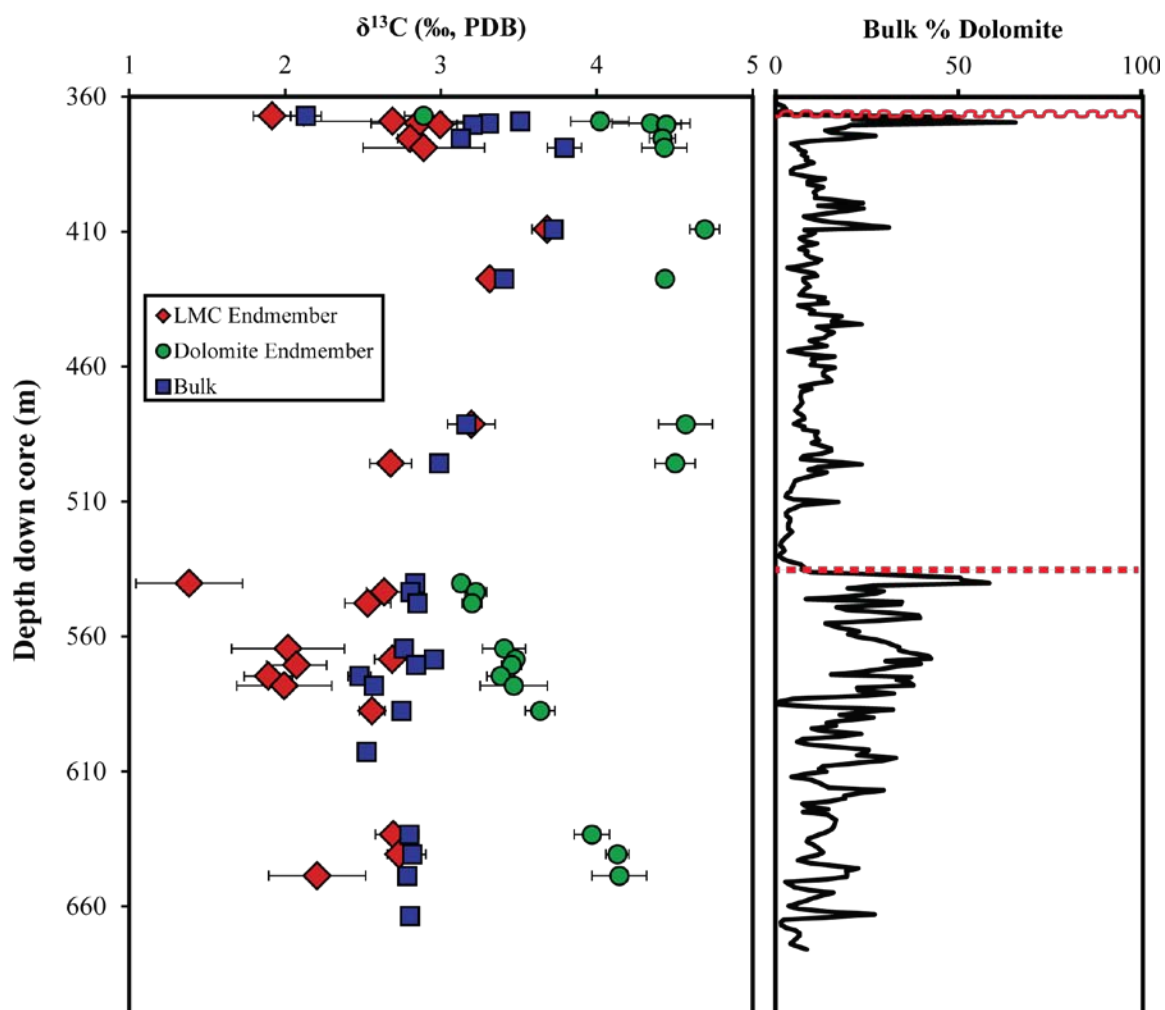
Figure 4.3 - The δ¹³C of Clino as presented through the measured bulk and dolomite endmembers as well as the low-mg calcite endmember calculated using a weighted least square regression. This is compared to the bulk dolomite percentage as determined by X-ray diffraction and the identified erosional (〰〰) surface and marine hardground (▪▪▪▪). Error bars represent ± 1σ.
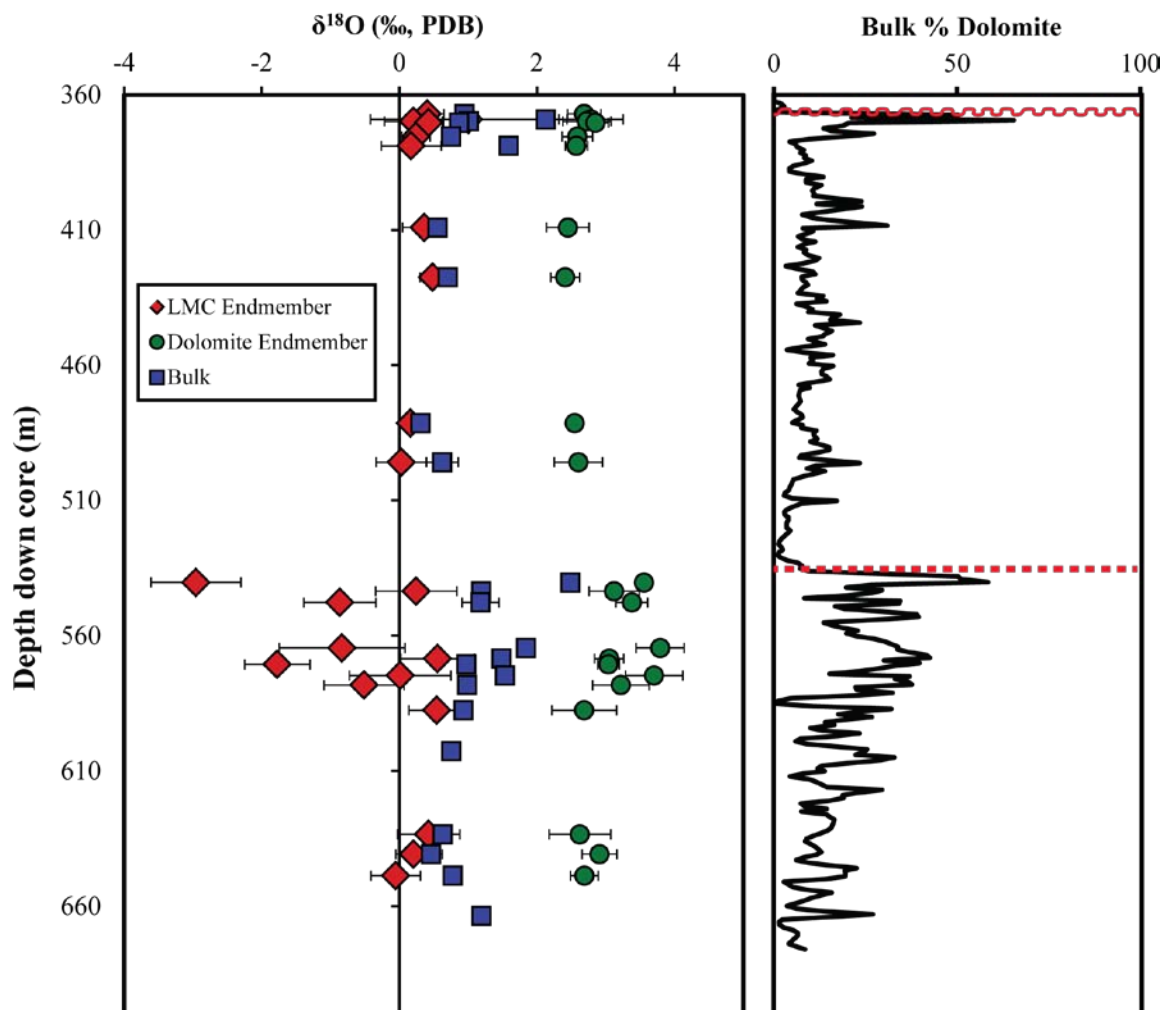
Figure 4.4 - The δ^{18}O of Clino as presented through the measured bulk and dolomite endmembers as well as the LMC endmember calculated using a weighted least square regression. This is compared to the bulk dolomite percentage as determined by X-ray diffraction and the identified erosional ($\sim\!\sim\!\sim$) surface and marine hardground ($\cdots\cdots$). Error bars represent $\pm$ 1σ.

heavier than the calcite endmember. If it can be presumed that the LMC and dolomite endmembers were derived from the same fluid, this 3‰ offset is in good agreement with observations made in other dolomite studies (Land, 1983; Swart and Melim, 2000). The $\delta^{13}C$ value also shows a trend towards heavier values in the dolomite endmember, by an average of 0.9‰ which is in agreement with the findings of Sheppard and Schwarcz (1970).

Scanning Electron Microscopy

The physical impact of the buffered acetic acid washes on the mineral crystals was observed through scanning electron microscopy; a sampling of select photos can be seen in Figure 4.5. Within the images, it was seen that both bulk and single acid-wash images show remnant amounts of calcite in abundance. The visible dolomite rhombs appear to be mostly intact will little evidence of dissolution. With each proceeding acid wash the amount of calcite was depleted as visible in the images and XRD, however, by the second and third acid wash, there was evidence of possible dissolution of the dolomite rhombs. What were presumed to have dissolved in these images are the less stable forms of calcian-dolomite. The effects of dissolution on the final results of this study are impossible to quantify, however there is little evidence to suggest it had a measurable effect on the clumped isotope measurements.

Clumped Isotopes (Measured)

The extrapolated Δ_{47} of the calcite endmembers from the measured samples ranged from 0.595-0.698‰ which translates to a temperature range of 28-53°C using the Ghosh et al. (2006) calibration converted to the CDES (Table 4.1). The dolomite
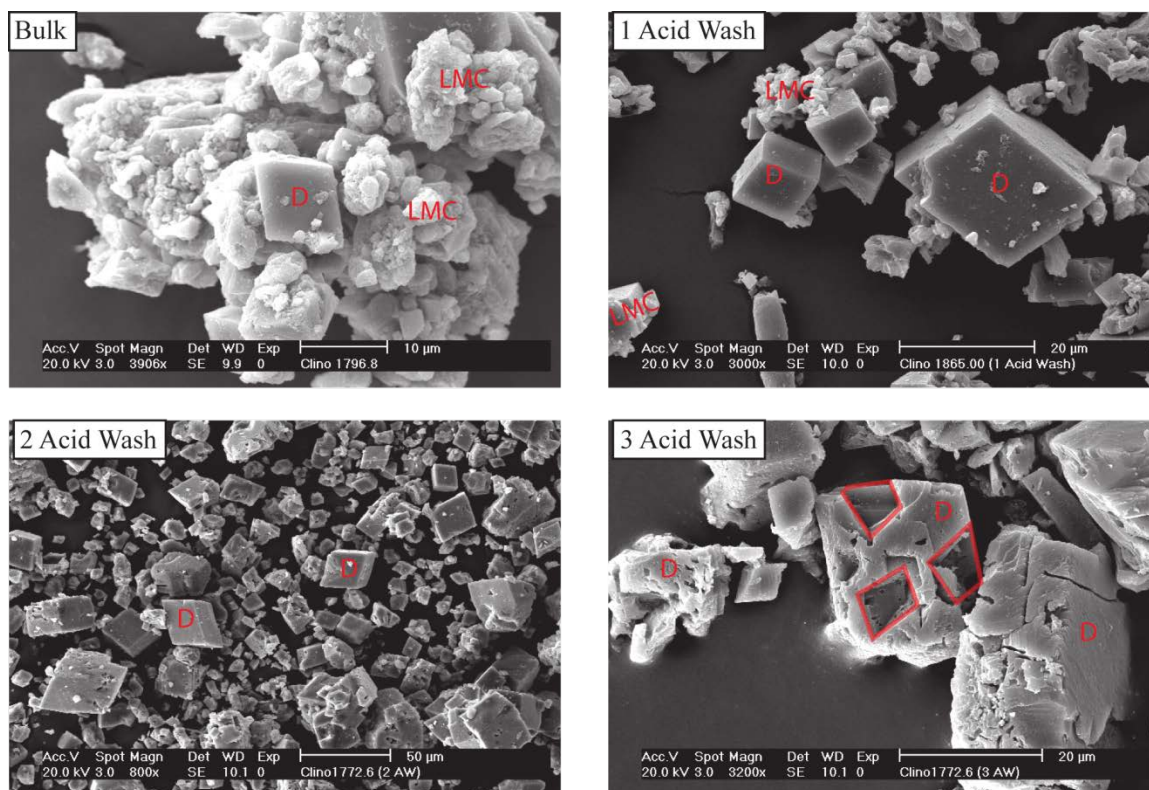
Figure 4.5 - SEM images showing the evolution of a bulk Clino sample through a series of treatments with buffered acetic acid. The red letters indicate mineralogy (D = dolomite, LMC = low-Mg calcite) as determined through visual inspection and electron dispersive X-ray spectroscopy. The third acid wash shows evidence of the dissolution of rhombic shapes out of the crystal structure (Outlined in red). These are believed to have been less stable forms of dolomite dissolving due to the treatments leaving only the most stoichiometric and stable dolomite endmembers.

Table 4.1 - Clino LMC Endmember

Depth (m)	δ¹⁸O Regression (‰)	Std. Dev.	δ¹³C Regression (‰)	Std. Dev.	Δ47_NOAF (‰)	Δ47 Regression (‰)	Std. Dev.	Δ47 Modeled (‰)	Ghosh et al. (2006) Regression (°C, CDES)	Ghosh et al. (2006) Modeled (°C, CDES)
367	0.4	0.2	1.9	0.1	0.523	0.615	0.023	0.617	47	47
369	1.0	1.4	2.7	0.6	0.558	0.650	0.140	0.653	38	38
370	0.2	0.4	2.9	0.3	0.503	0.595	0.028	0.597	53	52
370	0.4	0.2	3.0	0.1	0.557	0.649	0.036	0.650	39	38
375	0.2	0.2	2.8	0.1	0.524	0.616	0.046	0.618	47	46
379	0.2	0.4	2.9	0.4	0.509	0.601	0.038	0.605	51	50
409	0.4	0.3	3.7	0.1	0.544	0.636	0.029	0.637	42	42
427	0.5	0.2	3.3	0.0	0.517	0.609	0.034	0.609	49	49
481	0.2	0.1	3.2	0.2	0.557	0.649	0.020	0.650	39	39
496	0.0	0.4	2.7	0.1	0.572	0.664	0.019	0.666	35	35
540	-3.0	0.7	1.4	0.3	0.544	0.636	0.149	0.636	42	42
544	0.2	0.6	2.6	0.1	0.540	0.632	0.073	0.634	43	42
548	-0.9	0.5	2.5	0.1	0.513	0.605	0.041	0.608	50	49
564	-0.8	0.9	2.0	0.4	0.556	0.648	0.176	0.654	39	38
568	0.6	0.5	2.7	0.1	0.513	0.605	0.048	0.607	50	49
571	-1.8	0.5	2.1	0.2	0.591	0.683	0.110	0.689	31	30
575	0.0	0.7	1.9	0.2	0.606	0.698	0.033	0.701	28	27
578	-0.5	0.6	2.0	0.3	0.536	0.628	0.055	0.632	44	43
588	0.5	0.4	2.6	0.1	0.560	0.652	0.060	0.653	38	38
633	0.4	0.5	2.7	0.1	0.552	0.644	0.030	0.645	40	40
641	0.2	0.3	2.7	0.1	0.542	0.634	0.044	0.635	42	42
649	-0.1	0.4	2.2	0.3	0.528	0.620	0.038	0.623	46	45

- Results in columns designated as regressions were derived from a weighted least squares regression through all the data produced for that depth. Standard deviations were calculated using a 95% confidence interval. Results in the modeled columns are calculated from the end-member compositions for the Clino samples using the mixing model of Defliese and Lohmann (2015).

Table 4.2 - Clino Dolomite Endmember

Depth (m)	δ¹⁸O Regression (‰)	Std. Dev.	δ¹³C Regression (‰)	Std. Dev.	Δ₄₇_NOAF (‰)	Δ₄₇ Regression (‰)	Std. Dev.	Δ₄₇ Modeled (‰)	Ghosh et al. (2006) Regression (°C, CDES)	Ghosh et al. (2006) Modeled (°C, CDES)
367	2.7	0.2	2.9	0.1	0.524	0.677	0.023	0.677	32	32
369	2.8	0.5	4.0	0.2	0.539	0.692	0.046	0.692	29	29
370	2.7	0.3	4.3	0.3	0.527	0.680	0.026	0.681	32	32
370	2.9	0.2	4.4	0.1	0.537	0.690	0.032	0.691	29	29
375	2.6	0.2	4.4	0.1	0.522	0.675	0.049	0.676	33	33
379	2.6	0.2	4.4	0.1	0.550	0.703	0.014	0.703	27	27
409	2.4	0.3	4.7	0.1	0.549	0.702	0.028	0.702	27	27
427	2.4	0.2	4.4	0.0	0.524	0.677	0.039	0.677	32	32
481	2.6	0.1	4.6	0.2	0.580	0.733	0.023	0.733	21	20
496	2.6	0.4	4.5	0.1	0.558	0.711	0.018	0.711	25	25
540	3.6	0.1	3.1	0.0	0.568	0.721	0.013	0.721	23	23
544	3.1	0.4	3.2	0.1	0.590	0.743	0.045	0.743	19	18
548	3.4	0.2	3.2	0.1	0.590	0.743	0.018	0.743	19	18
564	3.8	0.3	3.4	0.1	0.554	0.707	0.067	0.708	26	26
568	3.1	0.2	3.5	0.0	0.538	0.691	0.019	0.691	29	29
571	3.0	0.2	3.5	0.1	0.546	0.699	0.036	0.700	27	27
575	3.7	0.4	3.4	0.1	0.536	0.689	0.019	0.690	30	30
578	3.2	0.4	3.5	0.2	0.570	0.723	0.039	0.723	23	23
588	2.7	0.5	3.6	0.1	0.537	0.690	0.070	0.691	29	29
633	2.6	0.4	4.0	0.1	0.557	0.710	0.030	0.710	25	25
641	2.9	0.3	4.1	0.1	0.536	0.689	0.043	0.689	30	30
649	2.7	0.2	4.1	0.2	0.533	0.686	0.021	0.687	30	30

- Results in columns designated as regressions were derived from a weighted least squares regression through all the data produced for that depth. Standard deviations were calculated using a 95% confidence interval. Results in the modeled columns are calculated from the end-member compositions for the Clino samples using the mixing model of Defliese and Lohmann (2015).

Table 4.3 - Clino Bulk Samples

Depth (m)	Dolomite (%)	δ¹⁸O (‰)	Std. Dev.	δ¹³C (‰)	Std. Dev.	Δ₄₇_NOAF (‰)	Δ₄₇ (‰)	Std. Dev.	Δ₄₇ Modeled (‰)	Ghosh et al. (2006) (°C, CDES)	Ghosh et al. (2006) Modeled (°C, CDES)
367	22%	0.9	0.1	2.1	0.1	0.522	0.627	0.007	0.629	44	44
369	61%	2.1	0.1	3.5	0.1	0.541	0.670	0.017	0.676	34	33
370	35%	1.0	0.0	3.3	0.0	0.513	0.627	0.002	0.625	44	45
370	17%	0.9	0.1	3.2	0.1	0.538	0.640	0.013	0.656	41	37
375	21%	0.8	0.1	3.1	0.0	0.517	0.621	0.011	0.628	46	44
379	59%	1.6	0.1	3.8	0.1	0.534	0.661	0.003	0.661	36	36
409	5%	0.6	0.1	3.7	0.0	0.533	0.628	0.016	0.640	44	41
427	7%	0.7	0.0	3.4	0.0	0.516	0.612	0.029	0.614	48	48
481	7%	0.3	0.1	3.2	0.0	0.557	0.653	0.028	0.655	38	37
496	20%	0.6	0.2	3.0	0.0	0.564	0.668	0.010	0.674	34	33
540	83%	2.5	0.1	2.8	0.0	0.564	0.707	0.021	0.707	26	26
544	31%	1.2	0.0	2.8	0.0	0.548	0.659	0.011	0.666	36	35
548	46%	1.2	0.3	2.9	0.1	0.539	0.659	0.011	0.668	36	34
564	55%	1.8	0.0	2.8	0.0	0.564	0.690	0.025	0.681	29	32
568	35%	1.5	0.1	3.0	0.0	0.523	0.636	0.017	0.635	42	42
571	56%	1.0	0.1	2.8	0.1	0.566	0.692	0.004	0.692	29	29
575	38%	1.5	0.1	2.5	0.1	0.578	0.693	0.010	0.695	29	28
578	42%	1.0	0.1	2.6	0.1	0.557	0.675	0.025	0.668	33	34
588	17%	0.9	0.1	2.7	0.0	0.553	0.656	0.001	0.659	37	36
633	7%	0.6	0.1	2.8	0.1	0.538	0.634	0.035	0.649	42	39
641	5%	0.5	0.2	2.8	0.1	0.547	0.642	0.039	0.637	40	42
649	28%	0.8	0.0	2.8	0.0	0.530	0.639	0.018	0.638	41	41

- Bulk Data is reported from measurements on untreated samples. The dolomite percentage was determined by x-ray diffraction. The Δ₄₇ final value was calculated using a linear mixing model to determine the applied acid fractionation (AF) based on the percent dolomite and acid fraction factors of 0.092‰ for the LMC endmember (Henkes et al., 2013) and 0.153‰ for the dolomite endmember (Murray et al., 2016). Modeled Δ₄₇ were based on the end-member mixing model of Defliese and Lohmann (2015) with results reported for the modeled sample with the same percent dolomite as within the bulk sample.

endmember's Δ_{47} values ranged from 0.675 to 0.743‰ which translates to a temperature range of 19-33°C (Table 4.2). The error on these temperature values averaged 7°C for the dolomites with a maximum error of 14°C, but the average for the calcite endmember was double that at 13°C with a maximum of 35°C. Fluid $\delta^{18}O$ values calculated from these temperatures using Fritz and Smith (1970) and Kim and O'Neil (1997) range from +1.8 to +7.8‰ for the calcites and +0.6 to +3.7‰ for the dolomites. A summary of the bulk material before any treatment can be found in Table 4.3.

Application of the Defliese et al. (2015) Mixing Model

As was suggested in the Defliese and Lohmann (2015), the effects of the model are minor on the final results of this study. The average difference between the measured Δ_{47} and that predicted by the model was 0.001‰ which is an order of magnitude less than the typically reported analytical uncertainty for a clumped isotope measurement (0.01‰). Therefore it has to be concluded that the non-linearity of clumped isotope measurements has little effect on the results of this particular study as the endmembers are too similar isotopically (Figure 4.6). That means any differences between the LMC and dolomite endmember clumped isotope results are indicative of real differences between the mineralogies.

Discussion

Possible Impact of Buffered Acid Washes

Multiple studies have used the technique applied here of treating bulk carbonates with a buffered acetic to remove the less stable carbonate endmembers from the dolomite and have reported no ill effects on their carbon and oxygen isotope values
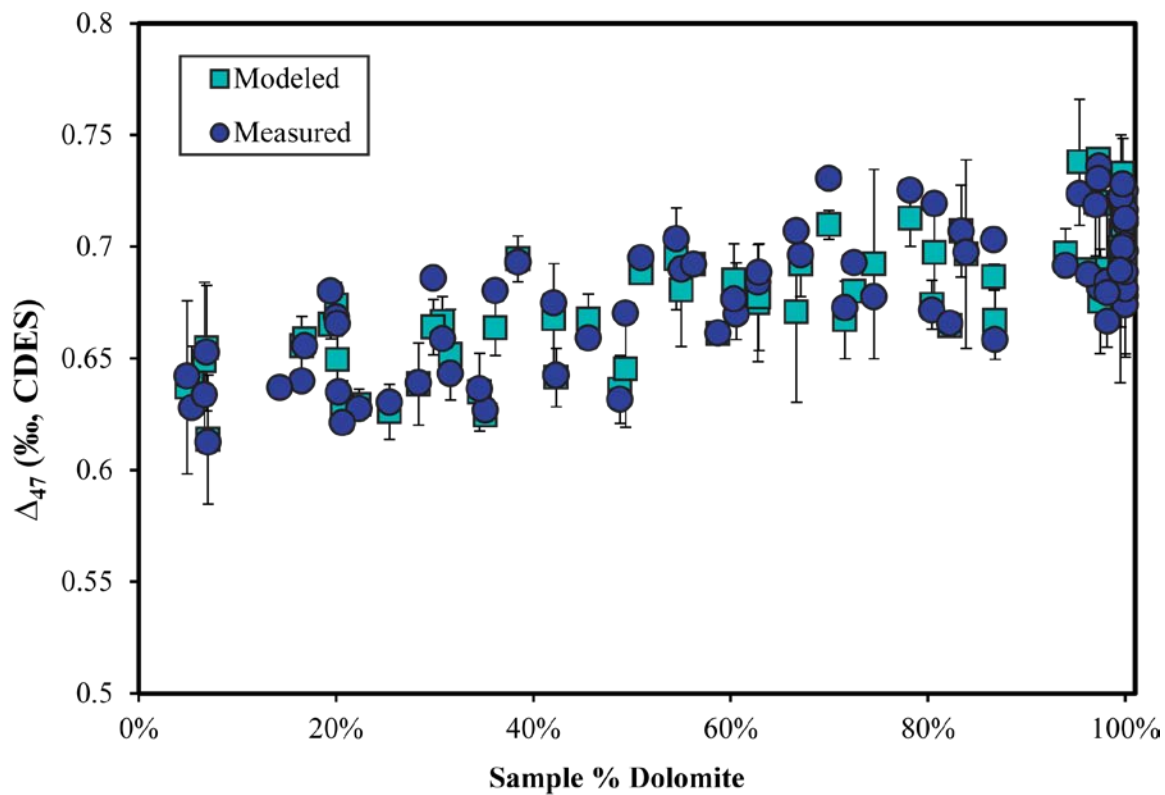
Figure 4.6 - Plot showing the similarity between measured Δ_{47} values for the treatments of Clino and the Δ_{47} estimated using the endmember composition of the individual samples with the non-linear clumped isotope mixing model from Defliese and Lohmann (2015). Error bars represent $\pm$ 1σ.

(Swart et al., 2005; Swart and Melim, 2000). In order to test the methods impact on clumped isotopes, sediments from depth 540.3m and 568.5m were treated with buffered acetic acid an additional time after having achieved 100% dolomite composition as determined by XRD. After measuring the samples for clumped isotopes, it is found that the additional treatment has no measureable statistically significant effect on the Δ_{47} value as both treatments are within error for each sample. It is possible that additional treatment would produce a measureable effect, but considering that no samples were progressively treated beyond 100% dolomite composition, it does not seem necessary to pursue such a case.

$\delta^{18}O$ and $\delta^{13}C$ Values of Endmembers

With respect to the $\delta^{18}O$ values of the LMC and dolomite endmembers, there is a variable 2 to 3‰ offset in the $\delta^{18}O_{LMC}$ value, typically fluctuating between 0 and 1‰, and the $\delta^{18}O_{dolomite}$ value ranging between 2.4 to 3.8‰. There is a spike to negative $\delta^{18}O_{LMC}$ values just beneath the 536.6 m hardground. This has been partially attributed to the error associated with extended extrapolations from high bulk dolomite % compositions as these samples also have the largest extrapolation errors of any of the LMC samples. However, the consistency of the signal across multiple samples with large degrees of variation in the bulk dolomite %, including samples with significantly less bulk % dolomite than other samples in the core that do not show such extrapolation signals, suggests that the trend toward negative $\delta^{18}O_{LMC}$ values is real. Based on the equilibrium fluid/temperature calibration of Kim and O'Neil (1997), to acquire such negative values in carbonates from normal seawater ($\delta^{18}O_{seawater} = 0‰$ VSMOW), would require fluid temperatures exceeding 50°C, of which no such body of water is known to

have existed in the Bahamas even at the depths of the core. This difficult to reconcile isotopic anomaly suggests the possibility for disequilibrium between the diagenetic sediments and the pore fluids.

The $\delta^{13}C_{\text{dolomite}}$ values show two unique trends distinctively separated by the 536.6 m hardground. Above this hardground (and just below the 367.04 m hardground) there is one sample at the top of the section, sample 367.1, with a $\delta^{13}C_{\text{dolomite}}$ value 1.5‰ more depleted than the rest of the section which has a narrow and constant range of 4.0 to 4.7‰ VPDB. The depleted value at the top of the section is most likely a product of the erosional boundary at the 367.04 m hardground and is not directly associated with the rest of the section. The $\delta^{13}C_{\text{LMC}}$ values in this same section parallel the trends seen in the dolomites, albeit 1‰ more depleted.

Just below the 536.6 m hardground, there is a linear increase in the $\delta^{13}C_{\text{dolomite}}$ value with depth increasing from 3.1 to 4.1‰ VPDB over 100 m core depth. This change is not associated with changes in the bulk % dolomite and not also seen in the LMC. This could be an indication of biological processes such as methanogenesis (Chapter 5) affecting the isotopic content of the pore waters through diffusional processes during dolomitization. The LMC endmember shows a similar negative spike just below the hardground, as seen in the $\delta^{13}C_{\text{LMC}}$ values depleting to between 1 to 2‰ VPDB, while the rest of the core has $\delta^{13}C_{\text{LMC}}$ values between 2 to 3‰ VPDB. Again, similar to the oxygen isotopes, the parallel trend seen above the 536.6 m hardground is followed by inconsistent trends below.

Swart and Melim (2000) suggested the difference between the sediments above the 536.6 m hardground and those below was the timing of diagenesis relative to

dolomitization. The results agree with this interpretation, though distinguishing whether the LMC or dolomite endmember formed first is difficult to determine.

Swart et al. (2001) measured Sr 87/86 ratio on the Clino core, looking at bulk sediments and the isolated dolomites. As has been discussed previously, the Sr isotopic values of carbonates were derived from the fluid they last equilibrated with (Swart et al., 1987; Vahrenkamp and Swart, 1990). If the Sr isotopic composition of the bulk material, which is predominantly LMC, had an 87/86 ratio that was equivalent to that in ocean fluid later in time than the dolomites, than there is good reason to believe that the LMC formed later than the dolomites. However, this was not the case. While there was some disparity in the sample location between the bulk and dolomite samples, any difference in the trends in Sr isotopes between the bulk and dolomite endmember samples were well within error of the individual measurements. The conclusion of Swart et al. (2001) was that within the resolution of the Sr-isotope curve created by the Clino measurements, all samples fell within an identical age range. The proposed Sr-isotope age range was more recent in time than the age of deposition, as determined by other chronostratigraphic techniques, suggesting that diagenesis occurred after deposition. Two distinct age intervals were present in the Sr isotopes; the first from 125.6 to 536 m depth with suggested ages of 2-5ma, then a sudden shift in isotopes below this from 0.709060 to 0.708900 suggesting an age of diagenesis from 5 to 9 ma. So there were at least two distinct diagenetic events in Clino, but these events were separated temporally by depth in core not mineralogy.
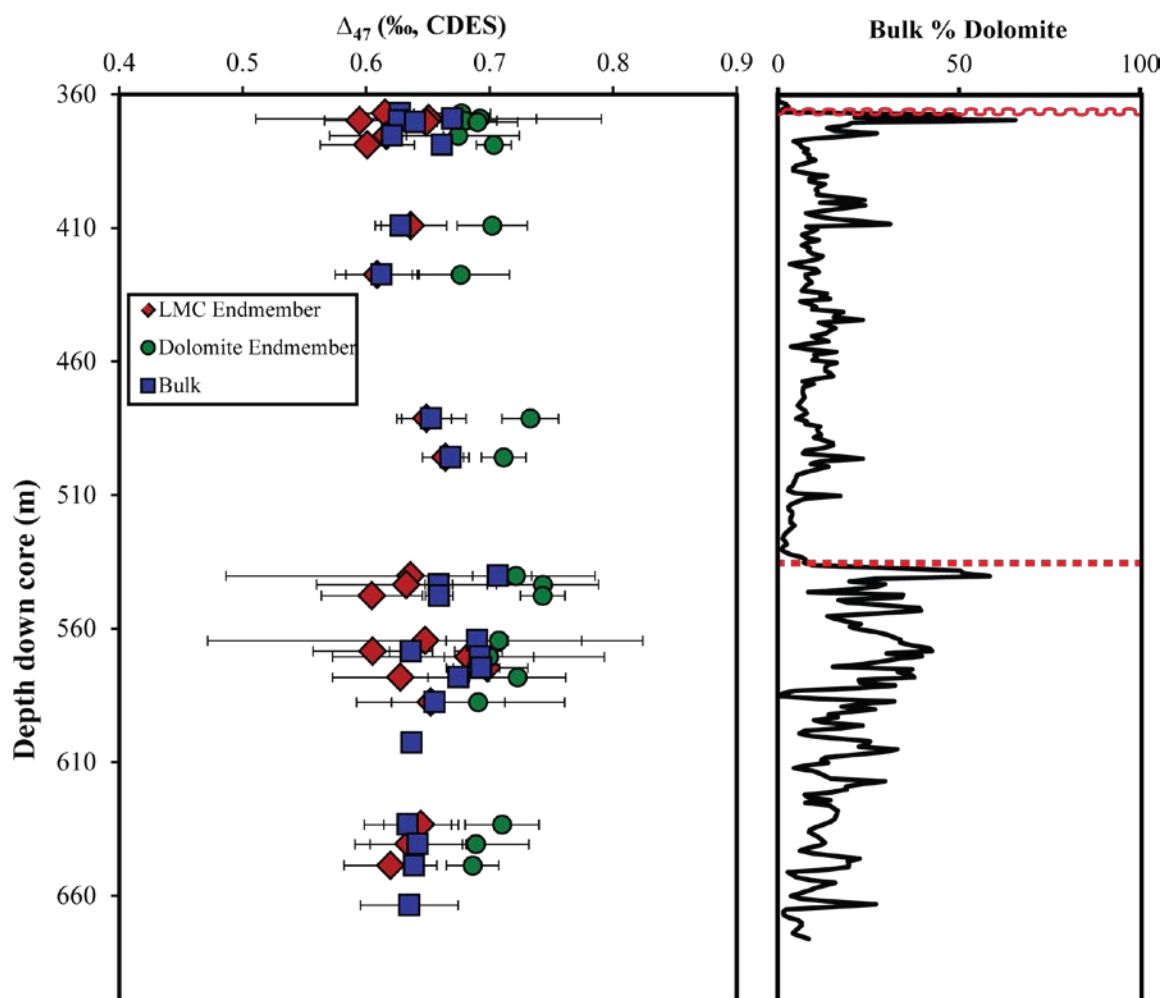
Figure 4.7 - The Δ_{47} of Clino as presented through the measured bulk and dolomite endmembers as well as the LMC endmember calculated using a weighted least square regression. This is compared to the bulk dolomite percentage as determined by X-ray diffraction and the identified erosional (〰️) surface and marine hardground (•••••). Error bars represent ± 1σ.

Implications of Differing Acid Fractionation Factors on Clumped Isotopes

There is an obvious separation in the Δ_{47} data between the LMC and dolomite

endmembers that would not necessarily exist if the difference was not forced by the

application of different acid fractionation factors (Figure 4.7). The consequence of this is

that the dolomites appear to have formed at a colder temperature than the LMC from the

same depth. While this is certainly a possibility that will be discussed below, some

skepticism can be brought forth as to whether these same trends and conclusions would

exist if a constant acid fractionation factor had been applied as was suggested in Defliese

et al. (2015). Using an identical acid fractionation factor for the two endmembers brings

more agreement in calculated temperatures, which has the effect of also imparting

temperatures on the dolomite endmembers which are too warm relative to the modeled

formation of Clino with temperatures averaging 41 ± 5°C with a maximum reported

temperature of 48°C. Such temperatures may be supported if the entire system were in

disequilibrium, however using a constant fractionation factor does not appear to improve

upon any of the main concerns with the data set.

Calcite and Dolomite Temperatures

There is a clearly defined difference in calculated clumped isotope temperatures

between the dolomite and calcite endmembers averaging 15 ± 7°C with the calcite

temperature endmembers averaging 42 ± 6°C and the dolomite endmember averaging 27

± 4°C. Considering the difference in temperature between the two endmembers and

discounting the suggested equilibrium of the nearly constant 3‰ offset in $\delta^{18}O$ values, it

would be concluded that these formation temperatures suggest different fluid sources.

However, there are no known fluid sources present in the Bahamas that can explain the

temperatures for the LMC samples and the dolomite temperatures are more similar to

Bahamian island sediments (Chapter 3) than they are to the deep bottom water

temperatures assumed to have played a role in their formation. With temperatures on

some LMC endmembers exceeding 50°C, even taking into account error produced by the

extrapolation of data, these temperatures could not be produced by interaction with

bottom waters.

There are two reasonable ways to explain such temperatures for the dolomite and

LMC endmember. The first is suggesting there was some kind of disequilibrium that

occurred during diagenesis that scrambled their isotopic values (explained in detail in

chapter 5). The other explanation would invoke the geothermal gradient and delayed

diagenesis with the dolomite forming earlier than the LMC upon burial. The latter

explanation requires a clear understanding of the timing of diagenesis but does agree with

the conclusions of Swart and Melim (2000) that dolomitization occurred after the

aragonite altered to LMC.

Temperatures calculated from clumped isotopes suggest that the dolomites

formed consistently from cooler temperatures than the LMC endmembers. This finding

goes against the conclusions of Swart and Melim (2000) that suggested that the dolomites

and LMC would have come into equilibrium with the same fluids based on oxygen

isotopic content of the carbonates and the Sr profile of the dolomites. The geothermal

gradient in the Bahamas has been measured in multiple studies with little agreement

between the studies possibly attributable to the large seasonal variation in the temperature

of the bottom waters. Some possible geothermal gradients suggested were 18.2 to

20.1°C/km as measured on Long Island, Bahamas (Epstein and Clark, 2009), 36°C/km
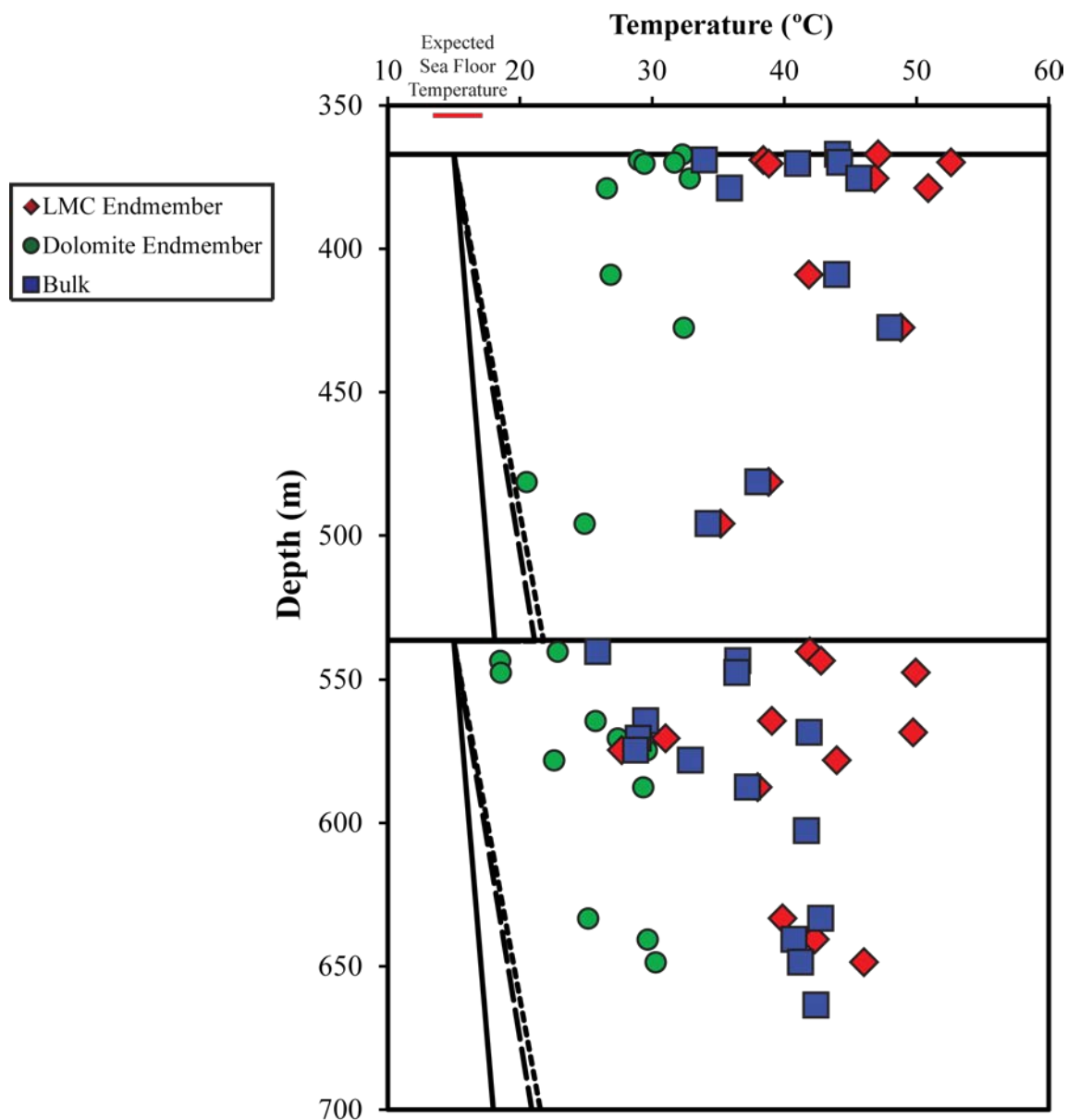
Figure 4.8 - The temperature of Clino as presented through the measured bulk and dolomite endmembers as well as the LMC endmember calculated using a weighted least square regression. Error bars have been omitted for clarity, but can be found in the data table. Vertical solid and dashed lines are representing different measured geothermal gradients across the Bahamas assuming a seafloor - sediment interface temperature of 15ºC (average of plausible values indicated by the red horizontal line). From left to right: 18.2 ºC/km (Epstein and Clark, 2009), 36 ºC/km (Melim et al., 2001), 40 ºC/km (Nagihara and Wang, 2000). Horizontal black lines represent the erosional surface at 367 m core depth and the hardground at 536.3 m core depth.

estimated off oxygen isotopes in Clino (Melim et al., 2001), and ≈40°C/km as modeled

for site 1004 of ODP Leg 166 which is located further out onto the rise than Clino

(Nagihara and Wang, 2000). Assuming seafloor bottom temperatures on Clino of 15°C,

than at 1 km depth, fluid temperatures could be anywhere from 33.2 to 55°C based on the

range of estimated geothermal gradients. The samples in this study are collected from

367to 649 m depth where a range of expected temperatures based on these geothermal

gradients would be 22 to 30°C at the top of the section to 27to 41°C at the bottom (Fig

4.8).

The average LMC clumped isotope temperature was at 42 ± 6°C which exceeds

the maximum predicted temperature based on the largest geothermal gradient. The

calculated temperatures of the dolomite endmember does fall within this range of

temperatures, however the temperatures tend to decrease with depth, not increase making

equilibration with geothermal gradient temperatures dubious.

The error associated with extrapolating the LMC endmember Δ_{47} value in many

of the samples is large enough to make the results questionable. Due to bulk samples

containing upwards of 83% dolomite material, there is a lot of interpretation made with

the calcite endmembers. The extrapolated Δ_{47} values for the LMC (Δ_{47_LMC}) endmember

are only more so confounded by the errors associated with measuring Δ_{47} from the mixed

carbonates themselves. There is a strong correlation ($r^2 = 0.523$) between increasing bulk

% dolomite and increasing error in the extrapolated Δ_{47_LMC} values. However, in the

sediments where the bulk % dolomite was low corresponding to lower errors in Δ_{47_LMC}

just greater than the analytical uncertainty, similar high formation temperatures (35 to

45°C) are calculated.

Interpretation of the measured Δ_{47} values for Clino is dependent upon the calculation of temperature. As has been discussed before, there are a multitude of Δ_{47}-temperature calibrations available, all of which could change the interpretations of this study. The calibration used is also significant due to the comparison of a LMC endmember and a dolomite endmember considering there is no measured-calibration for dolomite materials. Applying the calibrations of Dennis and Schrag (2010) and Defliese et al. (2015) in the CDES both produce more extreme temperatures for the LMC endmember with average temperatures >10°C more than those produced using Ghosh et al. (2006). Both the average temperature and range of temperatures for the dolomite endmembers do not change significantly using the other calibrations.

Conclusions

After using a series of buffered acetic acid treatments on the mixed carbonate sediments of Clino, it has been shown that the dolomite and LMC endmembers of these sediments display unique isotopic signatures suggesting different parent fluid sources. However, the Δ_{47} values for the samples produce temperatures that exceed any known fluids that are believed to have existed in the Bahamas since the Pliocene and exceed even the geothermal gradient. These temperatures cannot be accounted for by the non-linear mixing of endmembers associated with the calculation of Δ_{47} as determined using the modeling of Defliese and Lohmann (2015) and are therefore most likely evidence of either disequilibrium in the sediments or some unaccounted for consequence of measuring mixed carbonate samples.

Chapter 5 - Implications from the Measurement of $\delta^{34}S$ Values in Carbonate Associated Sulfate in San Salvador, Clino, and Unda

Introduction

Sulfur in the oceans is almost entirely derived from volcanic activity and the erosion of sulfur bearing minerals on continental surfaces which is then fed into the oceans through the hydrologic cycle. This sulfur, mainly in the biologically available form of sulfate (SO_4^{2-}), is utilized in both the bacterial mineralization of organic materials and as the electron acceptor for anaerobic methane oxidation in marine sediments (Bottrell and Newton, 2006; Kampschulte and Strauss, 2004).

The ratio of $^{34}S/^{32}S$, reported as $\delta^{34}S$ relative to Canyon Diablo Troilite (CDT) in the conventional form, has changed significantly through time in the world's oceans. The modern ocean has a $\delta^{34}S$ of $\approx+23‰$ CDT (Fig 5.1). In the ancient, the $\delta^{34}S$ value of seawater peaked in the Cambrian at around 33‰ before declining to a low of 10‰ in the Permo-Triassic and then steadily rising to the modern value of +23‰ (Claypool et al., 1980; Kampschulte and Strauss, 2004; Paytan et al., 1998; Strauss, 1999). The $\delta^{34}S$ value of seawater is heavily influenced by the amplitude of bacterial sulfate reduction (BSR). The process of BSR preferentially uses the lighter $^{32}SO_4^{2-}$ molecule in the reduction of sulfate which converts sulfate to sulfide:

$$SO_4^{2-} + 2CH_2O \rightarrow H_2S + 2HCO_3^- \qquad (5.1)$$
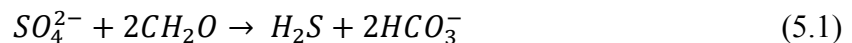
This reaction makes sulfur available for oxidation and the eventual formation of pyrite (FeS_2) that is depleted in ^{34}S relative to the surrounding seawater. Dependent upon the
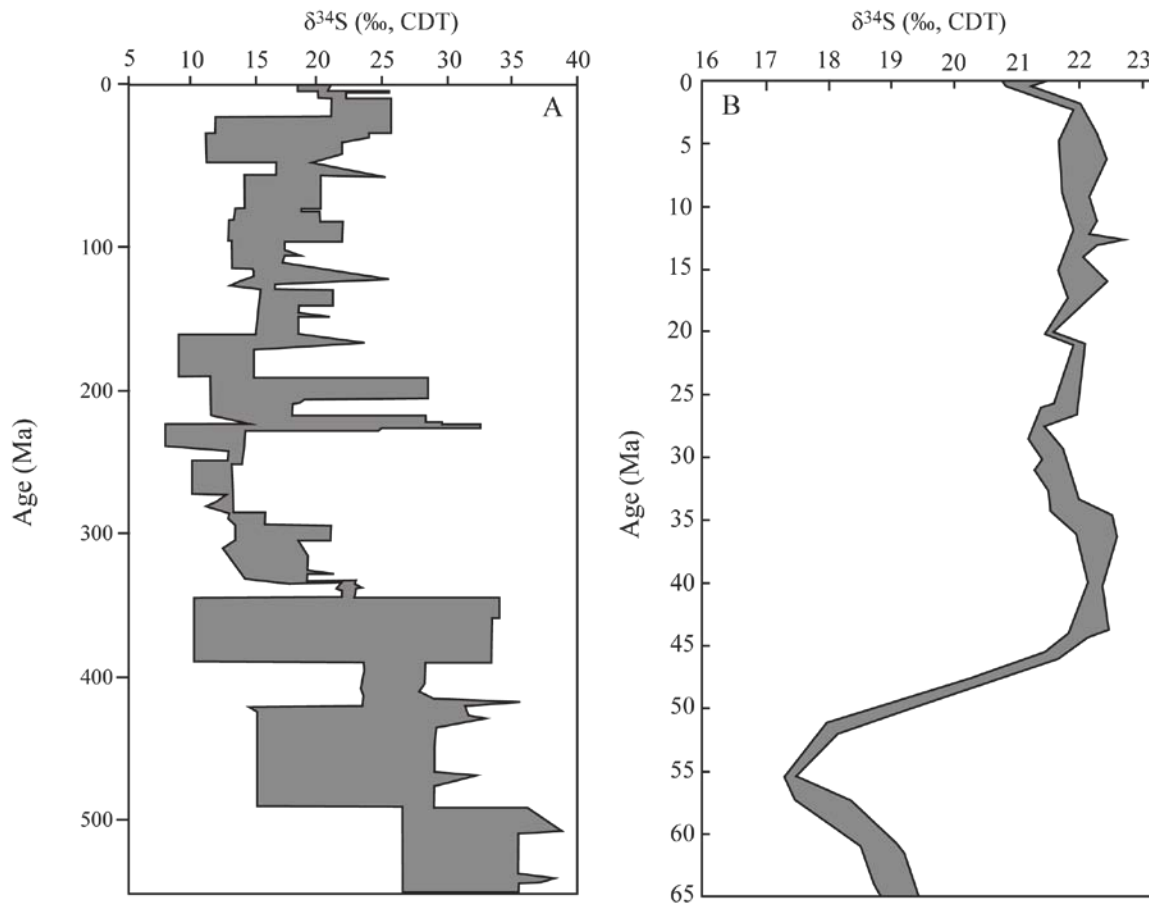
Figure 5.1 - The thickness of the gray line indicates the range of measured values.
A) Adapted from Kampschulte and Strauss (2004). Plot shows the sulfur isotopic content of Paleozoic and Mesozoic seawater as interpreted from measurements of carbonate associated sulfate and marine evaporites. B) Adapted from Paytan et al. (1998). Plot shows the compilation the sulfur isotopic content of Cenozoic seawater through time as measured in barite samples from multiple cores.

organic matter being decomposed by this reaction, other products could include water, phosphoric acid (H_3PO_4), and ammonia (NH_3) (Ben-Yaakov, 1973). The burial, and hence removal, of isotopically heavy sulfur is balanced by the weathering of tectonically uplifted pyrite and other sulfur bearing minerals which are then reintroduced to the sulfate pool via the hydrologic cycle.

The sulfur isotopic record has been developed predominantly through the measurement of gypsum and anhydrite, both sulfur bearing minerals which are commonly found in evaporite deposits, as well as in the marine biogenic barite record (Paytan et al., 1998). Because of the rapid scale of seawater mixing relative to residence time of sulfur in seawater (1 ky to 8,000 ky), it is assumed that the oceans are well mixed with respect to isotopic sulfur and that these measurements are representative of what the isotopic value of seawater was at the time of deposition (Bottrell and Newton, 2006). The problem with measuring evaporite minerals is that their existence, while not uncommon, is sparse throughout any single geologic sequence and requires a compilation of measurements from many different regions to compile a complete record of isotopic sulfur through time.

In marine carbonates, sulfate has been shown to structurally substitute for molecular carbonate in what has been aptly titled carbonate associated sulfate (CAS). This substitution occurs naturally, but has a relatively small impact on the total sulfur budget in the oceans ($\approx 0.58 \cdot 10^{13}$ gS $\cdot$ yr^{-1}) (Burdett et al., 1989; Kampschulte and Strauss, 2004; Strauss, 1999). With the use of CAS, it is possible to fill in the gaps in the oceanic sulfur isotope record left by sparse measurements using sulfur-bearing evaporites. The measurement of CAS has been shown to be representative of changes in

the sulfur content of overlying seawater with little to no fractionation (Burdett et al., 1989) and has also been suggested to be stable throughout the process of meteoric (Gill et al., 2008) and early marine burial (Rennie and Turchyn, 2014) diagenesis. Using this technique, it becomes possible to measure the changing sulfur isotopic content of seawater through time by measuring a single carbonate core (Bottrell and Newton, 2006; Burdett et al., 1989; Kampschulte et al., 2001; Kampschulte and Strauss, 2004; Paytan et al., 1998).

In this work, the measurement of CAS is applied to dolomitized cores from the island of San Salvador, Bahamas and two cores collected off of the western shelf of Great Bahama Bank: Unda and Clino (Eberli et al., 1997). The focus is to examine the influence of BSR on the clumped isotopic composition and dolomite formation. By pairing CAS analysis with the clumped isotopes and other proxies previously measured in other studies, we hope to gain a more complete understanding of the formation of dolomites in the Bahamas and derive implications for other systems. The samples used in this study are significantly younger (spanning the Cenozoic) and much better constrained in terms of their formation and dolomitization processes. Because of this, measuring CAS in these dolomites could play an essential role in determining the preservation potential of CAS through the process of dolomitization as well as the impact of BSR on clumped isotope temperatures.

Samples

Descriptions of the cores used in this work are given in chapters 3 and 4 of this dissertation but are summarized again in this chapter. Briefly, San Salvador is a carbonate island on the Eastern edge of the Bahamas. A 168 m deep core was obtained on the

northern tip of the island spanning Miocene to Pleistocene aged sediments. The upper

portion of the core is LMC formed by meteoric diagenesis. Below this interval, the core

is 100% dolomitized with a near stoichiometric, well ordered composition. Chapter 3 of

this work suggests these dolomites formed from two different fluid sources. The first is

normal marine seawater that would have flowed through the carbonate islands through

Kohout-convection, and the second is a warmer evaporative fluid that is most likely

derived from the circulation of fluids into ponds that formed all across the island from

infiltrated seawater. Multiple studies have examined the presence of modern day

microbial mat communities present within these pools that support large sulfate reducing

bacteria communities (Dupraz et al., 2013; Piggot, 2014; Puckett et al., 2011), but the

interaction between seasonality and the precipitation and dissolution of carbonates is not

well constrained.

Clino and Unda were both drilled as a part of the Bahamas Drilling Project on the

western edge of Great Bahama Bank (Eberli et al., 1997). Both cores were drilled into

Miocene to Pleistocene aged sediments that document the platform to slope transition

across the bank. Clino is the more distal of the two, about 5 km further off the bank than

Unda, and therefore documents more of the slope sediments while Unda is predominantly

reefal and platform derived sediments. Both cores are partially dolomitized throughout

their lower portions, with Unda having a reefal section that is almost 100% dolomitized

and Clino having various spurts of dolomitization that are associated with non-

depositional marine hardgrounds. The dolomite in Clino never composes more than 80%

of the sediment and is more generally between 20 to 40 %. The dolomite in these two

cores is calcian, 44 to 46% $MgCO_3$, and not as well organized as in San Salvador.

The measurement of Sr-concentrations in Clino and Unda suggest the pore fluids were composed of normal marine seawater (Swart and Melim, 2000). It has been found that dolomite abundance in these cores is negatively correlated with the Sr concentration in the dolomites. This is corroborated by the presence of celestite well below the dolomite abundance maximums, suggesting a trend by which dolomite precipitation is related to decreased abundance of Sr in the pore fluid. The Sr concentration measured in the dolomites increases to greater than 2000 ppm which is well beyond normal s for dolomites derived from seawater that are typically in the range of 70-250 ppm. (Vahrenkamp and Swart, 1990). It was suggested that in order for such high levels of Sr to be obtained without sudden precipitation of celestite that would occur above 600 μM Sr in normal seawaters, the abundance of SO_4^- in the pore waters needs to be well below typical values suggesting the fluids had been subjected to extensive sulfate reduction (Swart and Melim, 2000).

Carbonate Associated Sulfate

In the San Salvador core, 24 samples were collected from the dolomitized section of the core, almost entirely from the Pliocene aged sediments. In Unda, 12 samples were collected from the 70 m portion of core from the middle reefal section that was deposited during the Miocene and which is nearly completely dolomitized. In Clino, 38 samples were collected throughout the partially dolomitized lower half of the core with an attempt to acquire the changes in content associated with marine hardgrounds that are at 367.0 and 563.3 m depth in core. These are bulk samples, so the amount of dolomite within the Clino core samples varies significantly from 0.0-56.6% as determined by XRD.

Methods

Carbonate Associated Sulfate

Preparation of CAS samples followed the methods of Gill et al. (2011). Samples for CAS analysis were obtained by freshly cutting large chips out of the individual cores. Samples were powdered using short intervals in a Spex SamplePrep Mixer/Mill 8000. The powdered sediment was divided for XRD and CAS analysis. CAS samples consisted of 20-30 g of powdered sample which was soaked in a 10% NaCl solution for 24 hours followed by two consecutive rinses with DI water lasting 24 hours. Next was a 4% sodium hypochlorite solution soak for 48 hours to remove any organically formed sulfur compounds. This was followed by two more 24-hour DI water rinses before the samples were dissolved using a 4N hydrochloric acid solution. Upon complete dissolution of all carbonate material, any undissolved portions were removed from the supernatant via vacuum filtering through 45 μm filters. The filtered supernatant was then added to 100 mL of a saturated BaCl solution (250g/L), brought up to 1L total volume through the addition of DI water, and allowed to settle for three days. The precipitate was then removed from the remaining solution and dried over 72-hours in a 40°C oven before being sampled for analysis. If the dried samples contained evidence of crystalized hydrochloric acid, they were re-dissolved in a liter of DI water, allowed to settle overnight then dried. The second treatment was sometimes necessary as the volume of the beakers used (1 L) were not large enough to dilute the concentrated hydrochloric acid solution enough to remove it entirely. However, there is little indication that this had any effect on our samples.

The CAS sample analysis consisted of 1 mg of sample combined with 5 mg of vanadium-pentoxide (V_2O_5) in a single tin capsule. The tin capsules were combusted in a

modified Dumas group combustion furnace (Europa Scientific). The resulting SO_2 gas was analyzed via continuous flow on a CFIRMS 20-20 (Europa Scientific, Crewe, UK) isotope-ratio mass spectrometer. In order to homogenize the oxygen value in the SO_2, the gas was passed over quartz chips heated to 1000°C (Fry et al., 2002). The $\delta^{34}S$ value was determined by the measurement of masses 50/48 and was corrected to three different standards: an in-house standard calibrated to Vienna Canyon Diablo Troilite (V-CDT), and two IAEA standards, NBS 123, a seawater sulfate, and NBS 127, a sphalerite.

A linear drift correction was applied to each run of CAS samples by measuring a complete set of all three in house standards before and after the run with a single standard measured in the middle of the run. The amount of drift was typically less than 5% of the isotopic value of the standard but one run had large drifts of up to 60%. This run was scrutinized and each sample measured within it was re-measured multiple times after to confirm the results.

Clumped Isotopes and Estimating $\delta^{34}S$ Values of Samples

Clumped isotope samples were measured prior to beginning of this project from pre-ground sediments utilized in the initial studies on these cores. The methods follow those described in Chapter 1 of this work.

The samples used for the clumped isotope measurements of these cores were not always from identical sediments as those tested for CAS. In most cases, there was not enough of the originally sampled material for both CAS and clumped isotope analysis. In order to produce $\delta^{34}S$ values for the core depths where clumped isotope samples were measured, an estimate was produced using linear interpolation through least squares regression between CAS measurement depths, or in some cases where the depth

difference between the closest CAS sample and the clumped isotope sample was minimal
(< 3m), a linear extrapolation was used, . In San Salvador and Unda, trends in the data
were decided visually and multiple regressions were produced through subsets of the data
so as to best capture the trends suggested by the data. A different approach was taken for
Clino due to the frequent, significant changes in the δ^{34}S values throughout the core. To
interpolate δ^{34}S values, the nearest two CAS measurements were used to create the least
squares regression. If there was any clumped isotope samples that was measured at a
depth where there was a gap in the CAS measurement data of >15m or if there was a
sequence boundary associated with a sudden change in δ^{34}S values requiring a significant
extrapolation of data, the depth was discarded and not used in further analysis. Such cases
included clumped isotope samples at 481.4, 574.7, and 663.6 m depth. The accuracy of
our interpolations was checked against samples where both clumped and CAS
measurements were taken from the same sample which suggested fairly good agreement
with the method.

Results

δ^{34}S CAS Values from Bulk Samples

      Both the San Salvador and Unda cores showed little deviation in their δ^{34}S values
from the ambient seawater during the Plio-Pleistocene (Paytan et al., 1998). The San
Salvador core had a range of δ^{34}S values of +19.3 to +24.5‰ with little deviation from
the mean of +22.6‰ throughout the core except for a small negative deviation towards
the minimum reported value which corresponds to the low-temperature interval between
53 to 79 m depth as discussed in Chapter 3 (Fig 5.2). Unda showed less deviation
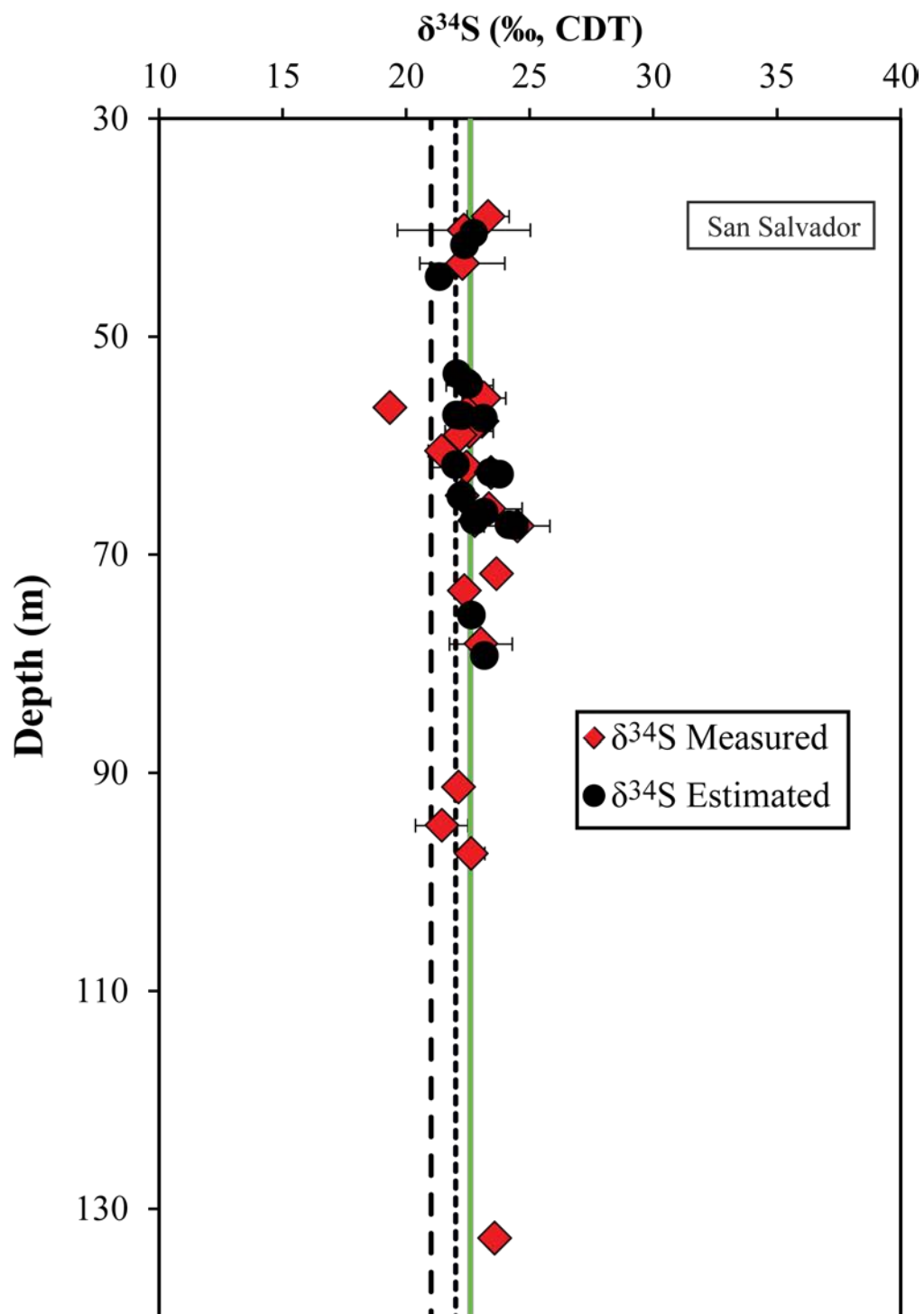
Figure 5.2 - Measured and estimated δ^{34}S values measured through CAS on the San Salvador core. Error bars represent ±1σ. Dashed and dotted lines represent seawater δ^{34}S values during the Mio-Pliocene and Pleistocene respectively as measured in Paytan et al. (1998). The green line is the average δ^{34}S of the measured San Salvador CAS samples.
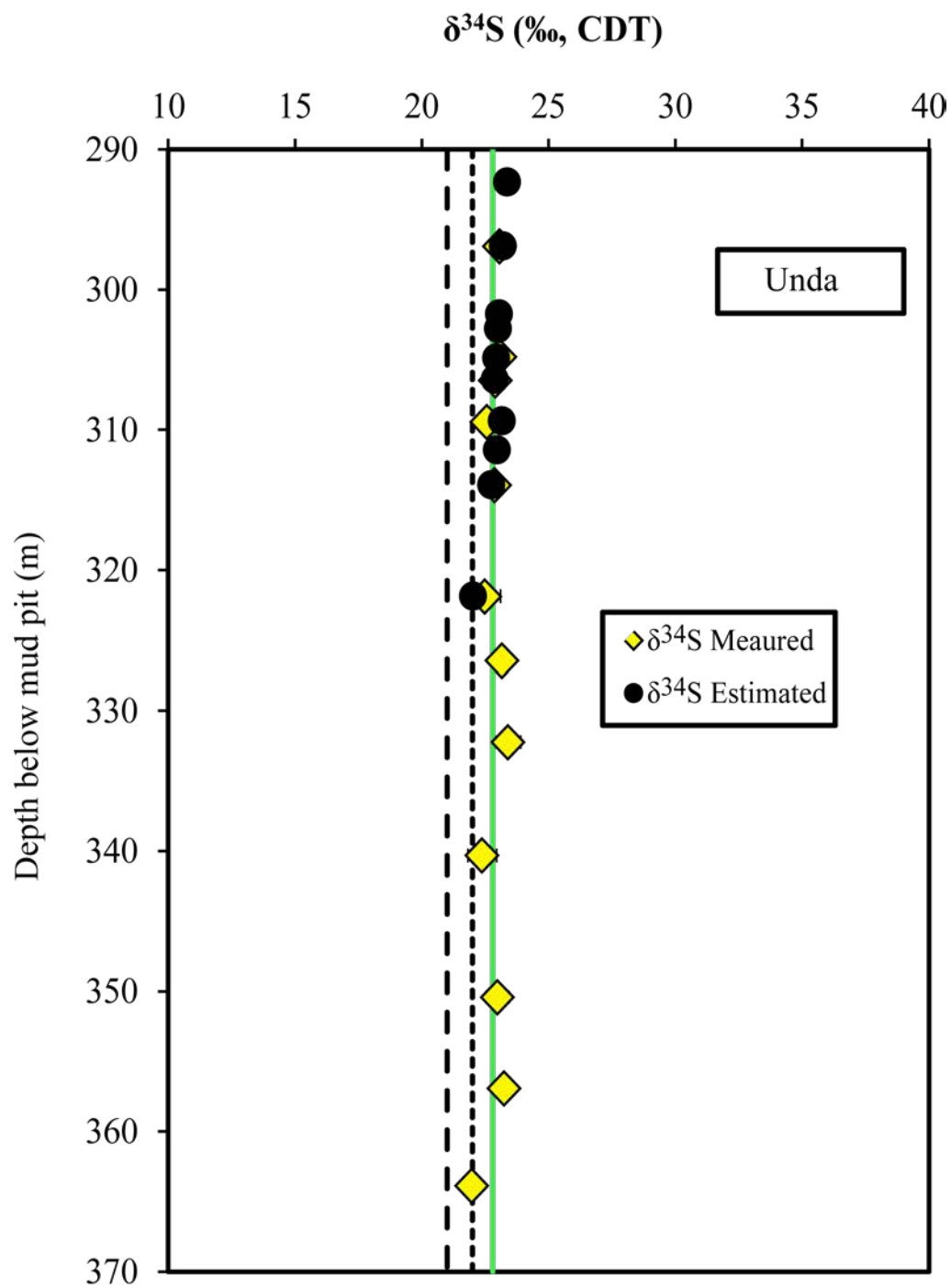
Figure 5.3 - Measured and estimated δ^{34}S values measured through CAS on the Unda core. Error bars represent ±1σ. Dashed and dotted lines represent seawater δ^{34}S values during the Mio-Pliocene and Pleistocene respectively as measured in Paytan et al. (1998). The green line is the average δ^{34}S of the measured Unda CAS samples.
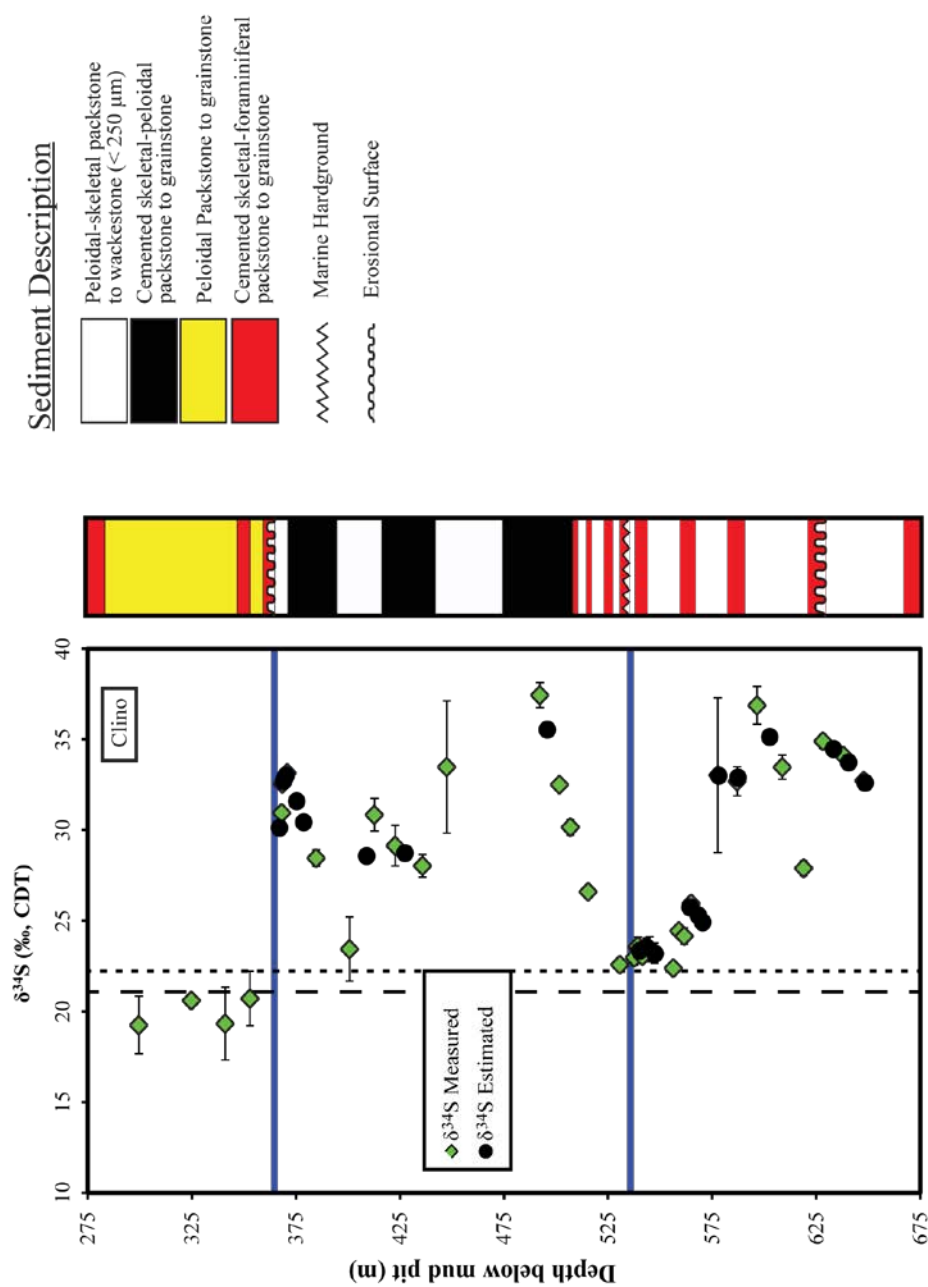
Figure 5.4 - Measured and estimated $\delta^{34}S$ values measured through carbonate associated sulfate on the Clino core. Error bars represent $\pm 1\sigma$. The blue horizontal lines indicate the identified erosional boundary at 367.0 m depth and the marine hardground at 536.3 m core depth. Dashed and dotted lines represent seawater $\delta^{34}S$ values during the Mio-Pliocene and Pleistocene respectively as measured in Paytan et al. (1998)

than San Salvador with a total range of measured values of less than 1.5‰ from +22.0 to +23.4‰ with an average value of +22.8‰ (Figure 5.3).

The Clino core showed significantly larger deviations from the expected seawater values of Plio-Pleistocene seawater with a range of δ^{34}S values from +19.2 to +37.4‰ (Figure 5.4). Above the 367.0 m hard ground, the δ^{34}S values were consistently below +21‰ which is the only period throughout the length of the core where values are depleted below the expected seawater values. Below this hardground, there are pulses of enrichment and depletion in δ^{34}S values that range from +22 to +37‰ and trends suggests a maximum value greater than what was measured in this study. Below the 536.6m hardground, values stay stable at ≈+23‰ for the first 20 m before increasing by 10‰ to the end of the measured core. (Table 5.1)

All individual CAS measurements can be found in supplementary table S.4.

Estimated δ^{34}S Values

The estimated results for the clumped isotope sample depths relative to measured CAS values from the same core depth can be seen in Table 5.2. The estimated values for both San Salvador and Unda suggested little deviation from the trends presented by the original CAS samples. The estimated values for Clino are left up to a greater amount of interpretation as the changing trends in enrichment and depletion in the δ^{34}S values make interpolating more of a risk if the trends are not continuous. However, it was believed that the all major trends were captured due to the apparent consistency of trends over depth in the core combined with the <10m resolution of samples. If a major shift were

Table 5.1 - δ^{34}S CAS Measurements

Depth (m)	n	δ^{34}S (‰, CDT)	Std. Dev. (‰, CDT)	% Dolomite	Depth (m)	n	δ^{34}S (‰, CDT)	Std. Dev. (‰, CDT)	% Dolomite
Clino					*San Salvador*				
299.5	2	19.2	1.6	0.0%	39.0	2	23.3	0.8	100.0%
324.8	2	20.6	0.2	0.4%	40.2	2	22.3	2.7	100.0%
341.1	2	19.3	2.0	0.0%	43.3	2	22.3	1.7	100.0%
353.0	2	20.7	1.5	0.1%	54.5	3	22.6	1.0	100.0%
368.2	2	30.9	0.1	25.3%	55.7	3	23.1	0.9	100.0%
368.5	2	32.6	0.1	28.3%	56.5	3	19.3	0.3	100.0%
370.9	2	33.1	0.2	19.6%	57.0	1	22.4	-	100.0%
384.8	3	28.5	0.5	9.3%	57.8	1	23.1	-	100.0%
400.8	2	23.4	1.8	17.4%	58.7	2	22.5	1.0	100.0%
412.8	2	30.8	0.9	7.1%	59.0	2	22.2	0.6	100.0%
422.7	2	29.1	1.1	6.2%	60.5	2	21.4	0.5	100.0%
435.9	2	28.0	0.6	25.8%	62.0	4	22.4	1.5	100.0%
447.5	2	33.5	3.6	20.9%	62.5	4	23.4	0.8	100.0%
492.3	2	37.4	0.7	29.1%	64.6	4	22.3	0.4	100.0%
501.7	2	32.5	0.3	9.7%	65.8	4	23.3	1.4	100.0%
506.9	2	30.2	0.4	5.3%	66.9	2	22.8	0.3	100.0%
515.4	2	26.6	0.2	1.9%	67.4	4	24.5	1.3	100.0%
530.7	2	22.6	0.2	1.2%	71.8	2	23.6	0.1	100.0%
537.7	2	23.0	0.4	37.6%	73.3	2	22.3	0.1	100.0%
538.6	2	23.6	0.3	50.5%	78.2	2	23.0	1.3	100.0%
539.3	2	23.6	0.5	38.0%	91.3	2	22.1	0.1	100.0%
541.5	2	23.0	0.2	14.9%	94.8	2	21.4	1.1	100.0%
543.5	2	23.5	0.5	17.9%	97.4	2	22.6	0.6	100.0%
544.9	2	23.4	0.7	23.4%	132.7	2	23.6	0.0	100.0%
547.4	2	23.2	0.6	17.6%					
556.3	2	22.4	0.0	13.8%	*Unda*				
559.1	2	24.4	0.1	31.6%	296.9	2	23.1	0.1	100.0%
561.6	2	24.2	0.5	20.9%	304.8	2	23.1	0.1	100.0%
564.9	2	26.0	0.1	32.4%	306.5	2	22.9	0.2	100.0%
568.1	2	25.4	0.1	56.1%	309.4	2	22.6	0.3	100.0%
577.7	2	33.0	4.3	56.6%	313.9	2	22.9	0.0	100.0%
587.0	2	32.7	0.8	27.0%	321.9	2	22.5	0.6	100.0%
596.5	2	36.9	1.0	22.9%	326.4	2	23.2	0.0	100.0%
608.7	2	33.5	0.7	10.7%	332.2	2	23.4	0.5	100.0%
619.0	2	27.9	0.4	26.5%	340.3	2	22.4	0.6	5.0%
628.2	2	34.9	0.4	17.1%	350.4	2	23.0	0.5	100.0%
638.0	1	34.1	-	18.9%	356.9	2	23.3	0.2	55.0%
647.9	2	32.7	0.4	13.9%	363.9	2	22.0	0.3	19.0%
Unknown	1	33.1	-	Celestite					

Table 5.2 - δ^{34}S Estimated Values

Depth (m)	δ^{34}S Measured (‰, CDT)	δ^{34}S Estimated (‰, CDT)	Depth (m)	δ^{34}S Measured (‰, CDT)	δ^{34}S Estimated (‰, CDT)
Clino			*San Salvador Cont.*		
367.1	-	30.1	177.9	-	22.4
369.1	-	32.7	178.5	22.6	22.5
369.8	-	32.9	187.7	-	22.0
370.3	-	33.0	187.9	-	22.3
375.5	-	31.6	188.7	-	23.1
378.9	-	30.4	202.7	-	22.0
409.1	-	28.6	205.0	-	23.4
427.5	-	28.7	205.6	-	23.8
495.9	-	35.5	212.0	-	22.3
540.3	-	23.4	212.2	22.3	22.2
543.5	23.5	23.5	217.0	-	23.2
547.7	-	23.2	219.5	-	22.8
564.5	-	25.7	220.8	-	24.2
568.5	-	25.3	220.9	-	24.3
570.6	-	24.9	221.0	24.5	24.4
578.2	-	33.0	248.0	-	22.7
587.5	-	32.9	260.2	-	23.2
602.7	-	35.1			
633.4	-	34.5	*Unda*		
640.7	-	33.7	292.3	-	23.4
648.7	-	32.6	296.9	23.1	23.2
			301.8	-	23.0
			302.8	-	23.0
San Salvador			304.9	23.1	22.9
124.0	-	23.7	306.4	22.9	22.9
125.5	-	23.5	309.4	22.6	23.2
133.0	-	22.7	311.5	-	23.0
136.5	-	22.4	313.9	22.9	22.8
146.1	-	21.4	321.9	22.5	22.0
175.3	-	22.1			

missed, the influence on the conclusions of this work would most likely be minimal as it would only have affected a small subset of the interpolated values.

The only major gap in the Clino data set between CAS measurements at 447.5 - 492.3 influenced a single clumped isotope pairing at 481.4 m. Based on the visual trends of a steepening enrichment to 33‰ before the gap and a steep depletion from 37‰ after the gap, it appeared that this depth would be the location of the most enriched $\delta^{34}S$ values in the core. However, without more data, it was difficult to justify including an interpolation between these endmembers as they clearly show different stages of BSR and/or sea level change and could not be properly quantified. Therefore, the sample 481.4 has been removed from any discussion involving $\delta^{34}S$ values.

An estimate of the maximum $\delta^{34}S$ value achievable was made using a simplified model of the diagenetic environment of BSR in Clino. The dissolution of 1g of aragonite with 50% porosity containing an initial 4000 ppm of sulfate into a BSR environment was modeled at a rate of 10% of the bulk remaining carbonate dissolving per interval. Seawater was expected to have an initial concentration of 28 mM SO_4^{2-} with an initial $\delta^{34}S$ value of 22‰ in both the aragonite and the seawater. Based on the work of Detmers et al. (2001), sulfate reducing bacteria were expected to induce a fractionation of 42‰ in the $\delta^{34}S$ value of seawater. With these conditions, it could be expected that the $\delta^{34}S$ value could have reached as high as 40‰ (Fig 5.5) which is in good agreement with the measured trends seen throughout Clino and a reasonable maxima for the gap in Clino data.

Clumped Isotopes

The clumped isotope results for all three sites were discussed in chapters 3 and 4 of this work. Briefly, both San Salvador and Unda clumped isotope temperatures agreed with previous models of formation for the dolomites. The calculated temperature for San Salvador ranged from 20 to 35°C with the bulk of the core forming at the warmer end of the spectrum most likely from the evaporative pools that form on the island. A small section of core between 56 to 78 m depth had predominantly cooler temperatures between 20 to 25°C which is indicative of formation by normal marine sea surface fluids as is normal in the Bahamas.

Considering the Unda core reached greater depths than San Salvador, it was expected to present clumped isotope signatures that were either indicative of cooler fluids than San Salvador, or in the case that diagenesis occurred during sea level low stands, a similar signature to San Salvador. All Unda samples had a narrow range of Δ_{47} values between 0.740 to 0.758‰ suggesting formation between 15 to 20°C using the calibration of Ghosh et al. (2006) in the CDES. The data suggests that Unda was formed by normal marine seawater.

Clino was significantly more complicated as calculated clumped isotope temperatures did not agree with formation by any fluid that was known to exist in the Bahamas. By treating the samples and isolating the dolomite endmember, it was found that dolomites yielded formation temperatures between 20 and 30°C while the LMC endmember gave extrapolated formation temperatures of between 28 and 54°C. The samples from the Clino core are from the deepest relative locality amongst any core in this work. There are several subaerial exposure surfaces in the upper 100 m of the Clino
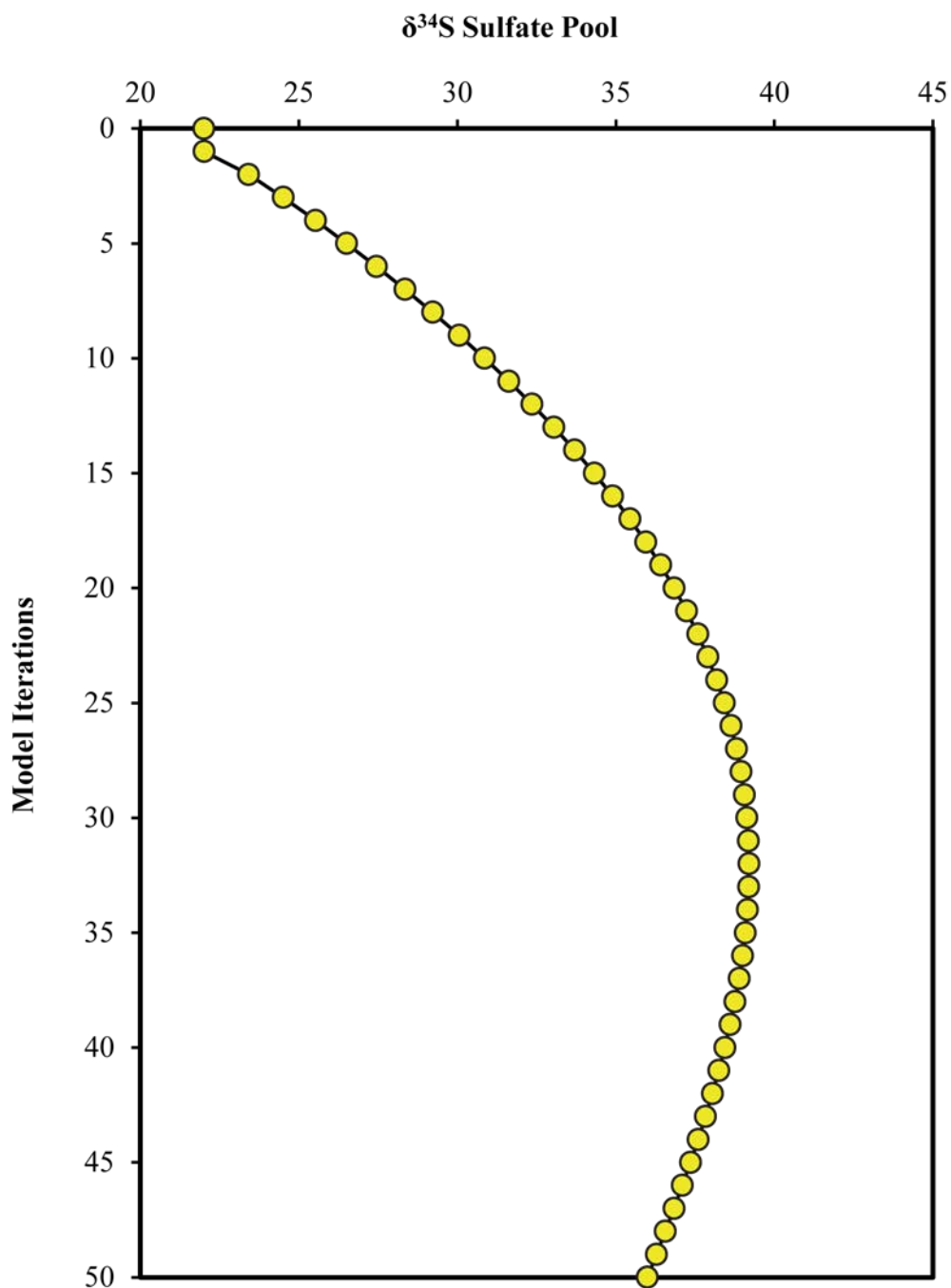
Figure 5.5 - Modeled pore water isotopic sulfur over multiple iterations of bacterial sulfate reduction with an alpha of 1.042 (Detmers et al. (2001)). The model is conceived as the evolution of pore water within a cubic centimeter block of aragonite with 50% porosity. The pore fluid and aragonite contain 28 mM and 41.6 mM of sulfate respectively. The $\delta^{34}S$ of both the pore water and aragonite is 22‰ (CDT). During each iteration, 10% of the remaining aragonite dissolves into the pore fluid.

core, however there are no known subaerial exposure surfaces or other evidence throughout the section of the core where our samples are located to suggest sea level was ever low enough to create such elevated temperatures. The clumped isotope temperatures also do not agree with formation along a geothermal gradient (Figure 4.8). It was therefore concluded that the Clino samples are evidence of some unknown variety of disequilibrium in the clumped isotope species.

Discussion

San Salvador

The bulk of samples from San Salvador focus on the unique isotopic region of the core where clumped isotope temperatures suggest two different fluid sources playing a role in the dolomitization process. Within this region, it is found that some significant deviations from the expected seawater $\delta^{34}S$ values. Throughout the length of the core where sulfate samples were measured, it can be seen that samples with elevated $\delta^{34}S$ values correlate also produce elevated temperatures (relatively). Statistically, the correlation between the $\delta^{34}S$ value and temperature is significant ($p = 0.04$). Looking specifically at the sea level cycle from 52 to 68 m core depth (Fig 5.6), $\delta^{34}S$ value is elevated at the bottom of the section where sea level was interpreted to be at a minimum (Dawans and Swart, 1988) and both clumped isotope temperatures and fluid $\delta^{18}O$ values were both at a maximum. As sea level is interpreted to rise through the middle of the section, $\delta^{34}S$ values are consistently within error of the expected seawater values.

Unda

The Unda CAS samples had little deviation from expected seawater values throughout the length of the section suggesting little to no sulfate reduction occurring

133
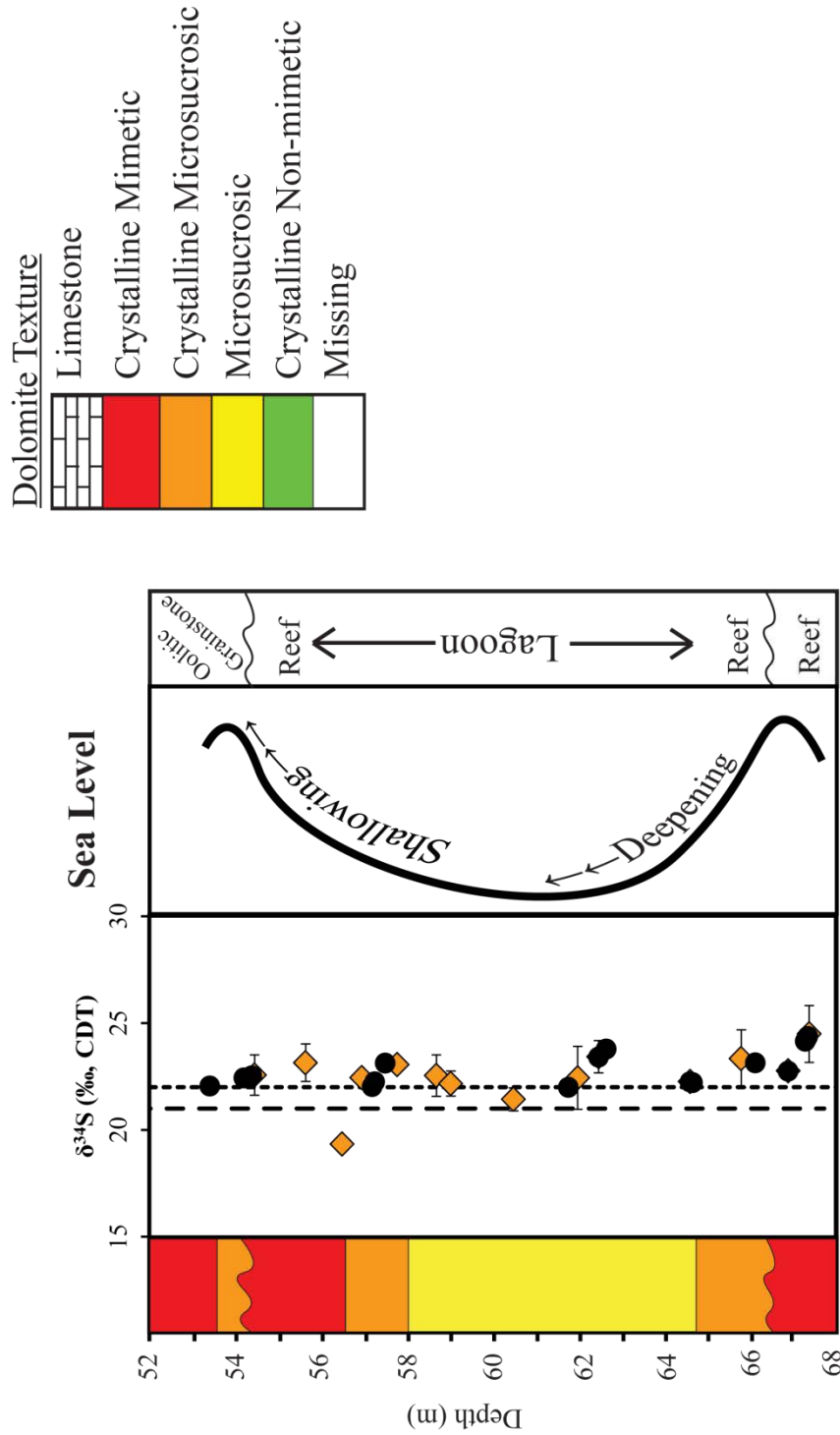
Figure 5.6 - Single interpreted sea level cycle within the San Salvador core with the sub aerial exposure surfaces indicated in the core texture description (∿∿). The green diamonds are measured sulfur isotope values from carbonate associated sulfate samples. The black circles are linearly estimated sulfur values for the depths where clumped isotope temperatures were measured. The vertical dashed line is the sea water δ³⁴S during the Pleistocene and the dotted line is the δ³⁴S during the Pliocene as determined in Paytan et al. (1998). Error bars represent ± 1σ standard deviation. Lithology is based on the work of Dawans and Swart (1988). Dashed and dotted lines represent seawater δ³⁴S values during theMio- Pliocene and Pleistocene respectively as measured in Paytan et al. (1998)

throughout the core. The largest deviation is found in the interpolated samples, and can most likely be attributed to the effects extended linear interpolation. The other small offsets from the lines of expected values are within error based on repeated runs and error associated with the correction of the data. Using a Mann-Whitney U-test comparing the $\delta^{34}S$ of the San Salvador and Unda CAS samples, no statistically significant difference (Mann-Whitney U = 118, n_1 = 24, n_2 = 12, p = .383 two-tailed) can be found between the San Salvador and Unda samples. Based on the mean $\delta^{34}S$ value from both cores (San Salvador = 22.6‰, Unda = 22.8‰), it can be suggested that both cores were dolomitized by Mio-Pliocene sea waters with little influence from bacterial sulfate reduction.

Clino

Clino is the only site of the three measured that showed significant offsets in the $\delta^{34}S$ CAS value compared to seawater values during the Plio-Pleistocene. Clino is also the only site to have clumped isotope temperatures that predominantly disagree with the expected range of temperatures for the site, and even exceed the plausible range of temperatures that fluids are known to exist at in the Bahamas. Therefore, the rest of this discussion will be focused on Clino and the trends and relationships associated with clumped isotope and CAS measurements and any possible implications that elevated $\delta^{34}S$ values could have on clumped isotope measurements.

CAS Samples

Two distinct groups were identified in the CAS measurements when comparing the bulk % dolomite and $\delta^{34}S$ values (Figure 5.7). The first (Group 1) incorporates the samples within the range 30 m below the non-depositional surface at 536.3 m depth. These samples display little change in $\delta^{34}S$ values with increasing
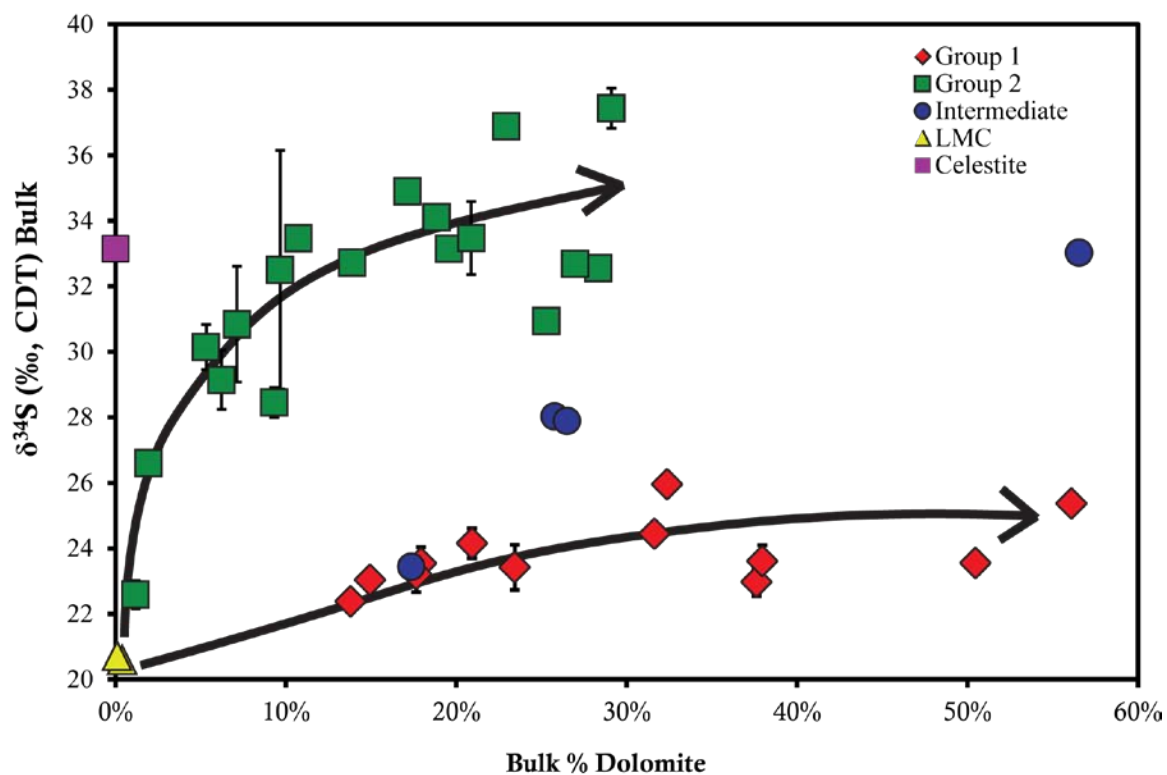
Figure 5.7 - Measured carbonate associated sulfate (CAS) results of the Clino core relative to the bulk % dolomite within each sample. Samples have been divided relative to the observed trends described as Group 1 and Group 2. The blue circles are samples that did not appear to fit in either trend based on either $\delta^{34}S$ or their depth in core. Celestite collected from an unspecified depth in Clino was also measured. Error bars represent $\pm 1\sigma$.

Table 5.3 - Sample Type Descriptions

Sample Group	Depth (m)	δ^{18}O Regression (VPDB, ‰)	Std. Dev.	δ^{13}C Regression (VPDB, ‰)	Std. Dev.	Δ$_{47\_NOAF}$ (‰)	Std. Dev.	Δ$_{47}$ Regression (‰)	Std. Dev.	δ^{34}S (‰, CDT)	Std. Dev.
1	536.6 - 570.6	1.5	0.6	2.8	0.1	0.551	0.017	0.674	0.027	24.3	1.1
2	367.1 - 495.9; 578.2 - 648.7	0.9	0.4	3.0	0.4	0.537	0.015	0.643	0.018	32.4	2.1

bulk percent dolomite ranging from ≈15 to 57% dolomite suggesting that little BSR was occurring within the upper 30 m of the sediment column while significant dolomitization was occurring. The other trend (Group 2) includes samples beneath the 30 m Group 1 interval and all samples above the 536.3 m hardground but below the 367.04 m hardground. These samples show elevated $\delta^{34}S$ values up to 37.4‰ but contain less bulk percent dolomite than the Group 1 samples with a maximum of only 29% (Table 5.3). The discussed trends are most likely associated with depth beneath the non-depositional surfaces. The proposed reason for why no Group 1 samples exist beneath the 367.04 m hardground is because it was an erosional boundary and all shallow sediments have been removed. The dolomite and LMC endmembers were not necessarily formed from the same fluids. Therefore, it is possible that the elevated sulfate is sequestered within one endmember.

Another erosional surface is suggested to exist around 625 m below mud pit in Eberli et al. (1997), however is not discussed in depth. This surface does correlate to a spike in $\delta^{34}S$ similar to that seen beneath the 367.04 m erosional surface. The measurements beneath this surface are not distinguishable from other Group 2 samples so they have been included with those.

Figure 5.7 suggests that within the Group 1 samples, this is not the case as all samples have relatively equivalent $\delta^{34}S$ values over a range of bulk % dolomite compositions. The Group 2 samples on the other hand have a strong correlation ($r^2 = 0.54$, $p < 0.001$, N = 18) between increasing bulk % dolomite and $\delta^{34}S$ value. Therefore, we can conclude that the dolomites formed in the 30 m just beneath the 536.6 m hardground were formed from the same fluids as the LMC endmember.

Elsewhere in the core, the dolomites appear to have formed during a period after the aragonite had transformed to LMC calcite and the dolomites formed later, probably in conjunction with elevated levels of BSR.

This unique isotopic distinction of the 30 m section beneath the 536.3 m hard ground was previously identified in Swart and Melim (2000). It was reported that a correlation was identified between the $\delta^{18}O_{dolomite}$ and $\delta^{18}O_{LMC}$ values in the sediment just beneath this hardground where no correlation exists elsewhere in the core. They suggested that this correlation meant that the precursor sediments were diagenetically altered before dolomitization occurred. This section has also been reported to have a unique Sr isotope signature that indicates it is a sudden transition zone between fluids that are 5 ma to fluids that are 2 ma (Swart et al., 2001). This suggests that the Group 1 samples were the slowly accrued sea floor surface sediments over a period of minimal deposition. If the sediments were never predominantly within the zone of BSR and organic materials were depleted prior to them reaching such depths due to the slow accretion rate thus inhibiting continued BSR, this could explain why the sediments have near ambient-seawater $\delta^{34}S$ values. Assuming BSR could play a role in the disequilibrium seen in the Clino clumped isotope data, the lack of association between these sediments and elevated BSR levels would indicate why some of the Group 1 samples have the lowest calculated and therefore closer to expected, temperatures of formation by clumped isotopes.

Some proposed dolomite formation mechanisms are coupled with an abundance of BSR. This concept was initially discussed in Baker and Kastner (1981) based on a natural observation of dolomite formation on continental margins where

dolomite formation commenced only when the abundance of sulfate in seawater was reduced. The theory was tested at high temperatures (200°C) and showed that the presence of sulfate did inhibit the dolomitization process (Baker and Kastner, 1981). However, this line of thinking goes against many examples of dolomites that have seemingly formed in environments where there is little evidence of BSR (Hardie, 1987), including Unda and San Salvador in this work.

The differences in the diagenetic environment between Clino and the other two sites, San Salvador and Unda, cannot be understated. The partial dolomitization of the sediments paired with the high abundance of BSR in probably stagnant pore waters suggests that Clino could be compared more closely with the modern dolomitizing sediments of Lagoa Vermelha, Brazil (Vasconcelos and McKenzie, 1997), than the porous sediments of San Salvador and Unda. Though no previous study on these samples has indicated as such, it is of this author's opinion that the dolomites in Clino are more closely associated with a dolomitization model including bacterial remediation than invoking the typical model of fluid flow and extensive amounts of time.

Clumped Isotope Samples with Interpolated $\delta^{34}S$ Values

Using Δ_{47} measurements from untreated bulk Clino samples and interpolated $\delta^{34}S$ values derived from the CAS measurements, it is found that the segregation between Group 1 and Group 2 samples is still apparent, though muddled by error on Δ_{47} measurements (Figure 5.8). There is a general trend of increasing Δ_{47} with

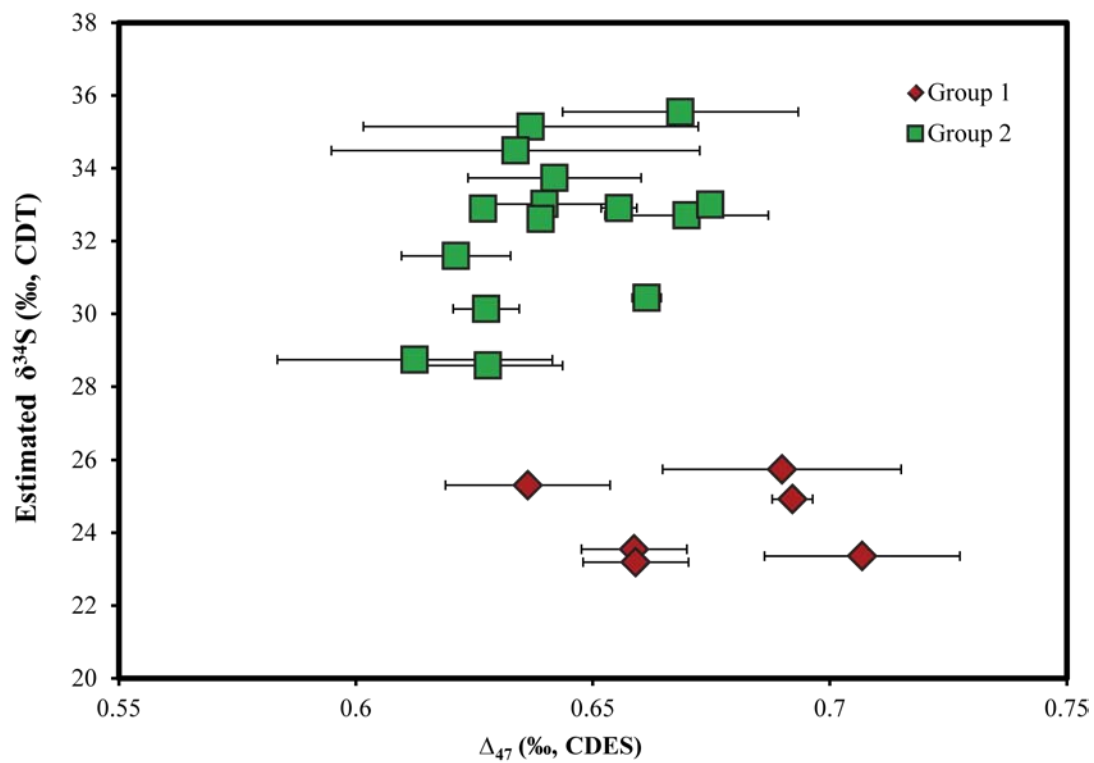Figure 5.8 - The estimated $\delta^{34}S$ of the clumped isotope samples from Clino based on the CAS Clino measurements. Error bars represent $\pm$ 1σ.

decreasing δ^{34}S values, though the trend is not statistically significant ($r^2 = 0.14$, $p = 0.10$).

Bacterial sulfate reduction in Clino

δ^{18}O and δ^{13}C Values

The bulk sample δ^{18}O values do vary significantly ($r^2 = 0.781$) with the bulk % dolomite in composition throughout the length of the core. This is to be expected, as dolomite endmembers have been repeatedly shown to have a 3‰ increase in their δ^{18}O value than the corresponding LMC endmembers (Land, 1980). However, the δ^{13}C values have been shown to be completely independent of the bulk % dolomite ($r^2 = 0.00$) as well as being poorly correlated with every other metric examined including δ^{18}O ($r^2 = 0.01$), Δ_{47} ($r^2 = 0.04$), or δ^{34}S ($r^2 = 0.01$).

Δ_{47} and δ^{34}S Values

Using a data set not distinguishing between Group 1 (N = 6) and Group 2 (*N* = 14) samples found statistically significant correlations between δ^{34}S values and the variables bulk % dolomite ($r^2 = 0.26$, $p = 0.02$) and δ^{18}O values ($r^2 = 0.24$, $p = 0.02$). When distinguishing between Group 1 and Group 2 samples and using bivariate correlations, the most striking difference between the two is a strong, though not statistically significant at the 95% confidence interval, correlation between δ^{34}S and Δ_{47} values for Group 2 samples ($r^2 = 0.26$, $p = 0.06$), where no such correlation exists for Group 1 samples ($r^2 = 0.01$, $p = 0.93$). The trend for Group 2 samples is strengthened when not utilizing acid digestion fractionation factors which could muddle the signal ($r^2 = 0.37$, $p = 0.02$). This suggests that at least for the Group 2 samples, there is a relationship between BSR and Δ_{47} values.

The other notable correlation is the strong relation between bulk % dolomite and Δ_{47} in both groups (G1: $r^2 = 0.78$, $p = 0.02$; G2: $r^2 = 0.37$, $p = 0.02$). This is to be expected due to the forcing in Δ_{47} associated with the increased acid fractionation for the dolomite endmember. The difference in the predictive capability of each correlation could be associated with the difference in sample size between the two groups, or could be a result of the differing dolomitization mechanisms that are seemingly at play between the two groups.

In summarizing the evidence, it has been shown that with increased depth beneath the hardground surfaces, the sediments in Clino transition from a clumped isotope equilibrium that is dominated by the bulk % dolomite into sediments that are more dominated by the abundance of BSR. This is paralleled by a depleting trend in bulk % dolomite with depth but no trending temperature change (as interpreted by clumped isotopes) with depth negating any interpretation that involved the geothermal gradient. It is also seen that the lowest clumped isotope temperatures with regards to the presumed model of formation are predominantly Group 1 and this is not directly associated with bulk % dolomite despite the fact that the LMC endmember has been shown to produce higher clumped isotope temperatures than the dolomite endmember (Chapter 4). This leads us to conclude that there is some connection between BSR, $\delta^{34}S$ values, and the exotic temperatures seen in Clino.

Influences of Bacterial Sulfate Reduction on Δ_{47}

Disequilibrium in Δ_{47} has been discussed in previous works with respect to speleothems (Affek et al., 2008; Daeron et al., 2011), shallow water corals (Saenger et al., 2012), bivalve mollusks (Eagle et al., 2013; Henkes et al., 2013), and DIC-H$_2$O pools (Henkes et al., 2013). This work is the first to suggest that disequilibrium
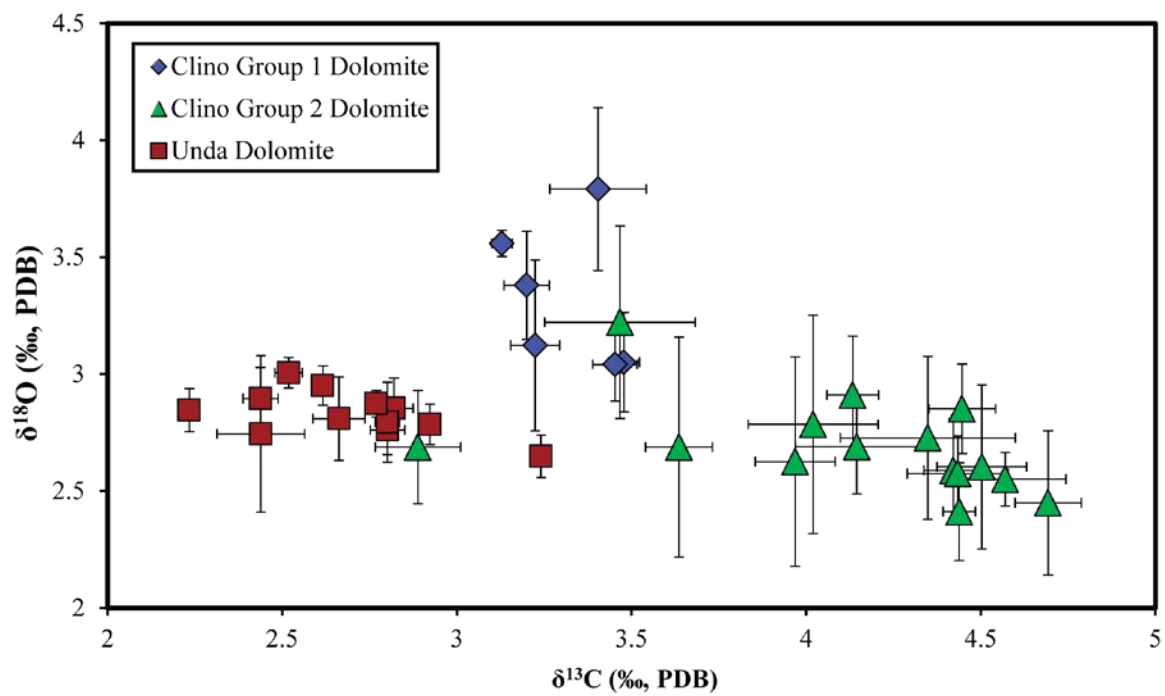
Figure 5.9 - Carbon and oxygen isotope measurements for the Unda and Clino clumped isotope samples. Clino has been separated into Group 1 and Group 2 designations. Error bars represent ± 1σ standard deviation.

in clumped isotopes could be associated with an overabundance of bacterial sulfate reduction. The proposed mechanisms for the other groups of disequilibrium include biological vital effects (Eagle et al., 2013; Henkes et al., 2013; Saenger et al., 2012), kinetic fractionation associated with fluid degassing of CO_2 and rapid precipitation (Daeron et al., 2011), diffused CO_2 in quickly growing organic precipitates, and large pH changes associated with biochemical precipitation (Henkes et al., 2013). In a similar fashion to some of the other mechanisms, BSR has been shown to fractionate both the oxygen (Fritz et al., 1989; Wortmann et al., 2007) and carbon pools (Londry and Des Marais, 2003). In a restricted fluid system, this mechanism could contribute to an isotopic disequilibrium in the pore fluids.

Based on the carbonate-water fractionation of Kim and O'Neil (1997), a model based on an expected fluid temperature of 10 to 15°C and using the LMC endmember $\delta^{18}O_{carbonate}$ value of 0.0 to 0.5‰, it would be expected that the fluids present at Clino would have had a $\delta^{18}O_{fluid}$ composition between -0.8 to +0.8‰ VSMOW. After taking into account the 3‰ offset associated with LMC and dolomite $\delta^{18}O$ value (Land, 1980), it is found that the dolomite endmembers in Clino are enriched by 1 to 2‰ than the modeled $\delta^{18}O_{fluid}$ value. It is difficult to say if there is enrichment in the $\delta^{13}C$ values in Clino as well. (Figure 5.9) Other sites that have been designated as having significant BSR influence on mineralogy, such as in the Gulf of California (Kelts and McKenzie, 1982), show upwards of +10‰ $\delta^{13}C$ values. The Clino bulk data shows no direct evidence of such elevated carbon values. Looking at the Clino separates that were produced in Chapter 4, it can be seen that the dolomites in Clino are more enriched relative to the Unda dolomites by up to

1.5‰ (Figure 5.8). Considering that Clino is located at the bottom of the slope of the platform that Unda presides, and that the source of Clino's sediments is believed to be the platform, this discrepancy could be evidence of isotopic enrichment in the fluids. However, discrepancies arise concerning the timing of dolomitization and diagenesis as well as the abundance of organics which could all have an influence on the $\delta^{13}C$ value.

Porewater pH

Changes in pore water pH could have also contributed to a muddled signal in the clumped isotope values. Tripati et al. (2015) found that changes in precipitation pH can contribute to 0.08‰ change in Δ_{47} as pH decreases from 12 to 7; however the steep transition in Δ_{47} values begin to level off between pH 7 to 9. The byproducts of BSR: hydrogen-sulfide, bicarbonate (2x), ammonia, and phosphoric acid, all contribute to a changing pH environment, but are balanced due to their near equal contribution and molar quantities in the reaction of sulfate reduction therefore contributing little to a changing pore water pH. However, these byproducts do increase alkalinity significantly over time, eventually making the pore waters supersaturated with respect to $CaCO_3$ which will eventually precipitate carbonate. Ben-Yaakov (1973) modeled the BSR reaction and its effects of pore waters and found that the pH was primarily dependent upon the byproducts of BSR, the transfer of charge between the proteolytic and non-proteolytic byproducts, and the eventual precipitation of metal sulfides and calcium-carbonate as the alkalinity changes from continued organic degradation. Unfortunately for this discussion, the results suggested that the pH ranged at most between 6.9 to 8.3, which both agrees with typical pore water pH measurements in shallow burial environments as well as

falling within the stable clumped isotope range presented in Tripati et al. (2015). This does not mean that carbonate precipitated or recrystallized under these conditions would be in equilibrium; just that pH change is not a likely contributor.

Methanogenesis

Methanogenesis is a process commonly associated with BSR, by which carbon in the form of CO_2 is utilized as an electron acceptor in the production of methane by anaerobic bacteria. The interaction between the two reducing environments was believed to be mutually exclusive with BSR preceding methanogenesis. The two processes are non-competing, but sulfate reducing bacteria can outcompete the methanogens for organic substrate while sulfate is prevalent in the pore fluid (Oremland and Taylor, 1978). Recent work on the Australian continental margin has suggested that this may not always be the case, as it was found that in lower sulfate conditions the two groups of reducers can coexist (Mitterer, 2010). That same study suggested that the coexistence of both sulfate reducing bacteria and methanogens could be prominent in the Bahamas, in particularly in sites 1005 and 1009 of the Ocean Drilling Project, due to similar sedimentary conditions and records of reduced hydrogen sulfide and methane. Sites 1005 and 1009 are two sites on the same geographically oriented drilling line as Clino, just further out onto the slope and rise of the Great Bahamas Bank platform.

Methanogenesis has also been shown to contribute to the fractionation on the carbon pool which has appeared in the isotopic records of sediments such as in the Gulf of California (Kelts and McKenzie, 1982). Methanogenesis was stated to have produced significant negative and positive shifts in the $\delta^{13}C$ values of dolomites

from the Gulf of California ranging from -70 to +15‰ associated with depth and abundance of BSR. Compared to the Gulf of California samples, Clino bulk sediment $\delta^{13}C$ values are much more homogenous with no trends associated with depth, and a consistent 1.0 to 1.5‰ offset between the LMC endmember and the dolomite endmember, both of which are slightly positive between +2 to +4‰. Relative to the bulk sediments, the dolomite endmember $\delta^{13}C$ value shows a unique trend with depth beneath the hard ground surface at 536.33m depth. The $\delta^{13}C$ values in these samples linearly increases from 3‰ to 4‰ over core depth 540.5 to 648.7 (Fig 4.2). The sediments above this hardground all have a fairly consistent $\delta^{13}C$ value of 4.5‰ except for the sample at the peak of the section, 367.1m, which has a depleted signal of 2.8‰. This is paralleled by no apparent change in the $\delta^{13}C$ value of the LMC endmember below the 536.33m hardground, disregarding the depths where error in extrapolation is significantly large, where values are a steady 2.5‰. Above this hard ground, the LMC endmember parallels the stable trend seen in the dolomites, albite 1‰ more depleted. While certainly not as drastic as the shift in $\delta^{13}C$ values reported in the Gulf of California, the linear increase with depth does suggest the possibility of increased methanogenesis occurring. Carbonate buffering of the system could have restricted the impact that methanogenesis had on the acquired values of the diagenetic sediments.

Direct Precipitation

One last possible contribution of the microorganisms present that could play a role in the Δ_{47} disequilibrium is the direct precipitation of carbonates. Many microorganisms have been found to directly precipitate carbonates (LMC, HMC,

dolomite, aragonite, etc.), and while some may be precipitating at equilibrium with respect to oxygen and carbon, there could still be biologically associated vital effects contributing to a disequilibrium in Δ_{47} values. This could explain the difference in correlations between the Group 1 and Group 2 sediments. If the Group 1 sediments were less influenced by bacterial mediation than the Group 2 sediments and instead were more dependent upon diagenetic alteration by interaction with seawater, this would explain why Group 1 sediments are all low in $\delta^{34}S$ values and have similar Δ_{47} values despite large variation in bulk dolomite %. The other possibility is that time played a role in these sediments. If the Group 1 sediments were dolomitized before the Group 2 samples through interaction with seawater, which then reduced the porosity of the sediments, induced anoxia and promoted sulfate reduction, methanogenesis, and bacterial remediated precipitation of carbonates, then the isotopic extremes would predominantly affect the deeper Group 2 sediments.

Conclusions

It has been suggested that there could be possible connections between high rates of bacterial sulfate reduction, as determined through the measurement of carbonate associated sulfate, and depleted or disequilibrated Δ_{47} values. In the two study sites of San Salvador and Unda, it was found that the sediments which were entirely dolomitized, had $\delta^{34}S$ values that varied little from the measured seawater composition (21-22‰) of the time periods through which dolomitization most likely occurred. The measured clumped isotope values and their calculated temperatures showed good agreement with expected temperature ranges based on previous geologic models for their formation. The third site, Clino, a mixed carbonate system, had elevated and variable $\delta^{34}S$ signatures,

from 20 to 37‰, that showed trends with depth beneath hard-ground surfaces found throughout the core. The trending $\delta^{34}S$ values were found to have different patterns with relation to the bulk % dolomite, which also translated into different relationships with measured Δ_{47} values.

No byproduct of bacterial sulfate reduction could be connected directly to these elevated clumped isotope temperatures. However, if bacterial sulfate reduction is found to be the culprit, the disequilibrium could be attributed to a combination of effects including pH changes, fractionation of the isotope pool, or biological vital effects if there are microorganisms that are directly contributing to the precipitation of carbonates. Further sample measurements need to be performed on sites similar to Clino to determine if sulfate reduction is actually the cause of the temperature offsets or if other unforeseen factors are also playing a role. This study should not discourage further clumped isotope work in sites where sulfate reduction is occurring until a direct mechanism is identified.

References

Affek, H., Bar-Matthers, M., Ayalon, A., Matthers, A., Eiler, J.M., 2008. Glacial/interglacial temperature variations in Soreq cave speleothems as recorded by 'clumped isotope' thermometry. Geochimica et Cosmochimica Acta 72, 5351-5360.

Affek, H., Eiler, J.M., 2006. Abundance of mass 47 CO_2 in urban air, car exhaust, and human breath. Geochimica et Cosmochimica Acta 70, 1-12.

Aharon, P., Socki, R.A., Chan, L., 1987. Dolomitization of atolls by sea water convection flow: Test of a hypothesis at Niue, South Pacific. The Journal of Geology 95, 187-203.

Badiozamani, K., 1973. Dorag dolomitization model-application to middle Ordovician of Wisconsin. Journal of Sedimentary Petrology 43, 965-984.

Baker, P.A., Kastner, M., 1981. Constraints on the formation of sedimentary dolomites. Science 213, 214-216.

Baldini, L.M., Walker, S.E., Railsback, L.B., Baldini, J.U.L., Crowe, D.E., 2007. Isotopic ecology of the modern land snail *Cerion*, San Salvador, Bahamas: Preliminary advances toward establishing a low-latitude island paleoenvironmental proxy. PALAIOS 22, 174-187.

Beach, D.K., 1982. Depositional and diagenetic history of Pliocene-Pleistocene carbonates of Northwestern Great Bahama Bank. Evolution of a carbonate platform, Comparative Sedimontology Laboratory. University of Miami, Florida.

Beach, D.K., Ginsburg, R.N., 1980. Facies Succession of Pliocene-Pleistocene Carbonates, Northwestern Great Bahama Bank. The American Association of Petroleum Geologists Bulletin 64, 1634-1642.

Ben-Yaakov, S., 1973. pH buffering of pore water of recent anoxic marine sediments. Limnology Oceanography 18, 86-94.

Bigeleisen, J., 1955. Statistical mechanics of isotopic systems with small quantum corrections. I. General considerations and the rule of the geometric mean. The Journal of Chemical Physics 23, 2264-2267.

Bonifacie, M., Ferry, J.M., Horita, J., Vasconcelos, C., Passey, B.H., Eiler, J.M., 2011. Calibration and applications of the dolomite clumped isotope thermometer to high temperatures, Mineralogical Magazine, p. 551.

Bottrell, S.H., Newton, R.J., 2006. Reconstruction of changes in global sulfur cycling from marine sulfate isotopes. Earth Science Reviews 75, 59-83.

Bristow, T.F., Bonifacie, M., Derkowski, A., Eiler, J.M., Grotzinger, J.P., 2011. A hydrothermal origin for isotopically anomalous cap dolostone cements from south China. Nature 474, 68-72.

Budd, D.A., 1997. Cenozoic dolomites of carbonate islands: their attributes and origin. Earth Science Reviews 42, 1-47.

Burdett, J.W., Arthur, M.A., Richardson, M., 1989. A Neogene seawater sulfur isotope age curve from calcareous pelagic microfossils. Earth and Planetary Science Letters 94, 189-198.

Burke, W.H., Denison, R.E., Hetherington, E.A., Koepnick, R.B., Nelson, H.F., Otto, J.B., 1982. Variation of seawater $^{87}Sr/^{86}Sr$ throughout Phanerozoic time. Geology 10, 516-519.

Came, R.E., Eiler, J.M., Veizer, J., Azmy, K., Brand, U., Weidman, C.R., 2007. Coupling of surface temperatures and atmospheric CO_2 concentrations during the Palaeozoic era. Letters to Nature 449, 199-202.

Carew, J.L., Mylroie, J.E., 1995. Quaternary tectonic stability of the Bahamian Archipelago: Evidence from fossil coral reefs and flank margin caves. Quaternary Science Reviews 14, 145-153.

Chen, J.H., Curran, H.A., White, B., Wasserburg, G.J., 1991. Precise Chronology of the last interglacial period: ^{234}U-^{230}Th data from fossil coral reefs in the Bahamas. Geological Society fo America Bulletin 103, 82-97.

Claypool, G.E., Holser, W.T., Kaplan, I.R., Sakai, H., Zak, I., 1980. The age curves of sulfur and oxygen isotopes in marine sulfate and their mutual interpretation. Chemical Geology 28, 199-260.

Conrad Neumann, A., Hearty, P.J., 1996. Rapid sea-level changes at the close of the last interglacial (substage 5e) recorded in Bahamian island geology. Geology 24, 775-778.

Craig, H., 1957. Isotopic standards for carbon and oxygen and correction factors for mass spectrometric analysis of carbon dioxide. Geochimica et Cosmochimica Acta 12, 133-149.

Daeron, M., Guo, W., Eiler, J.M., Genty, D., Blamart, D., Boch, R., Drysdale, R., Maire, R., Wainer, K., Zanchetta, G., 2011. $^{13}C^{18}O$ clumping in speleothems: Observations from natural caves and precipitation experiments. Geochimica et Cosmochimica Acta 75, 3303-3317.

Dale, A., John, C.M., Mozley, P.S., Smalley, P.C., Muggeridge, A.H., 2014. Time-capsule concretions: Unlocking burial diagenetic processes in the Mancos Shale using carbonate clumped isotopes. Earth and Planetary Science Letters, 30-37.

Davis, R.L., Johnson Jr., C.R., 1990. Karst hydrology of San Salvador, in: Mylroie, J.E. (Ed.), Proceedings of the fourth symposium on the geology of the Bahamas, pp. 118-135.

Dawans, J.M., Swart, P.K., 1988. Textural and geochemical alterations in Late Cenozoic Bahamian dolomites. Sedimentology 35, 385-403.

Defliese, W.F., Hren, M.T., Lohmann, K.C., 2015. Compositional and temperature effects of phosphoric acid fractionation on Δ47 analysis and implications for discrepant calibrations. Chemical Geology 396, 51-60.

Defliese, W.F., Lohmann, K.C., 2015. Non-linear mixing effects on mass-47 CO_2 clumped isotope thermometry: Patterns and implications. Rapid Communication Mass Spectrometry 29, 901-909.

Degens, E.T., Epstein, S., 1964. Oxygen and carbon isotope ratios in coexisting calcites and dolomites from recent and ancient sediments. Geochimica et Cosmochimica Acta 28, 23-44.

Dennis, K.J., Affek, H., Passey, B.H., Schrag, D.P., Eiler, J.M., 2011. Defining an absolute reference frame for 'clumped' isotope studies of CO2. Geochimica et Cosmochimica Acta 75, 7117-7131.

Dennis, K.J., Schrag, D.P., 2010. Clumped isotope thermometry of carbonatites as an indicator of diagenetic alteration. Geochimica et Cosmochimica Acta 74, 4110-4122.

DePaolo, D.J., 1986. Detailed record of the Neogene Sr isotopic evolution of seawater from DSDP Site 590B. Geology 14, 103-106.

Detmers, J., Bruchert, V., Habicht, K.S., Kuever, J., 2001. Diversity of sulfur isotope fractionations by sulfate-reducing prokaryotes. Applied and Environmental Microbiology 67, 888-894.

Dix, G.R., 2001. Origin of Sr-rich magnesian calcite mud in a Holocene pond basin (Lee Stocking Island, Bahamas). Journal of Sedimentary Research 71, 167-175.

Dupraz, C., Fowler, A., Tobias, C., Visscher, P., 2013. Stromatolitic knobs in Storr's Lake (San Salvador, Bahamas): a model system for formation and alteration of laminae. Geobiology 11, 527-548.

Dupraz, C., Visscher, P.T., Baumgartner, L.K., Reid, R.P., 2004. Microbe-mineral interactions: early carbonate precipitation in a hypersaline lake (Eleuthera Island, Bahamas). Sedimentology 51, 745-765.

Eagle, R.A., Eiler, J.M., Tripati, A.K., Ries, J.B., Freitas, P.S., Hiebenthal, C., Wanamaker Jr., A.D., Taviani, M., Elliot, M., Marenssi, S., Nakamura, K., Ramirez, P., Roy, K., 2013. The influence of temperature and seawater carbonate saturation state on $^{13}C–^{18}O$ bond ordering in bivalve mollusks. Biogeosciences 10, 4591-4606.

Eberli, G.P., Ginsburg, R.N., 1987. Segmentation and coalescence of Cenozoic carbonate platforms, northwestern great Bahama Bank. Geology 15, 75-79.

Eberli, G.P., Ginsburg, R.N., 1989. Cenozoic progradation of northwestern Great Bahama Bank, a record of lateral platform growth and sea-level fluctuations. SEPM Special Publication 44, 339-355.

Eberli, G.P., Swart, P.K., McNeill, D.F., Kenter, J.A.M., Anselmetti, F.S., Melim, L.A., Ginsburg, R.N., 1997. A synopsis of the bahamas drilling project: Results from two deep core borings drilled on the Great Bahama Bank, Proceedings of the Ocean Drilling Program, Initial Reports.

Eiler, J.M., 2007. "Clumped-isotope" geochemistry - The study of naturally occurring, multiply substituted isotopologues. Earth and Planetary Science Letters 262, 309-327.

Eiler, J.M., Schauble, E., 2004. $^{18}O^{13}C^{16}O$ in Earth's atmosphere. Geochimica et Cosmochimica Acta 68, 4767-4777.

Epstein, S.A., Clark, D., 2009. Hydrocarbon potential of the Mesozoic carbonates of the Bahamas. Carbonates and Evaporites 24, 97-138.

Fernandez, A., Tang, J., Rosenheim, B.E., 2014. Siderite 'clumped' isotope thermometry: A new paleoclimate proxy for humid continental environments. Geochimica et Cosmochimica Acta 126, 411-421.

Ferry, J.M., Passey, B.H., Vasconcelos, C., Eiler, J.M., 2011. Formation of dolomite at 40-80 C in the Latemar carbonate buildup, Dolomites, Italy, from clumped isotope thermometry. Geology 39, 571-574.

Friedman, I., Hall, W.E., 1963. Fractionation of O^{18}/O^{16} between coexisting calcite and dolomite. The journal of geology 71, 238-243.

Friedman, I., O'Neil, J.R., 1977. Compilation of stable isotope fractionation: Factors of geochemical interest, in: Fleischer, M. (Ed.), Data of Geochemistry 6th ed. Geology Survey Prof. Paper. USGS, Washington DC.

Fritz, P., Basharmal, G.M., Drimmie, R.J., Ibsen, J., Qureshi, R.M., 1989. Oxygen isotope exchange between sulphate and water during bacterial reduction of sulphate. Chemical Geology: Isotope Geoscience section 79, 99-105.

Fritz, P., Smith, D.G.W., 1970. The isotopic composition of secondary dolomites. Geochimica et Cosmochimica Acta 34, 1161-1173.

Fry, B., Silva, S.R., Kendall, C., Anderson, R.K., 2002. Oxygen isotope corrections for online d^{34}S analysis. Rapid Communication Mass Spectrometry 16, 854-858.

Ghosh, P., Adkins, J., Affek, H., Balta, B., Guo, W., Schauble, E.A., Schrag, D., Eiler, J.M., 2006. ^{13}C-^{18}O bonds in carbonate minerals: A new kind of paleothermometer. Geochimica et Cosmochimica Acta 70, 1439-1456.

Ghosh, P., Eiler, J.M., Campana, S.E., Feeney, R.F., 2007. Calibration of the carbonate 'clumped isotope' paleothermometer for otoliths. Geochimica et Cosmochimica Acta 71, 2736-2744.

Gill, B.C., Lyons, T.W., Frank, T.D., 2008. Behavior of carbonate-associated sulfate during meteoric diagenesis and implications for the sulfur isotope paleoproxy. Geochimica et Cosmochimica Acta 72, 4699-4711.

Gill, B.C., Lyons, T.W., Young, S.A., Kump, L.R., Knoll, A.H., Saltzman, M.R., 2011. Geochemical evidence for widespread euxinia in the Later Cambrian ocean. Letters to Nature 469, 80-83.

Glunk, C., Dupraz, C., Braissant, O., Gallagher, K.L., Verrecchia, E.P., Visscher, P.T., 2011. Microbially mediated carbonate precipitation in a hypersaline lake, Big Pond (Eleuthera, Bahamas). Sedimentology 58, 720-738.

Goldsmith, J.R., Graf, D.L., 1958. Structural and compositional variations in some natural dolomites. The Journal of Geology 66, 678-693.

Goodell, H.G., Garman, R.K., 1969. Carbonate geochemistry of Superior deep test well, Andros Island, Bahamas. AAPG Bulletin 53, 513-536.

Guo, W., Eiler, J.M., 2007. Temperature of aqueous alteration and evidence for methane generation on the parent bodies of the CM chondrites. Geochimica et Cosmochimica Acta 71, 5565-5575.

Guo, W., Mosenfelder, J.L., Goddard III, W.A., Eiler, J.M., 2009. Isotopic fractionations associated with phosphoric acid digestion of carbonate minerals: Insights from first principles theoretical modeling and clumped isotope measurements. Geochimica et Cosmochimica Acta 73, 7203-7225.

Hagey, F.M., Mylroie, J.E., 1995. Pleistocene lake and lagoon deposits, San Salvador island, Bahamas. Special Papers - Geological Society of America, 77-90.

Hardie, L.A., 1987. Dolomitization - A critical-view of some current views. Journal of Sedimentary Petrology 57, 166-183.

He, B., Olack, G.A., Colman, A.S., 2012. Pressure baseline correction and high-precision CO_2 clumped-isotope (D_{47}) measurements in bellows and micro-volume modes. Rapid Communication Mass Spectrometry 26, 2837-2853.

Hearty, P.J., Kindler, P., 1995. Sea-level highstand chronology from stable carbonate platforms (Bermuda and the Bahamas). Journal of Coastal Research 11, 675-689.

Henkes, G.A., Passey, B.H., Wanamaker Jr., A.D., Grossman, E.L., Ambrose Jr., W.G., Carroll, M.L., 2013. Carbonate clumped isotope compositions of modern marine mollusk and brachiopod shells. Geochimica et Cosmochimica Acta 106, 307-325.

Hoegh-Goldberg, O., 1999. Climate change, coral bleaching and the future of the world's coral reefs. Marine & Freshwater Research 50, 839-866.

Horita, J., 2014. Oxygen and carbon isotope fractionation in the system dolomite–water–CO2 to elevated temperatures. Geochimica et Cosmochimica Acta 129, 111-124.

Humphrey, J.D., 2000. New geochemical support for mixing-zone dolomitization at Golden Grove, Barbados. Journal of Sedimentary Research 70, 1160-1170.

Huntington, K.W., Eiler, J.M., Affek, H., Guo, W., Bonifacie, M., Yeung, L.Y., Thiagarajan, N., Passey, B.H., Tripati, A.K., Daeron, M., Came, R., 2009. Methods and limitations of 'clumped' CO_2 isotope (D_{47}) analysis by gas-source isotope ratio mass spectrometry. Journal of Mass Spectrometry.

Kampschulte, A., Bruckschen, P., Strauss, H., 2001. The sulphur isotopic composition of trace sulphates in Carboniferous brachiopods: implications for coeval seawater, correlation with other geochemical cycles and isotope stratigraphy. Chemical Geology 175, 149-173.

Kampschulte, A., Strauss, H., 2004. The sulfur isotopic evolution of Phanerozoic seawater based on the analysis of structurally substituted sulfate in carbonates. Chemical Geology 204, 255-286.

Kelts, K., McKenzie, J.A., 1982. Diagenetic dolomite formation in Quaternary anoxic diatomaceous muds of Deep Sea Drilling Project leg 64, Gulf of California, in: Blakeslee, J., Platt, L.W., Stout, L.N. (Eds.), Initial Reports of the Deep Sea Drilling Project, pp. 553-570.

Kim, S.-T., Mucci, A., Taylor, B.E., 2007. Phosphoric acid fractionation factors for calcite and aragonite between 25 and 75 °C: Revisited. Chemical Geology 246, 135-146.

Kim, S.-T., O'Neil, J.R., 1997. Equilibrium and nonequilibrium oxygen isotope effects in synthetic carbonates. Geochimica et Cosmochimica Acta 61, 3461-3475.

Kohout, F.A., 1967. Groundwater flow and the geothermal regime of the Floridian Plateau. Transactions of the Gulf Coast Assoc. of Geol. Societies XVII.

Land, L.S., 1980. The isotopic and trace element geochemistry of dolomite: The state of the art. SEPM Special Publication 28, 87-110.

Land, L.S., 1983. The application of stable isotopes to studies of the origin of dolomite and to problems of diagenesis of clastic cements, Stable Isotopes in Sedimentary Geology pp. 1-75.

Land, L.S., 1985. The origin of massive dolomite. Journal of Geology Education 33, 112-125.

Lechler, A.R., Niemi, N.A., Hren, M.T., Lohmann, K.C., 2012. Paleoelevation estimates for the northern and central proto-basin and bange from carbonate clumped isotope thermometry. Tectonics 32, 295 - 316.

Londry, K.L., Des Marais, D.J., 2003. Stable carbon isotope fractionation by sulfate reducing bacteria. Applied and Environmental Microbiology, 2942-2949.

Loyd, S.J., Corsetti, F.A., Eiler, J.M., Tripati, A.K., 2012. Determining the diagenetic conditions of concretion formation: Assessing temperatures and pore waters using clumped isotopes. Journal of Sedimentary Research 82, 1006-1016.

Lumsden, D.N., Chimahusky, J.S., 1980. Relationship between dolomite nonstoichiometry and carbonate facies parameters. SEPM Special Publication 28, 123-137.

Masaferro, J.L., Eberli, G.P., 1999. Jurassic-cenozoic structural evolution of the southern great Bahama bank, Sedimentary Basins of the World - Caribbean Basins, pp. 167-193.

Matthews, A., Katz, A., 1977. Oxygen isotope fractionation during the dolomitization of calcium carbonate. Geochimica et Cosmochimica Acta 41, 1431-1438.

Mazzullo, S.J., Bischoff, W.D., Teal, C.S., 1995. Holocene shallow-subtidal dolomitization by near-normal seawater, northern Belize. Geology 23, 341-344.

McNeill, D.F., 1989. Magnetostratigraphic dating and magnetization of cenozoic platform carbonates from the Bahamas, Marine Geology and Geophysics. University of Miami - Rosenstiel School of Marine and Atmospheric Science, p. 210.

McNeill, D.F., Ginsburg, R.N., Chang, S.-B.R., Kirschvink, J.L., 1988. Magnetostratigraphic dating of shallow-water carbonates from San Salvador Bahamas. Geology 16, 8-12.

McNeill, D.F., Lidz, B.H., Swart, P.K., Kenter, J.A.M., 2001. Chronostratigraphy of a prograded carbonate platform margin: A record of dynamic slope sedimentation Western Great Bahama Bank, Subsurface Geology of a Prograding Carbonate Platform Margin, Great Bahama Bank: Results of the Bahama Drilling Project. SEPM Special Publication, pp. 101-134.

Melim, L.A., Swart, P.K., Eberli, G.P., 2004. Mixing-zone diagenesis in the subsurface of Florida and The Bahamas. Journal of Sedimentary Research 74, 904-913.

Melim, L.A., Swart, P.K., Maliva, R.G., 1995. Meteoric-like fabrics forming in marine waters: Implications for the use of petrography to identify diagenetic environments. Geology 23, 755-758.

Melim, L.A., Swart, P.K., Maliva, R.G., 2001. Meteoric and marine-burial diagenesis in the subsurface of Great Bahama Bank, in: Geology, S.f.S. (Ed.), Subsurface Geology of a Prograding Carbonate Platform Margin, Great Bahama Bank: Results of the Bahamas Drilling Projec, SEPM Special Publications, pp. 137-161.

Melim, L.A., Westphal, H., Swart, P.K., Eberli, G.P., Munnecke, A., 2002. Questioning carbonate diagenetic paradigms: evidence from the Neogene of the Bahamas. Marine Geology 185, 27-53.

Meyerhoff, A.A., Hatten, C.W., 1974. Bahamas salient of North America: tectonic framework, stratigraphy, and petroleum potential. The American Association of Petroleum Geologists Bulletin 58, 1201-1239.

Mitterer, R.M., 2010. Methanogenesis and sulfate reduction in marine sediments: A new model. Earth and Planetary Science Letters 295, 358-366.

Murray, S.T., Arienzo, M.M., Swart, P.K., 2016. Determining the D_{47} acid fractionation in dolomites. Geochimica et Cosmochimica Acta 174, 42-53.

Nagihara, S., Wang, K., 2000. Geothermal regime of the wesetern margin of the Great Bahama Bank, in: Swart, P.K., Eberli, G.P., Malone, M.J., Sarg, J.F. (Eds.), Proceedings of the Ocean Drilling Program, Scientific Results. Ocean Drilling Program, College Station, TX, pp. 113-120.

Northrop, D.A., Clayton, R.N., 1966. Oxygen-isotope fractionations in systems containing dolomite. The Journal of Geology 74, 174-196.

O'Neil, J.R., Epstein, S., 1966. Oxygen isotope fractionation in the system dolomite-calcite-carbon dioxide. Science 152, 198-201.

Oremland, R.S., Taylor, B.F., 1978. Sulfate reduction and methanogenesis in marine sediments. Geochimica et Cosmochimica Acta 42, 209-214.

Paerl, H.W., Steppe, T.F., Buchan, K.C., Potts, M., 2003. Hypersaline cyanobacterial mats as indicators of elevated tropical hurricane activity and associated climate change. Ambio 32, 87-90.

Passey, B.H., Henkes, G.A., 2012. Carbonate clumped isotope bond reordering and geospeedometry. Earth and Planetary Science Letters 351-352, 223-236.

Passey, B.H., Levin, N.E., Cerling, T.E., Brown, F.H., Eiler, J.M., 2010. High temperature environments of human evolution in East Africa based on bond ordering in paleosol carbonates. PNAS 107, 11245 - 11249.

Paytan, A., Kastner, M., Campbell, D., Thiemens, M.H., 1998. Sulfur isotopic composition of cenozoic seawater sulfate. Science 282, 1459-1462.

Pierson, B.J., 1982. Cyclic sedimentation, limestone diagenesis and dolomitization in upper Cenozoic carbonates of the southeastern Bahamas.

Pierson, B.J., 1983. Cyclic sedimentation, limestone diagenesis and dolomitization in Upper Cenozoic carbonates of the Southeastern Bahamas, Marine Geology and Geophysics. University of Miami, unpublished, p. 343.

Piggot, A.M., 2014. Microbial Influences on Sedimentation and Early Diagenesis in Carbonate Environments.

Plummer, L.N., Vacher, H.L., MacKenzie, F.T., Bricker, O.P., Land, L.S., 1976. Hydrogeochemistry of Bermuda: A case history of ground water diagenesis of biocalcarenites. GSA Bulletin 87, 1301-1316.

Puckett, M.K., McNeal, K.S., Kirkland, B.L., Corley, M.E., Ezell, J.E., 2011. Biogeochemical stratification and carbonate dissolution-precipitation in hypersaline microbial mats (Salt Pond, San Salvador, The Bahamas). Aquatic geochemistry 17, 397-418.

Rennie, V.C.F., Turchyn, A.V., 2014. The preservation of $\delta^{34}S_{SO4}$ and $\delta^{18}O_{SO4}$ in carbonate associated sulfate during marine diagenesis: A 25 Myr test case using marine sediments. Earth and Planetary Science Letters 395, 13-23.

Rosenbaum, J., Sheppard, S.M., 1986. An isotopic study of siderites, dolomites and ankerites at high temperatures. Geochimica et Cosmochimica Acta 50, 1147-1150.

Rosenheim, B.E., Tang, J., Fernandez, A., 2013. Measurement of multiply substituted isotopologues ('clumped isotopes') of CO2 using a 5 kV compact isotope ratio mass spectrometer: Performance, reference frame, and carbonate paleothermometry. Rapid Communications in Mass Spectrometry 27, 1847-1857.

Saenger, C., Affek, H.P., Felis, T., Thiagarajan, N., Lough, J.M., Holcomb, M., 2012. Carbonate clumped isotope variability in shallow water corals:Temperature dependence and growth-related vital effect. Geochimica et Cosmochimica Acta 99, 224-242.

Saller, A.H., 1984. Petrologic and geochemical constraints on the origin of subsurface dolomite, Enewetak Atoll: An example of dolomitization by normal seawater. Geology 12, 217-220.

Schauble, E.A., Ghosh, P., Eiler, J.M., 2006. Preferential formation of ^{13}C-^{18}O bonds in carbonate minerals, estimated using first principle lattice dynamics. Geochimica et Cosmochimica Acta 70, 2510 - 2529.

Schlager, W., Austin, J., Comet, P., Droxler, A., Eberli, G.P., Fourcade, E., Freeman-Lynde, R., Fulthorpe, C., Harwood, G., Kuhn, G., Lavoie, D., Leckie, M., Melillo, A., Moore, A., Mullins, H., Palmer, A., Ravenne, C., Sager, W., Swart, P.K., Verbeek, J., Watkins, D., Williams, C., 1985. Ocean Drilling Program: Rise and fall of carbonate platforms in the Bahamas. Nature 315, 632-633.

Sena, C.M., John, C.M., Jourdan, A.-L., Vandeginste, V., Manning, C., 2014. Dolomitization of lower cretaceous peritidal carbonates by modified seawater: Constraints from clumped isotopic paleothermometry, elemental chemistry, and strontium isotopes. Journal of Sedimentary Research 84, 552 - 556.

Sharma, T., Clayton, R.N., 1965. Measurements of O^{18}/O^{16} ratios of total oxygen of carbonates. Geochimica et Cosmochimica Acta 29, 1347-1353.

Sheppard, S.M.F., Schwarcz, H.P., 1970. Fractionation of carbon and oxygen isotopes and magnesium between coexisting metamorphic calcite and dolomite. Contr. Mineral. and Petrol. 26, 161-198.

Sibley, D.F., 1982. The origin of common dolomite fabrics: clued from the Pliocene. Journal of Sedimentary Petrology 52, 1087-1100.

Simms, M., 1984. Dolomitization by groundwater flow systems in carbonate platforms. Transactions Gulf Coast Association Geological Society 34, 411-420.

Smart, P.L., Dawans, J.M., Whitaker, F., 1988. Carbonate dissolution in a modern mixing zone. Nature 335, 811-813.

Stoessell, R.K., Ward, W.C., Ford, B.H., Schuffert, J.D., 1989. Water chemistry and $CaCO_3$ dissolution in the saline part of an open-flow mixing zone, coastal Yucatan Peninsula, Mexico. Geological Society of America Bulletin 101, 159-169.

Strauss, H., 1999. Geological evolution from isotope proxy signals - sulfur. Chemical Geology 161, 89-101.

Supko, P.R., 1970. Depositional and diagenetic features in subsurface Bahamian rocks, Marine Science. University of Miami, Proquest Dissertation and Theses, p. 180.

Supko, P.R., 1977. Subsurface Dolomites, San Salvador Bahamas. Journal of Sediment Petrology 47, 1063-1077.

Swanson, E.M., Wernicke, B.P., Eiler, J.M., Losh, S., 2012. Temperatures and fluids on faults based on carbonate clumped-isotope thermometry. American Journal of Science 312, 1-21.

Swart, P.K., Burns, S.J., Leder, J.J., 1991. Fractionation of the stable isotopes of oxygen and carbon in carbon dioxide during the reaction of calcite with phosphoric acid as a function of temperature and technique. Chemical Geology 86, 89-96.

Swart, P.K., Cantrell, D.L., Westphal, H., Handford, C.R., Kendall, C.G., 2005. Origin of dolomites in the Arab-D reservoir from the Ghawar Field, Saudi Arabia: Evidence from petrographic and geochemical constraints. Journal of Sedimentary Research 75, 476-491.

Swart, P.K., Elderfield, H., Beets, K., 2001. The ^{87}Sr/^{86}Sr ratios of carbonates, phosphorites, and fluids collected during the Bahamas Drilling Project cores Clino and Unda: Implications for dating and diagenesis. SEPM Special Publication 70, 175-185.

Swart, P.K., Guzikowski, M., 1988. Interstitial-water chemistry and diagenesis or periplatform sediments from the Bahamas, ODP leg 101, in: Austin Jr., J.A., Schlager, W. (Eds.), Proceedings of the Ocean Drilling Program, Scientific Results.

Swart, P.K., Melim, L.A., 2000. The origin of dolomites in tertiary sediments from the margin of Great Bahama Bank. Journal of Sedimentary Research 70, 738-748.

Swart, P.K., Ruiz, J., Holmes, C.W., 1987. Use of strontium isotopes to constrain the timing and mode of dolomitization of upper Cenozoic sediments in a core from San Salvador, Bahamas. Geology 5, 262-265.

Teeter, J.W., 1995. Holocene saline lake history, San Salvador Island, Bahamas. Special papers - Geological Society of America, 117-124.

Tripati, A.K., Hill, P.S., Eagle, R.A., Mosenfelder, J.L., Tang, J., Schauble, E.A., Eiler, J.M., Zeebe, R.E., Uchikawa, J., Coplen, T.B., Ries, J.B., Henry, D., 2015. Beyond temperature: Clumped isotope signatures in dissolved inorganic carbon species and the influence of solution chemistry on carbonate mineral composition. Geochimica et Cosmochimica Acta 166, 344-371.

Urey, H., 1947. The thermodynamic properties of isotopic substances. Journal of Chemical Society, 562-581.

Vahrenkamp, V.C., 1988. Constrains on the formation of platform dolomites: A geochemical study of late tertiary dolomite from Little Bahama Bank, Bahamas, Marine Geology and Geophysics. University of Miami, p. 434.

Vahrenkamp, V.C., Swart, P.K., 1990. New distribution coefficient for the incorporation of strontium into dolomite and its implications for the formation of ancient dolomites. Geology 18, 387-391.

Vahrenkamp, V.C., Swart, P.K., 1994. Late Cenozoic dolomite of the Bahamas: metastable analogues for the genesis of ancient platform dolomites. Special Publications Int. Ass. Sediment 21, 133-153.

Vahrenkamp, V.C., Swart, P.K., Ruiz, J., 1991. Episodic dolomitization of late Cenozoic carbonates in the Bahamas: Evidence from strontium isotopes. Journal of Sedimentary Petrology 61, 1002-1014.

Van De Velde, J.H., Bowen, G.J., Passey, B.H., Bowen, B.B., 2013. Climatic and diagenetic signals in the stable isotope geochemistry of dolomitic paleosols spanning the Paleocene-Eocene boundary. Geochimica et Cosmochimica Acta 109, 254-267.

Vasconcelos, C., McKenzie, J.A., 1997. Microbial mediation of modern dolomite precipitation and diagenesis under anoxic conditions (Lagoa Vermelha, Rio de Janeiro, Brazil). Journal of Sedimentary Research 67, 378-390.

Vasconcelos, C., McKenzie, J.A., Warthmann, R., Bernasconi, S.M., 2005. Calibration of the $\delta^{18}O$ paleothermometer for dolomite precipitated in microbial cultures and natural environmnets. Geology 33, 317-320.

Wacker, U., Fiebig, J., Schoene, B.R., 2013. Clumped isotope analysis of carbonates: comparison of two different acid digestion techniques. Rapid Communication Mass Spectrometry 27, 1631-1642.

Wacker, U., Fiebig, J., Todter, J., Schone, B.R., Bahr, A., Friedrich, O., Tutken, T., Gischler, E., Joachimski, M.M., 2014. Empirical calibration of the clumped isotope paleothermometer using calcites of various origins. Geochimica et Cosmochimica Acta 141, 127-144.

Wang, Z., Schauble, E.A., Eiler, J.M., 2004. Equilibrium thermodynamics of multiply substituted isotopologues of molecular gases. Geochimica et Cosmochimica Acta 68, 4779-4797.

Ward, W.C., Halley, R.B., 1985. Dolomitization in a mixing zone of near-seawater composition, Late Pleistocene, Northeastern Uvatan Peninsula. Journal of Sedimentary Petrology 55, 407-420.

Warren, J., 2000. Dolomite: occurence, evolution and economically important associations. Earth Science Reviews 52, 1-81.

Whitaker, F.F., Smart, P.L., 1990. Active circulation of saline ground waters in carbonate platforms: Evidence from the Great Bahama Bank. Geology 18, 200-203.

Whitaker, F.F., Smart, P.L., 1993. Circulation of saline ground water in carbonate platforms - A review and case study from the Bahamas, in: Horbury, A.D., Robinson, A.G. (Eds.), Studies in Geology 36: Diagenesis and Basin Development, pp. 113-134.

Wilf, P., 2000. Late Paleocene–early Eocene climate changes in southwestern Wyoming: Paleobotanical analysis. GSA Bulletin 112, 292-307.

Williams, S.C., 1985. Stratigraphy, facies evolution, and diagenesis of late cenozoic limestones and dolomites, Little Bahama Bank, Bahamas, Marine Geology and Geophysics. University of Miami, Coral Gables, Florida.

Wilson, M.A., Palmer, T.J., 1992. Hardgrounds and hardground faunas. University of Wales, Aberystwyth.

Wortmann, U.G., Chernyavsky, B., Bernasconi, S.M., Brunner, B., Böttcher, M.E., Swart, P.K., 2007. Oxygen isotope biogeochemistry of pore water sulfate in the deep biosphere: Dominance of isotope exchange reactions with ambient water during microbial sulfate reduction (ODP Site 1130). Geochimica et Cosmochimica Acta 71, 4221-4232.

Yuan, J., Zhang, Z., Zhang, Y., 2014. 13C-18O bonds in precipitated calcite and aragonite: An ab initio study. Open Journal of Geology 4, 436-480.

Zaarur, S., Affek, H.P., Brandon, M.T., 2013. A revised calibration of the clumped isotope thermometer. Earth and Planetary Science Letters 382, 47-57.

Zenger, D.H., Dunham, J.D., Ethington, R.L., 1980. Concepts and models of dolomitization: SEPM Special Publication. 320.

Zheng, Y.-F., 1999. Oxygen isotope fractionation in carbonate and sulfate minerals. Geochemical Journal 33, 109-126.